Feasibility Study on the Utilization of Soybean Oil and Butanol Blends as an Alternative Fuel Source for Combustion Applications

A THESIS
SUBMITTED TO THE FACULTY OF
UNIVERSITY OF MINNESOTA
BY

Reilly Jay Schoo

IN PARTIAL FULFILLMENT OF THE REQUIREMENTS
FOR THE DEGREE OF
MASTERS OF SCIENCE IN ENGINEERING MANAGEMENT

Advisor: Dr. Alison Hoxie

October 2012

Acknowledgements

I would like to acknowledge and thank all staff and faculty members of the MIE and MSEM departments at the University of Minnesota Duluth. The guidance and support from my advisor Dr. Alison Hoxie has made the completion of this thesis possible. I would also like to acknowledge Dr. Daniel Pope for continually taking the time to help me progress in the research work I have completed at UMD.

I am especially thankful for the research and teaching assistant opportunities which I was given while I furthered my education by completing the MSEM program. I would like to acknowledge my fellow students who I have been fortunate to share an office with and collaborate with throughout my graduate studies.

I would like to acknowledge undergraduates Jay Drescher and Molly Clabots for their contribution to the research project which this paper is based upon. I would also like to thank Darrel Anderson for all the time and effort he has put into our research project as well as the guidance and knowledge he has provided.

Dedication

This thesis is dedicated to my family.
Without their patience and support my graduate school experience
would not have been possible.

ABSTRACT

A variety of concepts have been investigated in an effort to categorize simply mixed blends of soybean oil-butanol fuel as a suitable alternative fuel source for combustion applications. Basic physical property testing carried out in accordance with ASTM standardized methods proved that the addition of butanol to the highly viscous soybean oil (SBO) lowered viscosity, density, and surface tension and improved cold flow properties. The high energy density of pure SBO proved to increase the heating value of the fuel blend. Mixing rules and estimation methods were developed to predict basic property values as a function of temperature and composition with good accuracy. Evaporation studies on single fuel droplets revealed that there is a diffusion-like gasification mechanism present when SBO/butanol blends are exposed to pure vaporization at or below 225°C. All blends exhibit evaporation constants similar to pure butanol suggesting that the mass diffusion of butanol toward the surface is faster than the surface regression rate of the droplet. Combustion tests results suggested that there is a mixed mode gasification mechanism dominated by that of a diffusion rate limiting one present during combustion of single SBO/butanol droplets. Disruptive burning and microexplosions occur because of the mass diffusion of butanol toward the droplet surface being slower than that of the surface regression during combustion. This results in the trapping of butanol within the surface of the droplet allowing for it to be superheated and causing obliteration of the fuel droplet. All blends proved to exhibit incomplete combustion however it was less likely for droplets of near equal concentrations. Blends of near equal concentration (Bu50 and Bu40) proved to have a higher tendency for microexplosions to occur and they were more violent. Strategic droplet size measurements throughout their lifetime provided insight that this is likely due to the amount of butanol burned prior to droplet microexplosions. An economical analysis provided information suggesting that simply mixed SBO/butanol blends could be a feasible alternative fuel source for various combustion applications.

Table of Contents

List of Tables

List of Figures

List of Symbols

Nomenclature

AAD	Absolute average deviation
a, b, c	Regression coefficients
x	Mole fraction of x
y	Mole fraction of y
V	Volume fraction
T	Temperature
P	Pressure
n	Number of components
NP	Number of experimental points
$G_{i,j}$	Interaction parameter between the i_{th} and j_{th} components
P_i	Parachor of component i
$\mathcal{A}$	Partial molar surface area
R	Universal gas constant ($R = 8.314\ \frac{J}{mol \cdot K}$)
$\dot{m}$	Mass flow rate
r_s	Radius of the droplet
v	Surface flux
Pe	Peclet number
K_s	Surface regression rate
$\mathcal{D}$	Liquid phase mass diffusivity
$\mathcal{D}^{\circ}_{\alpha\beta}$	Infinate Diffusivity of A into B
K	Evaporation constant
S, F, I	Parameter values suggested by Nakanishi for the Nakanishi Correlation
t	Time

D	Diameter
D_{final}	Final diameter
D_0	Initial diameter
Vol_{final}	Final volume
Vol_0	Initial volume

Greek Symbols

φ	Fuel property
ρ	Density
ρ_l	Liquid phase density
ρ_g	Gas phase density
η	Kinematic viscosity
μ	Absolute viscosity
$\bar{\mu}$	Mean absolute viscosity
Δ	Contribution Table value
σ	Surface tension
γ	Activity coefficient
π	Pi ($\pi \approx 3.14$)
ξ	Thermal correction factor

Subscripts

SBO	Soybean oil
Bu	Butanol
M	Mixture
i	Referring to the i_{th} component
j	Referring to the j_{th} component
EXP	Experimental value

PR	Predicted value
α	Referring to component A
β	Referring to Component B

Superscripts

B	Referring to the bulk
S	Referring to the surface

1.0 Introduction

The focus of this research is experimental and analytical analysis of properties, vaporization and combustion characteristics of refined, bleached and deodorized (RBD) soybean oil-butanol blends. Investigation into economical information associated with the use of RBD soybean oil-butanol blends as an alternative fuel source for power generation and other combustion applications was also of concern. As a result of high cost and demand of common fuel sources currently in use for combustion applications, bio-derived oils (BDOs) such as soybean oil (SBO) are becoming increasingly attractive for use as an alternative fuel source. Providing different, cost effective methods of making the use of BDOs possible including mixing with miscible alcohols like butanol has been a common concept in the fuel research industry. The main objective of this work was to provide meaningful and accurate information to prove the feasibility and economical/environmental benefits of using SBO simply mixed with butanol as an effective and low cost alternative fuel source for the relevant applications. Properties governing behavior of combustion are important when categorizing fuels as useful or not. Consequently, the overall goal was to provide experimental results that compare the effectiveness and suitability of mixtures of SBO/butanol blends based on mixture concentrations and ambient temperatures. Flashpoint data were compared with results obtained via current standardized testing method for flashpoint (ASTM D93) and combustion behavior of blends of different concentrations were investigated. Other basic properties (viscosity, density, surface tension, higher heating values and cold flow properties) were tested using standardized methods and mixing rules and procedures developed for estimating such properties based on composition and temperature. A quick, cost effective testing facility was developed in order to provide both qualitative and quantitative results which were used to provide insight on how mixture composition affects the gasification process during standard vaporization at low temperatures and during combustion. An economic analysis was performed in order to provide information on the possible benefits of utilizing SBO/butanol mixtures as an alternative fuel source.

The increasing attention in the research community on the use of BDOs is focused on providing efficient, clean burning alternatives to petroleum-based fuels. The testing methods used to categorize these types of fuels as suitable for particular applications have not been standardized due to the such different physical properties these fuels exhibit. Biofuels do have the advantage of being domestically grown thus benefiting local economies. Concerns over environmental issues such as global warming and sulfur related acid rain put biomass-derived fuels at a significant advantage over fossil fuel based fuels as well. This is due to their substantially shorter CO_2 life cycle and the fact that BDOs contain negligible or zero levels of sulfur. However, the high viscosity and low vapor pressure inherent in BDOs lead to poor atomization thus making ignition and efficient combustion difficult to achieve. The two most common biofuels currently being used for combustion applications are biodiesel and ethanol. Biodiesel has seen wide use as a drop in fuel for diesel engines dating back to the 1940s. Biodiesel is produced from BDOs of various feed stocks through transesterification. Transesterification lowers viscosity and flash point thus overcoming some challenges in utilizing neat BDOs. Currently many states have biodiesel mandates, with some as high as 5%, which means that 5% of diesel fuel used in automotive transportation must consist of biodiesel. As a result of more recent biofuel mandates ethanol has been the additive of choice for reformulated gasoline since 2006. The energy intensive batch nature of biodiesel production leads to higher prices over neat BDOs and the main feedstock used for ethanol fermentation, corn, competes with food sources. Consequently, investigation into simpler methods for bringing BDOs and other alcohols to the market is warranted. In a recent article by Chung K. Law butanol is considered the most attractive alcohol for use as alternative fuel source because of its high energy content and volatility surpassing the commonly used ethanol. The abundance of soybean oil stocks in the United States make it the most economical BDO for producing BDO/alcohol blends. For these reasons investigation into the simple mixing of these two fluids as an alternative food source is very justifiable.

Basic property data for binary blends of RBD soybean oil with 99% 1-butanol is presented in this thesis. The pure components were tested as well as blends of 25, 50 and 75% composition by volume of SBO. The mixtures are referred to as Bu100, Bu75, Bu50, Bu25 and Bu0 where the number represents the composition of butanol in the mixture. For example, Bu50 means that the blend contains 50% by volume of butanol and thus the other 50% is pure SBO. The purpose of the property testing within this work is to establish appropriate mixing rules and estimation methods to predict basic properties (i.e. relative density, kinematic viscosity, higher heating values (HHV), surface tension and cold flow properties) of SBO/butanol blends based on composition and temperature. The mixing rules and estimation methods found most suitable are reported.

In most combustion applications fuel is injected into a combustion chamber through a nozzle. The atomization, or breaking up of fuel into many small droplets, is very important for efficient combustion to occur making investigation of single fuel droplets an attractive approach to study combustion characteristics. Innovative studies of the two pure components and blends of Bu75, Bu50, Bu40 and Bu25 provide qualitative and quantitative information useful to correlate gasification mechanisms during vaporization at low temperatures and combustion to the burning behavior of single fuel droplets. Resultant phenomena such as incomplete combustion and microexplosions of single mixed droplets are investigated, analyzed and compared for the different mixtures. The experimental results were be obtained using a combustion facility developed particularly for fuels of such nature as BDO/alcohol mixtures and was useful in predicting combustion behavior as a function of blend composition. The gasification mechanism of single mixed fuel droplets during vaporization at low temperatures and during combustion is analyzed by comparing previous research groups' findings with experimental data. The concepts were tested and theories provided to confidently and accurately describe combustion activity based on the gasification process and the physical characteristics of the droplets. The understanding of such information for single droplets is useful knowledge when attempting to predict how a spray will burn and helps to predict a range of compositions which would be desirable for use in various

combustion applications. The repeatability and accuracy of certain components of the test facility are reported. Ignition technique and temperature collection methods are described and compared with those of previous research groups working with single mixed fuel droplets. Suggestions to improve the test process will be provided.

Cost, availability, CO_2 life cycle and emission characteristics of these fuels were analyzed using published information. The analysis provides valuable information to determine the economic and environmental feasibility of using the simply mixed SBO/butanol fuel blends as an alternative fuel source for various applications. Impacts on consumer costs, fuel consumption, greenhouse gas (GHG) emissions and the petroleum trade market are reported.

2.0 Literature Review

2.1 Biofuels as a Viable Alternative

In the United States the most available feedstock for BDOs is soybean oil with over 19 billion pounds produced yearly. Stores of soybean oil not being utilized are in the 2 to 3 billion pound range yearly [1]. Efforts to burn BDOs like SBO in diesel engines date back to its invention, however the engine was developed and tailored to work with petroleum based diesel. Since then research has continued in an effort to utilize neat SBO in diesel engines, however problems with coking of fuel injectors, ring carbonization, and varnish in the fuel system have been common [2-6]. Methods to alleviate the problems associated with the high viscosity of SBO in general have included dilution, heating, microemulsification, pyrolysis and transesterification [3], [7-11]. Dunn et al. have reported a number of studies investigating co-solvent blending as an alternative solution to biodiesel for application in diesel engines. These studies mixed neat soybean oil with short-chain alcohols such as ethanol and methanol along with a stabilizing agent to prevent separation and improve cold flow properties [6], [11].

Studies focused on the use of biofuels in gas turbine engines and fuel burners are far more recent than diesel engines, but show promise as gas turbines operate under steady

conditions thus alleviating a strong dependence on cetane and octane numbers [12]. The research has primarily consisted of practical engine studies with biodiesel as the primary fuel [13-15]. However, Panchasara et al. and Sequera et al. conducted a more fundamental study of the atomization and combustion performance of biofuels—including a soybean oil-diesel blend—in a model atmospheric combustor [12], [16]. Boucher et al. evaluated a bio-oil obtained through vacuum pyrolysis of softwood bark blended with methanol as a candidate gas turbine fuel finding promising property characteristics [17]. Chiaramonti et al. have performed studies on BDOs used in a modified tractor while Andrews et al. have performed tests using BDOs for power generation in a 2.5MW gas turbine engine. Both groups found promising results documenting the modifications made to the engines so that the BDOs could be effectively used in their applications [18-19]. Proper mixing of BDOs with alcohols like butanol would result in fewer engine modifications. There are no studies these authors are aware of however evaluating the properties of SBO blended with butanol as an alternative fuel blend for use in combustion applications. Butanol, an alcohol that can be produced from a large variety of biomass sources, exhibits characteristics such as octane number similar to that of gasoline and is more energy dense than ethanol and methanol. Also, a lower vapor pressure and higher miscibility than ethanol and methanol make butanol a more desirable alcohol to pair with SBO. Furthermore, butanol is not corrosive and is knock resistant. For these reasons commercial production of butanol through fermentation is targeted for the next two to three years [20]. Blending butanol with SBO reduces the viscosity thus enhancing atomization. The lower flash point of butanol should also improve the ignitability of SBO eliminating the need for preheating and duel fuel tank systems.

Experts claim that markets exist worldwide for various applications utilizing renewable and environmental fuels, and energy systems [18].The high cost of electricity and petroleum as well as environmental concerns are some of the main incentives. Agricultural waste and stores of renewable energy sources such as SBO are among others. Industrial engines for power generation and transportation remain among the

most sought after uses for these types of fuels [18]. The SBO/butanol fuel blend is a promising future fuel for use in combustion applications such as gas turbine engines and boilers. The use of this fuel as an alternative for aviation fuel in modern aircraft is also a considerable possibility.

2.2 Property Testing

2.2.1 SBO/butanol mixture

In order to categorize fuels as feasible or not for various applications and whether or not certain specifications will be met it is necessary to know the basic properties of the fuels such as density, viscosity, heating values, surface tension and cold flow properties. Binary mixtures similar to SBO/butanol mixtures have been studied and are well documented. Equations called mixing rules and prediction methods have been developed for such mixtures to estimate these basic properties based on composition, pressure and temperature however SBO/butanol mixtures in particular remain undocumented. It is essential to have an evaluation method to determine the suitability of these equations. A widely used evaluation method is the absolute average deviation (AAD), which compares experimental results with mixing rules [21]. The AAD is calculated using Eq. (1).

$$AAD = \frac{100}{NP}\sum_{i=1}^{NP}\left|\frac{\varphi_{EXP}-\varphi_{PR}}{\varphi_{EXP}}\right| \quad (1)$$

Mixing rules and prediction methods have been established to estimate fuel properties for biodiesel-diesel fuel blends made with soybean oils, palm oils, fish oils and other BDOs. Multiple works have shown agreement with Kay's mixing rule for estimating specific gravity as well as a monotonic relationship with temperature for various biodiesel mixtures similar to that of pure diesel [7], [22-24]. The same studies showed an exponential relationship between kinematic viscosity and temperature of biofuels similar to that of neat fuels. Tat and Van Gerpen suggest viscosity increases with the increase in percentage of biodiesel and can be estimated with an absolute average deviation (AAD) less than 4% of measured values using a blending rule similar to the one proposed by

Arrhenius and described by Grunberg and Nissan [25], [26]. Benjumea et al. suggest similar behaviors and mixing rule for estimating viscosities of palm oil biodiesel-diesel fuel blends. Heating values have also been accurately predicted using Kay's mixing rule for similar fuel blends by Benjumea et al. [7]. Alptekin and Canakci showed that surface tension increases with increasing composition of biodiesel and decreases with temperature [23].

2.2.2 Relative Density (Specific Gravity)

The density of any fuel is used as a categorization parameter. Poling et al. suggests that the equation for predicting relative density as a function of temperature is of the form:

$$\rho_M = a(T) + b \tag{2}$$

where ρ_M is the blends relative density (unitless) of the mixture and T is the temperature (°C). Researchers have achieved very accurate results using this approach and have shown R^2 values above 0.99 for regression analysis using this equation.

Kay's mixing rule is a commonly used method for predicting properties such as relative density as a function of composition [7]. Kay's mixing rule is shown in Eq. (3).

$$\varphi_M = \sum_{i=1}^{n} x_i \varphi_i \tag{3}$$

where φ_M is the calculated property of the fuel mixture. For a binary mixture of SBO and butanol, using volume fractions instead of molar fractions, this mixing rule takes the form of an arithmetic volume average shown in Eq. (4).

$$\varphi_M = V_{SBO} \cdot \varphi_{SBO} + V_{Bu} \cdot \varphi_{Bu} \tag{4}$$

Kay's mixing rule has proved to be very accurate for predicting the composition-specific gravity relationship for similar mixtures with researchers achieving very low AAD values of less than 0.20% [7]

2.2.3 Kinematic Viscosity

Viscosity is an important property to consider when categorizing fuels because a lower viscosity will lead to better atomization of fuel sprays. A common representation for the variation in kinematic viscosity with temperature for different types of fluids is the Andrade equation shown in Eq. (5) [7].

$$\eta = e^{(a+\frac{b}{T}+\frac{c}{T^2})} \tag{5}$$

where η is the kinematic viscosity (mm/s) and T is the absolute temperature (K). Experts suggest that R^2 values around 0.99 can be achieved when curve fitting data using this equation [7], [27].

By comparing similar studies Poling et al. suggests that there are numerous available equations to estimate viscosity of mixtures based on their composition and that the Grunberg-Nissan equation is a widely used method and suitable for binary liquid mixtures under these conditions. The Grunberg- Nissan equation is:

$$\ln \bar{\mu}_M = \sum_{i=1}^{n} x_i \ln \mu_i + \sum_{i=1}^{n} \sum_{j=1}^{n} x_i x_j G_{i,j} \tag{6}$$

In most cases of binary mixtures where the two components have similar chemical structure it is assumed that they do not interact and the interaction parameter $G_{i,j}$ is neglected ($G_{i,j} = 0$, for $i = j$). This is the case in biodiesel-diesel mixtures because both liquids are non-polar, completely miscible and additive [7]. SBO-butanol mixtures are miscible and additive however SBO is highly non-polar while butanol exhibits a low level of polarity therefore the interaction parameter G_{ij} should not be neglected.

Poling et al. suggests that the value for $G_{i,j}$ is a function of the component composition as well as the temperature therefore it is possible to predict a mixture's viscosity based on these two variables [21]. Using volume fractions instead of the molar fractions and kinematic viscosity instead of absolute viscosity, Eq. (6) for a binary mixture of SBO and butanol takes the form:

$$\ln \eta_M = V_{SBO} \ln \eta_{SBO} + V_{Bu} \ln \eta_{Bu} + V_{SBO} V_{Bu} G_{SBO,Bu} \quad (7)$$

Poling et al. states that the binary interaction parameter, G_{ij}, has been more extensively examined than any other liquid mixture-viscosity correlation. They present a group contribution method proposed by Isdale et al. in 1985 to estimate G_{ij} based on the chemical structure of each component and the temperature of many systems [21]. The method suggests that G_{ij} at 298 K can be estimated using Eq. (8). The *i*th and *j*th component must be chosen using a hierarchical list of rules based on the chemical structure of the components. In this particular case the butanol is the *i*th component because it is an alcohol.

$$G_{ij} = \sum \Delta_i - \sum \Delta_j \quad (8)$$

Δ are values from a group contribution table provided by Poling et al. [21]. Once G_{ij} for 298 K is calculated, Eq. (9) can be used to adjust the interaction parameter G_{ij} for a desired temperature.

$$G_{ij}(T) = 1 - \left[1 - G_{ij}(298)\right]^{\frac{573-T}{275}} \quad (9)$$

Typical AAD values obtained by researchers using the Grunberg Nissan approach to estimate viscosity of fuel mixtures similar to the ones studied here are usually less than 3.74% [7], [21].

2.2.4 Higher Heating Value

Higher heating value (HHV) is a measurement of the amount of energy released during combustion of a fuel. Lower heating values can be directly calculated if the HHV is known [7]. Literature suggests that for binary mixtures similar in nature to SBO-butanol the HHV exhibits a linear relationship as a function of composition and Kay's mixing rule can be used to estimate these values with AAD values typically less than 2% [7].

2.2.5 Surface Tension

Atomization is very dependent on surface tension making it an important property to analyze. Surface tension is a much more challenging property to estimate as a function of composition and temperature [21]. This is because the composition at the surface of a mixture is not the same as the bulk composition and is actually very difficult to estimate. The tendency of the pure component with a lower surface tension to move towards the surface may have an effect on combustion behaviors as well. A common method for predicting surface tension of organic liquid mixtures is using the Macleod-Sudden correlation or some variation of it [28]. The Macleod-Sugden correlation equation for mixtures is:

$$\sigma_M^{1/4} = \sum_{i=1}^{n} [P_i]\left(\rho_{lM} x_i - \rho_{gM} y_i\right) \tag{10}$$

where σ_M is the surface tension of the mixture (dyne/cm), and ρ_{lM} and ρ_{gM} the liquid and vapor densities (mole/cm^3) of the mixture respectfully.

At low pressures the terms involving vapor density and composition may be neglected. The parachor $[P_i]$ may either be obtained from a general group contribution table provided by Reid et al. or by regression of experimental data. The latter method is used by most authors [28]. Neglecting the vapor terms since this work was done at low pressures, Eq. (10) may also be written as Eq. (11) because $[P_i] = \sigma_i^{1/4}/\rho_{Li}$ [28].

$$\sigma_M^{1/4} = \rho_{lM} \sum_{i=1}^{n} \frac{x_i \sigma_i^{1/4}}{\rho_{li}} \tag{11}$$

Another empirical relation recommended by Reid et al. for surface tension prediction is Eq. (12) [28].

$$\sigma_M^{-1} = \sum_{i=1}^{n} x_i \sigma_i^{-1} \tag{12}$$

The benefit of using Eq. (10) is that no experimental data for surface tension of the pure components are needed however depending on the parachor $[P_i]$ chosen the values at the

extreme compositions may not reduce to the appropriate limiting value whereas using Eqs. (11) and (12) will yield the correct values because $\sigma_M \rightarrow \sigma_i$ as $x_i \rightarrow 1$.

There are thermodynamic correlations derived from statistical and classical thermodynamics that can be used to estimate surface tension which may be more accurate since they take into account surface composition whereas the empirical methods employ bulk compositions to characterize the mixtures [28]. Eq. (13), suggested by Reid et al. is a common form of an equation derived from thermodynamics.

$$\sum_{i=1}^{n}\left(\frac{x_i^B\gamma_i^B}{\gamma_i^S}\right) exp\frac{\mathcal{A}_i(\sigma_M-\sigma_i)}{RT} = 1 \tag{13}$$

where x_i^B is the mole fraction of i in the bulk liquid, γ_i^B the activity coefficient in i normalized so that $\gamma_i^B \rightarrow 1$ as $x_i \rightarrow 1$, γ_i^σ the activity coefficient of i in the surface phase normalized so that $\gamma_i^\sigma \rightarrow 1$ as the surface phase becomes identical with that of pure i, $\mathcal{A}_i$ the partial molar surface area of i (cm^2/mole) approximated as $(V_i)^{2/3}(N_0)^{1/3}$ where V_i is the pure liquid molal volume and N_0 is Avogadro's number.

A common method to simplify Eq. (13) is to assume an ideal-liquid mixture ($\gamma_i^B = \gamma_i^\sigma = 1$). Doing this the equation for this binary system reduces to:

$$\sigma_M = x_{SBO}\sigma_{SBO} + x_{Bu}\sigma_{Bu} - \frac{\mathcal{A}}{2RT}(\sigma_{SBO} - \sigma_{Bu})^2 x_{SBO}x_{Bu} \tag{14}$$

where the terms are as defined previously with x_{SBO} and x_{Bu} the bulk mole fractions of SBO and butanol and $\mathcal{A}$ is an average surface area for the molecules constituting the system.

2.2.6 Cold Flow Properties

Cold flow properties such as cloud point (CP), cold filter plugging point (CFPP) and pour point (PP) of fuels like SBO-butanol blends are very important for categorizing fuels especially in climates similar to that of Minnesota. The CP is defined as the temperature at which dissolved solids in fuels are no longer soluble resulting in the tendency to plug

filters. The CFPP is similar to the cloud point and represents the lowest temperature a fuel will pass through a standardized filtration device. The PP of a liquid is the lowest temperature before it becomes a semi-solid and loses its flow characteristics. These properties describe how well a fuel of certain composition will perform at or above these temperatures. It is suggested in literature that mixing BDOs with alcohols will improve cold flow properties (i.e. lower the CP, CFPP and PP) however no prediction methods are available to estimate quantitative effects.

2.3 Droplet Evaporation and Combustion

2.3.1 Facility

In most applications liquid fuel is injected into a combustion chamber via a nozzle resulting in a fuel spray. There are many physical processes involved in spray combustion including atomization, vaporization, heat and mass transfer during droplet-air and vapor-air mixing, ignition, pre-mixed and or diffusion flames, pollutant production (soot), etc. [29]. Atomization, which is arguably one of the most important topics when considering a combustion process, is the production of many small fuel droplets usually ranging from a few microns to around 500 μm through a nozzle [29]. Understanding how a single droplet will behave during the combustion process can give insight on how a spray will burn.

There have been many methods used for testing single fuel droplets. Some methods include reduced gravity or "microgravity" conditions in an effort to keep droplets and flames spherical and reduce the effect of convection for testing purposes [30], [31]. Others are done in normal gravity [32-37] and some compare the two [38], [39]. Some researchers use the method of free falling droplets [32-35], [37] while others [30], [38] use fibers of small diameter to supports the droplet (7um – 110um) which are usually made from silicon carbide (SiC) or other high temperature ceramic. Ikegami et al. preferred the method of suspending droplets off of a thermocouple bead [31]. Placing droplets on the cross section of two intersecting microfibers has proven to be the best

method for producing geometrically spherical droplets [30], [38]. The microfibers also exhibit a low thermal conductivity reducing their contribution to evaporation to nearly nothing [30]. Auto ignition in combustion chambers at temperatures above 980 K were used by the majority of research groups [32-35] but other ignition methods such as spark [30] or resistance elements [36], [38], [40] were also found to be suitable for certain testing applications. The primary interests of experts performing tests on single droplets were ignition delay time [41], burning characteristics such as soot formation [34], burning rates [30], [40], microexplosions and disruptive burning [32-36]. Ambient temperature, pressure, droplet size and concentrations are often the variables in the studies. The use of high speed cameras to capture combustion and evaporation behavior is common for most groups performing droplet studies. No research groups were found to be relating flashpoint or ignition temperature measurements to the combustion of single droplets

Xu et al. used a furnace set at 1173 K which was lowered surrounding 0.6 – 1.7 mm initial diameter (D_0) droplets of light cycle oil mixed with diesel light oil suspended from a single silica fiber to investigate ignition delay and burning rates [36]. They took initial droplet diameter measurements via high speed video analysis at the instance before the droplet entered the furnace and considered the passing of the furnace by the suspended droplet to be time zero in their study assuming the furnace chamber was a constant temperature throughout [36]. Pan et al. studied burning rates and characteristics of biodiesel mixed with diesel or alkanes using a drop tower facility. They suspended fuel droplets (445 μm < D_0 <528 μm) of biodiesel mixed with diesel or alkanes on the cross section of two SiC microfibers with a diameter of 7 μm. The chamber was not heated and was dropped prior to ignition producing a reduced gravity effect. Ignition was achieved by hot wires made of kanthal (90 W in 336 ms) which were attached to a set of push-pull solenoids. Two cameras were attached to the falling chamber. A black and white camera was positioned on top of the droplet and was used to monitor droplet diameter and soot shell. A color CCD camera was used to capture the shape and

luminosity of the flame. The reduced gravity conditions allowed for more symmetrical flames for analysis [38].

2.3.2 Droplet Evaporation

Droplet vaporization is of particular interest when considering fuels in nearly any application using spray combustion. This is because most droplets injected into a combustion chamber evaporate or change composition before combustion takes place. The concentration of a fuel vapor or droplet is governed by the rate of evaporation, usually referred to as (K). The concentration of droplets at the time of ignition has a significant impact on the combustion process especially with mixtures like SBO - butanol. Binary mixtures of this nature where the two components have very different boiling points can exhibit disruptive combustion behavior that could affect the performance of the relevant application. The evaporation rates of these types of mixtures must be analyzed so that complete and effective combustion can be achieved. Along with Poling et al's suggestion that the pure component with lower surface tension tends to concentrate at the surface a number of research groups suggest that there is a mass diffusion mechanism of the more volatile component moving outwards of a mixed fuel droplet to the surface as it vaporizes [32-35], [37]. The initial composition and droplet size will govern the combustion process [32-35] however droplet size and concentrations are changing with time prior to ignition during spray combustion. Consequently it is important to correlate evaporation analysis with combustion characteristics. The mass per unit time leaving a droplet of a pure fluid (vaporization) can be calculated using Eq. (15) which can be rewritten as Eq. (16) [29].

$$-\frac{d}{dt}\left(\frac{4}{3}\pi\rho_l r_s^3\right) = \dot{m} \tag{15}$$

$$-4\pi\rho_l r_s^2 \frac{dr_s}{dt} = 4\pi r_s^2 \cdot \rho_g v \tag{16}$$

where $\dot{m}$ the mass flow rate leaving the droplet and v the surface flux surrounding the droplet. Simplifying and rearranging Eq. (16) yields:

$$\frac{dr_s}{dt} = -\frac{\rho_g}{\rho_l} v \tag{17}$$

Matalon suggests that ρ_g/ρ_l typically ranges from ~ 10^{-2} to 10^{-3} which would mean that the droplet size regresses very slowly compared to the diffusion process [29]. If the suggestions by Poling et al. and Wang et al. are true then, at temperatures below the boiling point of SBO ($T_{b\text{-}SBO}$), the butanol in the mixture would be diffusing to the surface fast enough to exhibit evaporation rates resembling that of pure butanol until the droplet has become purely SBO.

There have been numerous research groups that have studied evaporation rates of pure fuel droplets varying initial droplet size, ambient pressures and temperatures as well as considered low gravity versus regular gravity situations. Fuel mixtures however become much more challenging especially when the vapor phase is considered [32]. A few groups studying multicomponent droplets have determined that the gasification mechanism during evaporation and combustion is either distillation-like, diffusion-like or a mixture of both depending on the components properties. Zhang et al. suggests that diffusion-limited gasification is favored for rapid gasification rates (during combustion) and components with large volatility differences and distillation-like gasification is favored otherwise [42]. Volatility is defined as the tendency of a liquid to vaporize and is usually categorized by a substances boiling point. The volatility difference between the two components studied in this work is high as pure butanol will vaporize at room temperature and has a boiling point of 118°C while pure SBO has no boiling point but rather a smoke point around 240°C. In earlier work, Makino and Law have shown that an instantaneous Peclet number for mass diffusion in the liquid phase can be used to predict whether the gasification process will be distillation-like or diffusion-like [43]. They define this Peclet number as:

$$Pe(t) = \frac{K_s(t)}{\mathcal{D}} \tag{18}$$

where $\mathcal{D}$ is the liquid phase mass diffusivity and $K_s(t)$ is the droplet surface regression rate defined as:

$$K_s(t) = -\frac{1}{2}\frac{dr_s{}^2}{dt} \tag{19}$$

where $r_s(t)$ is the instantaneous droplet radius. They suggest that for $P_e << 1$ the process should be distillation-like and for the $P_e >> 1$ it should be strongly diffusion limited. The diffusion coefficient in Eq. (18) is complicated to estimate. Poling et al. shows a variety of estimation methods for infinitely dilute systems (low concentrations of A into B) along with their accuracy for multiple binary systems [21]. They show that the method proposed by Nakanishi in 1978 is the most accurate for binary mixtures of oleic acid solute in solvent n-butanol (the binary system closest in chemical structure to the SBO – butanol mixture) The Nakanishi correlation is [21]:

$$\mathcal{D}^{\circ}_{\alpha\beta} = \left[\frac{9.97\times10^{-8}}{(I_\alpha V_\alpha)^{1/3}} + \frac{2.40\times10^{-8} F_\beta S_\beta V_\beta}{I_\alpha S_\alpha V_\alpha}\right]\frac{T}{\eta_\beta} \tag{20}$$

where $\mathcal{D}^{\circ}_{\alpha\beta}$ is the diffusivity of solute A into solvent B at low concentrations, cm^3/s. V_α and V_β are the liquid molar volumes of A and B at 298 K, cm^3/mol, and the factors I_α, S_α, S_β, and F_β are parameter values suggested by Nakanishi and provided by Poling et al. The parameter values depend on the compound. η_β is the solvent viscosity in cP, and T is the system absolute temperature (K).

Diffusion coefficients are dependent on concentration as well as temperature (and pressure) and Poling et al. shows many methods of predicting diffusion coefficients based on these parameters. Most of these methods are functions of the infinite dilute diffusivities, the molar concentrations and a thermal correction factor similar to the one shown in Eq. (21) [21].

$$\mathcal{D}_{\alpha\beta} = \left[x_\alpha\left(\mathcal{D}^{\circ}_{\beta\alpha} - \mathcal{D}^{\circ}_{\alpha\beta}\right) + \mathcal{D}^{\circ}_{\alpha\beta}\right]\xi \tag{21}$$

where $\mathcal{D}_{\alpha\beta}$ is the concentration based diffusivity of A into B, x_α is the molar concentration of A, and ξ is a thermal correction factor ($\xi = [(\partial \ln \xi_\alpha / \partial \ln x_\alpha)]_{T,P}$). However Poling et al. suggests that no single correlation is accurate in estimating the

concentration dependent diffusion coefficient for any mixture and furthermore the correction factor (ξ) is nearly impossible to estimate without experimental data [21].

Understanding evaporation rates and behavior in these conditions is a significant step for analysis of similar droplets in more realistic environments where they would be experiencing more intense convection and elevated pressures. If the gasification mode is found to be diffusion limited then instantaneous concentrations throughout the fuel droplets lifetime could be estimated and the assumption that mixed fuel droplets will share the same evaporation rates as pure butanol at $T < T_{b\text{-}SBO}$ could be made. As a result, the combustion behaviors can be correlated with droplet concentrations at the time of ignition.

2.3.3 Droplet Combustion

Combustion characteristics of single, mixed fuel droplets such as burning behavior and ignition delay have been extensively studied by a select group of researchers since the 1950's. Some multicomponent fuel droplets have been reported to experience "disruptive burning", or a staged burning behavior, while others exhibit a steady burn similar to a pure fuel. Authors describe the staged burning of multicomponent droplets similarly such that it is a three-staged burn. The first stage is an almost steady process where the more volatile component is preferentially burned. The second stage is a short transient period where the flame becomes feeble (flame shrinkage) and the dominant surface concentration transitions from the more volatile to the less volatile component. As the surface temperature increases towards the boiling point of the less volatile component a third stage of combustion is observed which often includes a "microexplosion" of the droplet followed by the co-burning of the less volatile component and what remains of the more volatile component [32-35], [42]. Microexplosions are the boiling and exploding of the liquid fuel droplet. Botero et al. suggests that the occurrence of microexplosions starts a secondary atomization and could significantly facilitate the overall burning rate of fuel droplets because the rupturing of the droplet into the gas medium improves mixing with the oxidizing gasses. This in turn reduces the sooting

propensity and NO_x formation [35]. Other experts agree that microexplosions may help to improve the energy utilization and emission characteristics in practical combustion systems. Because of these potential benefits research into droplet burning behavior is warranted. In an effort to understand what governs the combustion behavior of multi-component fuel droplets experts have used mixtures of a wide variety of different fuel types with different chemical properties. Biodiesels, alcohols, n-alkanes, n-alkenes and their mixtures have proved to be the most widely studied. The effects of initial droplet size [41] and concentration [32-35] are the most highly studied variables in their tests. Changes in pressure and droplet generation techniques have also been shown to affect combustion characteristics [34].

The physiochemical properties of the fuels have proved to be the most influential on whether or not a mixed fuel droplet will experience the disruptive burning phenomenon. Experts agree that for a mixed fuel droplet to exhibit microexplosions and staged burning (i.e. disruptive burning) the droplet must experience a diffusion-rate limited gasification mechanism during combustion. The more volatile fuel in the mixture must be trapped within the surface due to diffusional resistance. At that point the interior of the droplet can be superheated (experience temperatures above the boiling point of the more volatile component) to the point of homogeneous nucleation where it boils and explodes obliterating the droplet [32-35], [42]. In contrary, steady burning of mixed droplets has been linked to a distillation-like mechanism. Most authors agree that the gasification mechanism is controlled by the volatility (i.e. tendency to vaporize) differentials and liquid phase mass diffusivities of the fuels as well as the droplet surface regression rate [32-35], [42]. Surface regression (i.e. shrinkage due to gasification) of liquid fuel droplets may be rapid or very slow. During combustion the surface regression rate will be higher because the surface temperature will be approaching the boiling point of the fuel present at the surface. Alternatively the surface regression rate will be much lower when the droplet is undergoing pure evaporation at low temperatures but will increase with ambient temperature. The gasification mechanism, which can be diffusion-like, distillation-like or what is referred to as mixed mode (mixture of the two) is the deciding

factor of whether fuel droplets will exhibit microexplosions or not [32]. It is important to note that a diffusion limiting mechanism is necessary for a microexplosion to occur however disruptive burning and a diffusion-like gasification mechanism can still be present without the occurrence of a microexplosion. Research groups however have not reported any behaviors of incomplete combustion but rather only the tendency for the combustion process to be disruptive or not.

A diffusion-like, or diffusion limiting, gasification mechanism is one in which one of the components (the more volatile of the two) is moving outwards towards the droplet surface as it is undergoing liquid to gas vaporization there. It is limited by the diffusion rate because the rate of liquid-phase mass diffusion is slow relative to the rate of surface regression and liquid phase thermal diffusion [32]. This results in the more volatile component preferentially gasified leaving a higher concentration of the less volatile component at the surface. The more volatile component is essentially trapped in the interior where the composition is again nearly uniform. The droplet temperature then approaches the boiling point of the less volatile component, which can cause superheating of the interior and homogeneous nucleation (i.e. boiling of the more volatile component) in the interior resulting in microexplosions. High volatility differentials and fast surface regression rates are likely causes of a diffusion-like gasification mechanism [44]. In a distillation-like gasification mechanism there would not be superheating of the interior of the droplet because the vaporization is not dependent on the liquid-phase mass diffusion. Instead, the droplet remains uniform and the gasification rates are controlled by the volatility differentials of the components. Contrary to the diffusion limited mechanism, slow surface regression rates and mixtures of components with similar volatilities are likely to result in a distillation-like gasification mechanism [42]. A mixed mode mechanism would suggest that the droplet starts burning as it would in the distillation-like case suggesting uniform surface compositions and then reaches a steady state limit where concentration in the inner core remains uniform surrounded by a concentration layer at the surface. The difference between the diffusion-rate limited mechanism and the mixed mode is that the concentration at the surface layer rapidly

adjusts to satisfy the requirements of the volatility differentials and as the droplet heats, liquid-phase diffusional resistance weakens. Then, toward the end of the droplet lifetime mass diffusion of the volatile component outward becomes efficient again and the burning is more distillation-like. With a mixed mode mechanism microexplosions can still occur it is just suggested that the mode of gasification is temperature dependent and thus dependent on the changing diffusivity. Very few research groups have actually studied the gasification modes in depth but rather fuel droplets susceptibility to experience disruptive burning or not based on specific fuel characteristics and testing techniques. The actual gasification mode is usually overlooked and just accepted to be dominated by diffusion limitations. The select groups which have been trying to understand what gasification mechanism droplets are undergoing have now leaned toward the mixed-mode mechanism in the most recent studies utilizing a variety of tests in an effort to prove this [32], [34], [42].

Wang et al. use burning rate plots to compare slopes of the third burning stage stating that for a distillation-like mechanism the slope would be equal to the burning rate of the less volatile component and for a diffusion-like mechanism the slope should depend on the initial concentration of the more volatile component. They also attempt to compare volumes of the droplet throughout its lifetime stating that at flame shrinkage (between the 2^{nd} and 3^{rd} stage) the droplet should have a volume equal to the fraction of the less volatile component for a distillation-like process and adversely the volume would be larger for a diffusion-like mechanism suggesting there is still concentrations of the more volatile fuel present in the droplet after the first stage. They investigate flame color during the first and third stages to distinguish whether the more volatile component is still present in the third stage suggesting a diffusion controlled mechanism [32]. Makino and Law have shown that the Peclet number, which depends on the diffusivity, can be used to predict if the gasification mode is diffusion limited or distillation-like. The same researchers show that since diffusivities increase with temperature the mode can change throughout the droplet lifetime indicating the possibility of mixed mode behavior [43]. Randolph, Makino and Law have experimentally shown mixed-mode behavior for mixed

droplets with significant volatility differentials [44]. They do this by instantaneously determining the droplet size and composition throughout the droplets lifetime using microphotography and sampling.

A variety of ignition and droplet positioning techniques have been used to study disruptive burning of mixed fuel droplets with diameters ranging from 220 μm [35] to 1.9 mm [40]. Volatility differentials, initial droplet size and initial concentrations remain the most influential factors on whether or not disruptive burning and microexplosions will occur. Takei et al. examine the combustion of n-heptane/n-hexadecane and study the effect of initial droplet size on ignition delay using an auto ignition technique. They correlate initial droplet diameter of mixed fuels with that of the pure fuels to explain how the diffusion mechanism of the more volatile component affects the ignition process. They have found that for smaller diameter droplets (<0.65mm) ignition was impossible because the vapor mass flux of the volatile heptane, is quite large and has vaporized from the surface before ignition could occur.

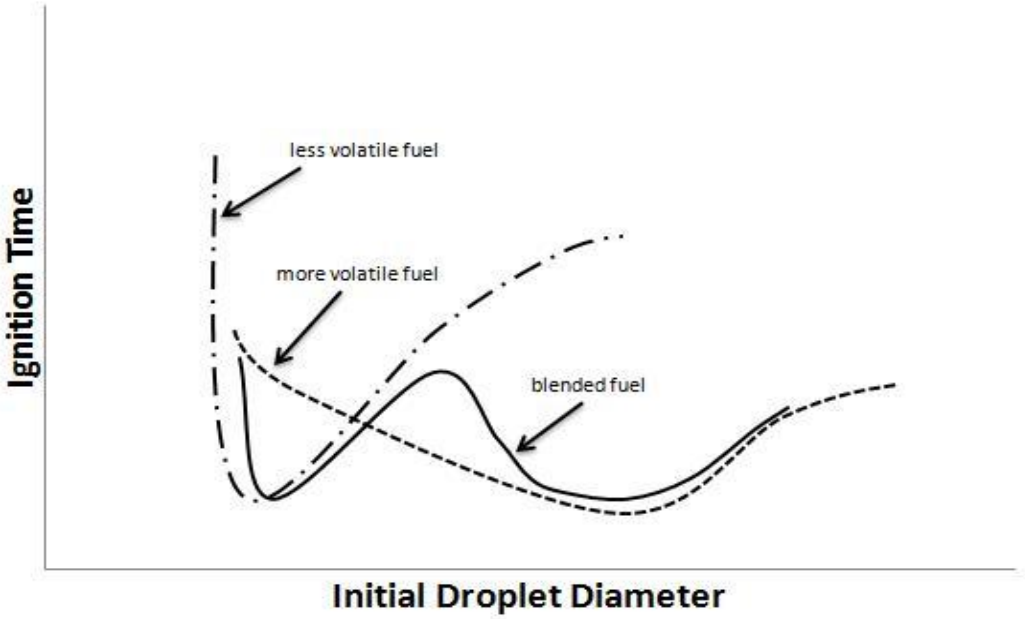

Fig. 2.1. Plot of ignition time versus initial droplet diameter similar to that of Takei et al. in their study using n-heptane/n-hexadecane droplets [41]

They also show using plots like the one shown in Fig. 2.1 that for smaller sized droplets (< ~1mm) the ignition delay pattern resembles that of pure hexadecane and for droplets of larger diameter the pattern resembles pure heptane. They explain that with smaller droplets the concentration of liquid heptane on the surface decreases rapidly and since the diffusion coefficient of liquid heptane is very small it is trapped within the surface of the droplet at the time of ignition. Consequently the concentration of hexadecane on the surface becomes high and therefore the ignition is induced by the hexadecane gasification. Alternatively for large droplets they suggest the vapor mass flux of heptane is slower and as a result the ignition is induced by the heptane/oxygen reaction. This behavior is similar to the staged burning phenomena, caused by diffusional resistance, described by Lasheras and Wang et al. because ignition depends on the time it takes to reach the boiling point of the dominant fuel at the droplet surface [41]. Lasheras et al. have used free falling droplets of a range of n-propanol/n-paraffin and ethanol/n-paraffin solutions and emulsions in a hot air chamber at atmospheric pressure to study disruptive burning. They use a high speed camera to correlate initial composition, properties (vaporization temperatures and relative concentration) and the combustion behavior (droplet diameter, slip velocity, temperature and oxidizer concentration) to disruptive burning. They provide evidence that the disruptive burning behavior is a function of difference in normal boiling points of the pure components and their relative concentrations. They show that disruptive burning occurs for a larger range of propanol and ethanol concentrations as the carbon number of the n-paraffins increase (i.e. volatility differential becomes larger) [37]. They use their results to propose a prediction method for the minimum concentration of alcohol required to produce the disruptive burning. Lasheras et al. further clarify the diffusion-like gasification mechanism and explain that the microexplosion is caused as a result of homogeneous bubble nucleation (spontaneous and random bubble formation within the droplet caused by superheating the interior) within the droplet as the local temperature reaches that of the nucleation temperature (> the boiling point of the more volatile component) of the solution. They suggest that the intensity of the microexplosion is determined by the number of nucleation centers and the physical properties of the components. They claim that the microexplosion phenomenon

is more likely to occur with greater volatility differentials between the two pure components and when the concentrations are nearly equal (i.e. 50/50 mixtures) [37]. Lasheras et al. provides a plot similar to the one shown in Fig. 2.2 which qualitatively suggests that the lowest concentration of the more volatile component for disruption to occur can be estimated by determining the mixture at which the homogeneous nucleation temperature is the same as the normal boiling point of the heavier component. For mixtures with larger initial concentrations of the less volatile component the maximum surface temperature approaches that of its boiling point but for mixtures with small initial concentrations of the less volatile component the maximum surface temperature may be significantly lower [37].

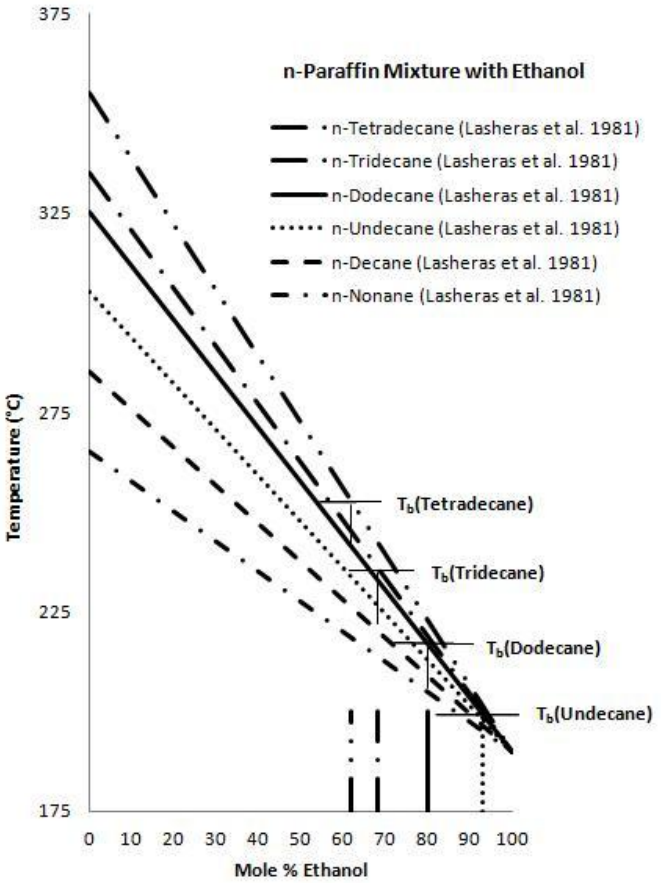

Fig. 2.2. Plot of boiling temperature versus ethanol concentration similar to the one provided by Lasheras et al. in their disruptive burning study using ethanol/n-paraffin blends [33]

Wang et al. have performed similar studies to that of the Lasheras group to study the combustion process of pure n-alkanes, alcohols and aromatics as well as binary and tertiary mixtures of these components. Their main focus was the disruptive burning behavior of mixed fuel droplets and investigating how the gasification mechanisms which the droplets undergo during combustion may relate. This group as well suggests that disruptive burning of these mixtures occurs because of internal superheating caused by volatility differentials and a

diffusion dominant gasification mechanism. They show that for mixtures of similar volatilities disruptive burning does not occur and the burning rates are dependent on the initial concentrations. This suggests a distillation-like gasification mode throughout the droplet lifetime. They explain the three-stage burning phenomenon of droplets with different volatilities similar to other groups where the first stage is a period where the more volatile component is preferentially gasified followed by a second transient period where flame shrinkage due to internal droplet heating occurs. After the droplet has been heated it assumes a steady burning of both components in the third stage. For certain mixtures where there exists high enough volatility differentials the high boiling point of the less volatile component will allow for the inner core to be heated to a temperature at which homogeneous nucleation is possible resulting in internal gasification or microexplosion. However they claim that, since the droplet is uniform at ignition, the initial gasification period (first burning stage) is more distillation-like because the volatile component is preferentially gasified at a relatively low surface temperature establishing a higher concentration of the less volatile component. This indicates mixed-mode gasification throughout the droplet lifetime [32]. Botero et al. use similar experimental methods as the Wang research group studying combustion characteristics (burning rate, microexplosion and sooting propensity) of ethanol, diesel, castor oil biodiesel and their mixtures. They show agreement with other research groups explaining that the requirement for microexplosions to occur depends on the volatility differences of the components and their relative concentrations. They use plots of normalized diameter squared versus normalized time plots such as the one shown in Fig. 2.3 to investigate these behaviors [35]. They explain the three stage combustion process as one which exhibits two relatively straight segments corresponding to nearly steady droplet burning separated by a nearly horizontal segment. In the first stage the more volatile component is preferentially gasified until it has nearly depleted from the surface. Then a transient period occurs during which the droplet surface temperature increases approaching the boiling point of the less volatile component which is then more abundant at the surface. They explain that this heating process slows down the gasification rate and thus flame size. After sufficient heating has occurred the gasification is sustained by vaporization of

both components and if the components are such that would promote a microexplosion it will occur here [35]. They prove in their research that higher volatility differences and near equi-volumetric compositions of binary mixtures are most likely to experience microexplosions and at a greater intensity. Higher concentrations of the more volatile component also result in microexplosions but they happen later in the droplet lifetime and are less intense. This is consistent with the Lasheras group's findings.

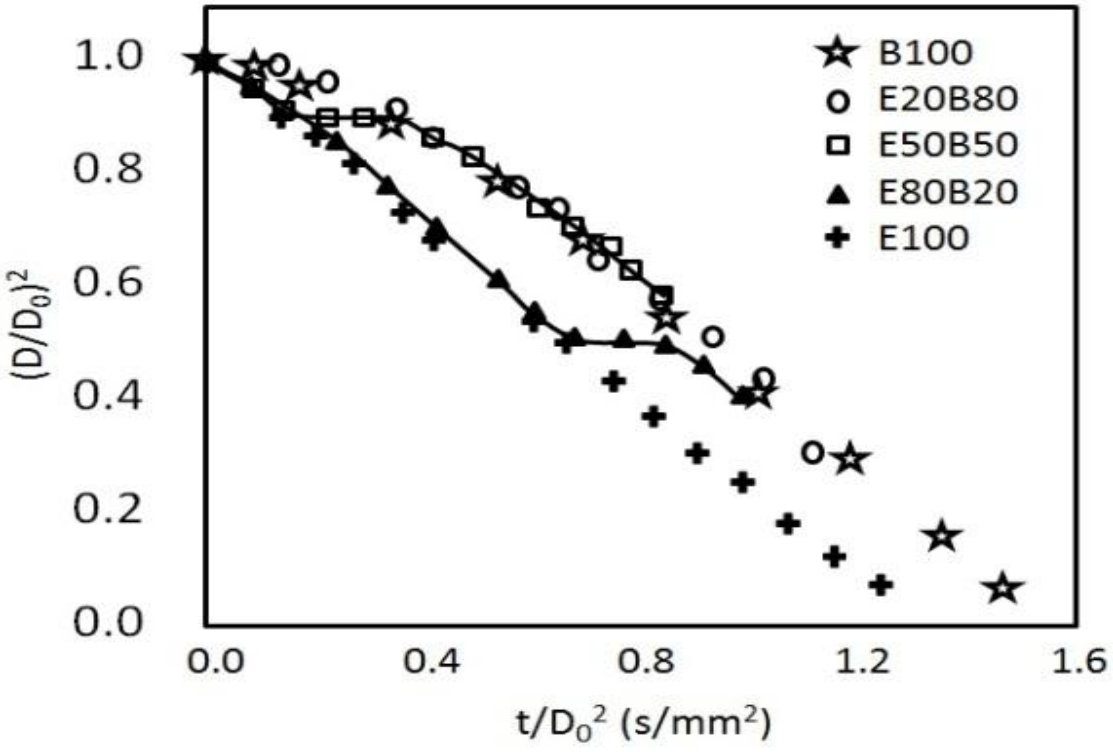

Fig. 2.3. Plot of normalized droplet diameter as a function of time during combustion similar to the plot provided by Botero et al. in their single droplet study using ethanol/castor oil biodiesel blends [35]

The effect of droplet generation on the microexplosion phenomenon has also been explored. In a more recent study Wang et al uses heptanes/hexadecane droplets to show that disruptive burning is less likely to occur for stably produced single, premixed droplets reaching a spherical shape close to the nozzle than otherwise [34]. They also show that collision induced mixed droplets which would resemble the atomization process are more likely to experience microexplosions. They provide evidence in the

study that the non-disruptive combustion characteristics including ignition delay, flame shrinkage and burning rates are not affected by the different generation modes. This suggests that a diffusion dominant gasification mechanism (however the initial stage is more diffusion-like because the initial droplet is uniform and surface temperature rather low) is still present with changing droplet generation and that microexplosions need not be present to signify this. The flame shrinkage and burning rates prove this. They also analyze past research groups droplet generation methods explaining that even for premixed droplets of the same mixtures microexplosions are likely to occur with an unstable mode of droplet generation [34]. For example, the Lasheras group's apparatus via the chopping method to produce droplets are a form of unstable premixed droplet generation. Most of the current research groups are using free falling single fuel droplets to study disruptive burning however droplets suspended from filaments have been used in the past. The filaments are not believed to play a part in the occurrence of microexplosions in mixed fuel droplets however because the fibers do not influence the burning process of pure fuels [30], [40].

Considering that most combustion applications would occur under elevated pressure mixed fuel droplets were also studied in such environments by a couple groups. The droplet experiments reported thus far have been done at relatively low pressure. The Lasheras group, using their results, explains that they believe with elevated pressure that microexplosions are more likely to occur and would possibly be more violent. They attribute this to the fact that boiling points and nucleation temperatures of liquids increase with pressure thus allowing the droplet to heat to a higher temperature before bubble nucleation occurs. They further explain that since both temperatures increase with pressure at similar rates that if microexplosions occur at atmospheric pressure they will to at any higher pressure [37]. In one of Wang et al's studies, they conclude that the occurrence of microexplosions is generally enhanced in low pressures ranging up to 0.5 MPa [40]. Niioka and Soto investigated the effect of increasing pressure (up to 2.0 MPa) on combustion of n-heptane/n-hexadecane (the same fuels used by Wang and Lasheras) droplets and found that increasing pressure beyond 0.5 MPa reduces the staged burning

and the micro-explosion effect. They suggest that the range of pressures which microexplosions will occur depend on the limit of superheat for the relevant mixture and the boiling point of the less volatile component [40]. They do not comment on the gasification mode or how it would change at elevated pressures. This contrasts Lasheras et al's prediction that disruptive burning will occur at elevated pressures if it is found to occur at atmospheric pressure. In a more recent study Zhang and Law show consistent results with the Niioka group claiming that as pressure is increased the occurrence of microexplosions diminishes [42]. They claim however, that this is due to the fact that the liquid-phase mass diffusivities can be substantially increased with pressure. With a higher temperature increase which coincides with the increased boiling points at elevated pressure the diffusional resistance diminishes. Consequently the transport of the volatile component to the droplet surface is facilitated. They claim that facilitation becomes stronger with increasing pressure and that the gasification mechanism actually becomes more distillation-like. The disagreement between the Lasheras group and the Zhang group suggests that possibly for n-heptane/n-hexadecane mixtures the gasification mode changes with increased pressures and that difference in volatility may not be the only factor disruptive burning is dependent on. Zhang and Law's results further show the diffusivities of components dependence on temperature and they agree on the mixed mode gasification throughout a droplets lifetime [42]. It also reinforces that the Peclet number can be useful in estimating gasification modes because diffusivities are a function of temperature.

Disruptive burning could impact the effectiveness of fuel in various atomization applications constituting the research on what causes this behavior [34], [35], [37]. Experts claim that microexplosions break up the fuel more, better mixing the liquid with the oxidizing gases and could be beneficial to combustion. Incomplete combustion, however not referred to in previous research, would be undesirable in any application. Consequently, predicting SBO/butanol mixtures combustion behavior depending on initial characteristics (droplet size and composition) is important. Droplets of SBO/butanol mixtures have not previously been tested but the vast difference in boiling

points (118° C for butanol while pure SBO does not have a boiling point) would suggest that droplets of SBO/butanol would experience disruptive burning and microexplosions. According to past research this would however depend on the initial conditions (droplet size and concentration) and droplet generation mode. Using evaporation rates in various atmospheric conditions to estimate the relative concentrations at the ignition time can be used to help understand the combustion process.

2.4 Economic and Environmental Impact

Sustainable energy, being the problem of the 21st century, has had increased focus in the research industry in the past few years. This is especially true for bio-derived fuels for use as an alternative fuel source in the transportation sector and for the production of heat. The use of bio-derived fuels can potentially provide economic and environmental benefits because they are sustainable and could reduce the use of conventional fossil fuels. This is the driving force promoting their production and use [45]. There is good reason for the increased attention toward finding and testing suitable renewable alternative fuel sources. In 2010 approximately 37% of the energy consumed in the United States came from petroleum, 25% natural gas, and 20.8% coal (i.e. fossil fuels) [46]. Biodiesel and ethanol fuels (biofuels) contributed less than 2% to the annual energy consumption in 2010 [46]. This includes energy used in the transportation, industrial, residential, commercial and electric power generation sectors. Sustainable energy systems including biofuels could be potential alternatives in each of these sectors. Biofuels in general would primarily have impacts on the transportation and industrial sectors serving as an alternative for petroleum based fuels (petro-fuels) sources such as gasoline, jet fuel and fuel oil [46].

Petroleum fuels are the most widely used energy source in the U.S. today [46]. In 2010 approximately 7 trillion barrels of petroleum were consumed (~ 19.15 million barrels per day) compared to about 314 million barrels of ethanol fuel. Over half of the petroleum consumed was imported, which means that any future issue concerning oil supply could have a significant impact on the energy use sectors especially that of transportation and in

turn have a negative impact on the economy [47]. Greenhouse gas (GHG) emissions are also of concern when discussing the use of petro-fuels. Petro-fuels contributed to 39.5% of carbon dioxide (CO_2) emissions in 2010 compared to 1.2% contributed by biofuels. Since there was more petro-fuel consumed this is expected but, when comparing the amounts of each used to their contribution to the total CO_2 emissions, on average this equates to petro-fuels contributing almost twice as much CO_2 emissions per barrel when burned. For these reasons the increased production and usage of renewable biofuels like ethanol and biodiesel provides a promising solution to help boost the economy and reduce negative environmental effects from energy usage.

Production and utilization of biofuels is mostly dependent on tax incentives and mandates [58]. If mandates become more binding and tax credits more attractive the demand for biofuels increases [49]. For example, the National Energy Act of 1078 gave ethanol blends of 10% by volume a 40-cent-per-gallon exemption from the Federal motor fuel tax. As a result production and consumption of ethanol increased. Congress passed the Clean Air Act Amendments of 1990 (CAAA 90), which mandated the use of oxygenated fuels to reduce carbon monoxide emissions in specific regions of the U.S. in the winter months. The 2005 Energy Policy Act and several of its provisions maintained air quality standards, resulting in a continued need for reformulated gasoline. Since the addition of ethanol in petroleum gasoline was the most common and effective way to increase oxygen content it became the oxygenate of choice for the reformulated gasoline program by 2006 [49]. The 2005 Energy Policy Act also created the Renewable Fuel Standard (RFS) which mandated 4.0 billion gallons of renewable fuel be blended into gasoline in 2006 and increased this number to 7.5 billion gallons by 2012 [49]. There is currently a new mandate in place referred to as RFS2. Specific RFS2 mandates were created for subcategories of biofuels which are defined by feedstock types and lifecycle GHG emissions [49]. One of these subcategories are called advanced biofuels which are defined as any renewable fuel other than those derived from corn starch, which can apply to a variety of fuels, including biodiesel, cellulosic, and other alcohols [49]. RFS2 requires specific volumes of biodiesel and cellulosic biofuels however the rest of the

specified volumes for advanced biofuel usage could be met by "others" that satisfy the feedstock and GHG-reduction requirements. Butanol blends with gasoline as well as with SBO would fall into the "other" category. According to RFS2 the mandate for these "other" advanced biofuels will increase significantly by the year 2022 [49]. This means that the production and demand for such fuel sources as butanol and pure SBO will likely increase. This makes butanol, which is a light alcohol similar to ethanol, very attractive for fuel blending applications. Currently ethanol is primarily produced using corn as feedstock (corn ethanol). Butanol can be made from a wider variety of nonfood feedstocks than ethanol such as cheese whey [50]. By utilizing other sources than corn it reduces competition with food sources as well as utilizes feedstocks which provide a shorter CO_2 lifecycle. Butanol has a higher energy content than ethanol and has the same range of volatility as gasoline [20]. Butanol is also infinitely miscible with gasoline and other fuel sources, non-corrosive and nock resistant [20]. Because of these properties butanol is considered by experts as a better fuel source than ethanol and has a significant potential for use in land transportation [20]. Increased commercial production of butanol through fermentation is targeted for the next two or three years, which will lower production costs [20]. The specific energy content of butanol is the closest to jet fuel of alcohols and is only surpassed by biodiesel and Fischer-Tropsch synthetic fuels. Its lower energy content makes its direct use as an aviation fuel unsuitable but mixing with energy dense BDOs like soybean oil could make this a possibility.

Research focusses on fuels which are cost effective, economically sound and environmentally friendly. Although biodiesel has been successfully used for decades the transesterification process required to produce it consumes energy (usually provided by fossil fuels) and is costly. Biodiesel is the second most common bio-mass derived fuel currently in use today [46]. The United States produced a monthly record, 109 million gallons, of biodiesel in December of 2011 [46]. Soybean oil was the number one feedstock for biodiesel during 2011, more than doubling all other feedstocks combined, with 4,153 million pounds consumed. Soybean oil is the most available feedstock in the U.S. with over 19 billion pounds produced yearly. Stores of soybean oil not being

utilized are in the 2 to 3 billion pound range yearly [1]. The utilization of soybean oil for feedstocks is environmentally helpful because it reduces the need for competition with food sources, diminishes storage space while using a fuel that has a short CO_2 lifecycle and very low levels of sulfur. However, the National Biodiesel Board reported that in 2010 only 11.6 % of the United States' annual production capacity (2.69 billion gallons in 2009) was produced. This was due to the profitability of producing biodiesel. Although the feedstocks (soybean oil) used in biodiesel account for the majority of the cost to produce it the transesterification process is energy intensive and costly. In a recent report by the USDA the economic returns from producing biodiesel from soybean oil were shown to be low in the last few years [49]. The price of biodiesel is only about $1 per gallon more, at the most, than the price of strait soybean oil between 2008 and 2011. The same report projects that the price of soybean oil will be lower than that of regular diesel fuel in the next five years and by 2020 it will be about 50 cents per gallon lower than diesel fuel. For these reasons along with the environmental benefits it merits the study of other ways SBO could potentially be used as an alternative renewable resource.

Possible uses for such a fuel blend as SBO/butanol include but are not limited to use for power generation in gas turbines, transportation (land and air), boilers for heat generation and more. As a result the importing and usage of conventional fossil fuels could be reduced. It is important to analyze specific SBO/butanol fuel mixtures for economical and sustainable effectiveness for various combustion applications. Although current soybean oil and butanol prices are quite significant an increased demand for their use would likely lower costs. Cost versus usage comparisons between fuel blends of SBO/butanol and widely used fossil fuels could provide incentive for increased production usage.

3.0 Experimental Methods

3.1 Property Testing Procedures

3.1.1 Blend Preparation

Blends of 25%, 50%, and 75% RBD soybean oil and pure 99% 1-butanol were produced on a volume basis at room temperature. CHS in Mankato Minnesota processed the food grade RBD soybean oil. Table 3.1 shows the chemical composition of the RBD soybean oil provided by CHS. The butanol was 99% extra pure 1-butanol purchased from Cole-Parmer. The butanol isomer has a molecular weight of 74.12 g/mol with a chemical formula of CH3(CH2)2CH2OH resulting in an elemental composition by weight of 64.9% Carbon, 21.6% oxygen and 13.5 % hydrogen.

Table 3.1

Chemical composition of RBD soybean oil

Fatty Acid	Mass Percent
C14:0	0.08
C16:0	10.16
C16:1	0.10
C17:0	0.13
C17:1	0.07
C18:0	4.83
C18:1	22.25
C18:2	53.00
C18:3	8.37
C20:0	0.37
C22:0	0.38
C24:0	0.13
Total Saturated (S)	16.78
Total Unsaturated (U)	83.22
U:S Ratio	5.66

3.1.2 Experimental Procedure

All property tests were performed in triplicate for accuracy. Values are reported as averages with calculated error bars. Tests were conducted at a barometric pressure of 0.974 atm and at the following temperatures when applicable: 20, 25, 30, 40, 50, 60, 80 and 100° Celsius. The temperature was controlled by a Cannon CT-1000 constant temperature bath which maintains temperatures to within 0.01°C. The temperature was also monitored using a Type K thermocouple with resolution 0.1° C. Special consideration was taken during measurements to minimize the evaporation of fuel blends.

Specific gravity measurements used to calculate fluid density were carried out in accordance with ASTM D1298 [51]. Glass hydrometers calibrated at 60°/60° F were used in the process. Viscosity measurements were determined following ASTM D445 [52]. Four Cannon-Fenske routine viscometers of sizes 25, 75, 150 and 200 were used to test viscosities over a range of pure butanol to pure SBO at the desired temperatures. The manufacturer supplied calibration constants and expanded uncertainties, for each viscometer. Higher heating values were determined using an IKA C 200 automated bomb calorimeter, following ASTM D240 [53]. Surface tension was measured with a calibrated Cole-Parmer EW-59780-90 surface tension apparatus employing the capillary rise method.

Cold filter plugging point was measured according to ASTM D6371 using a certified Cannon AFP-102 cold filter plugging point tester in conjunction with a coolant circulator [54]. Pour point and cloud point were measured according to ASTM D6749 and D2500 respectively using a Cannon MPC-1021certified mini-pour/cloud point tester [55], [56].

3.1.3 Property Analysis

This work develops equations or mixing rules which help to predict basic fuel properties for mixtures as a function of the relevant pure fuel properties, temperature and mixture content. The properties in each test are plotted against temperature and mixture

composition. These plots are then analyzed to develop a mixing rule for property prediction with an acceptable AAD.

3.2 Evaporation and Combustion

3.2.1 Test Facility

The evaporation and combustion studies in this work were performed in the same facility which was designed and built using concepts described in section 2.3.1. It was desired to perform evaporation and combustion studies at elevated temperatures and atmospheric pressures in normal gravity. Evaporation rates, droplet temperatures at ignition and combustion behavior of droplets of various initial diameters (0.61 – 1.00 mm) were of primary concern. Consequently the facility shown in Fig. 3.1 was chosen to be the most effective design to accomplish the goals of the research. The concept is a mixture of the Pan et al. microgravity facility and the Xu et al. drop furnace facility [36], [38]. The main component of the facility is a 10x10x10 inch (I.D.) custom built top hat furnace from Deltech. Inc. Three 6.35 cm (2.5") diameter circular sight ports are located on the front and two sides of the furnace for lighting and visualization. A 5.08 cm (2") diameter thru hole is located in the center of the bottom of the furnace which allows access for the igniter. The temperature of the heated chamber is controlled by a Eurotherm 3504 PID controller which is monitored by a Type K thermocouple. The PID controller was auto tuned for increased accuracy at temperature settings relevant to this work. An IDT NR4-S2 color, high speed camera equipped with two Nikon 2x teleconverters attached to a 105mm Sigma macro lens (set at f2.8) is attached to a tripod situated on the main table which keeps the camera in position about 7.62 cm (3") away and focusing through the right sight port. Frame rates for evaporation studies ranged from 100 – 250 fps the latter being used at higher temperatures while the exposure was set at 1000 μs to allow for more light to enter the lens. The room temperature evaporation studies were done at 30 fps and an exposure of 800 μs. The combustion studies were done at 200 fps and an exposure of 1000 μs. Provided that the focus of this paper did not include burning rates 200 fps was a reasonable frame rate to achieve droplet diameter measurements prior to,

during and after the initial burning stage (±5μs) as well as provide visual information on the flame color and combustion behavior. The lighting was provided by a 50 Watt Solarc^{TM} light box equipped with a liquid light guide attached to a 15° full aperture Visi-Spotlight mounted on a magic arm clamped to the main table. The Visi-Spotlight is positioned just below and in front of the camera lens. This provided sufficient light to bounce back off the white interior walls of the furnace and backlight the droplet so that video analysis could be done on the evaporation and combustion process. The other two sight ports were used for the experimentalist's observation only but could be used for back lighting or side lighting if necessary. The igniter used for combustion studies was a Mini-Igniter^{TM} model 301 micro igniter. The igniter was charged by a voltage of 120V at 12Amps (1440 W) and held in place for ~ 20 – 40 μs.

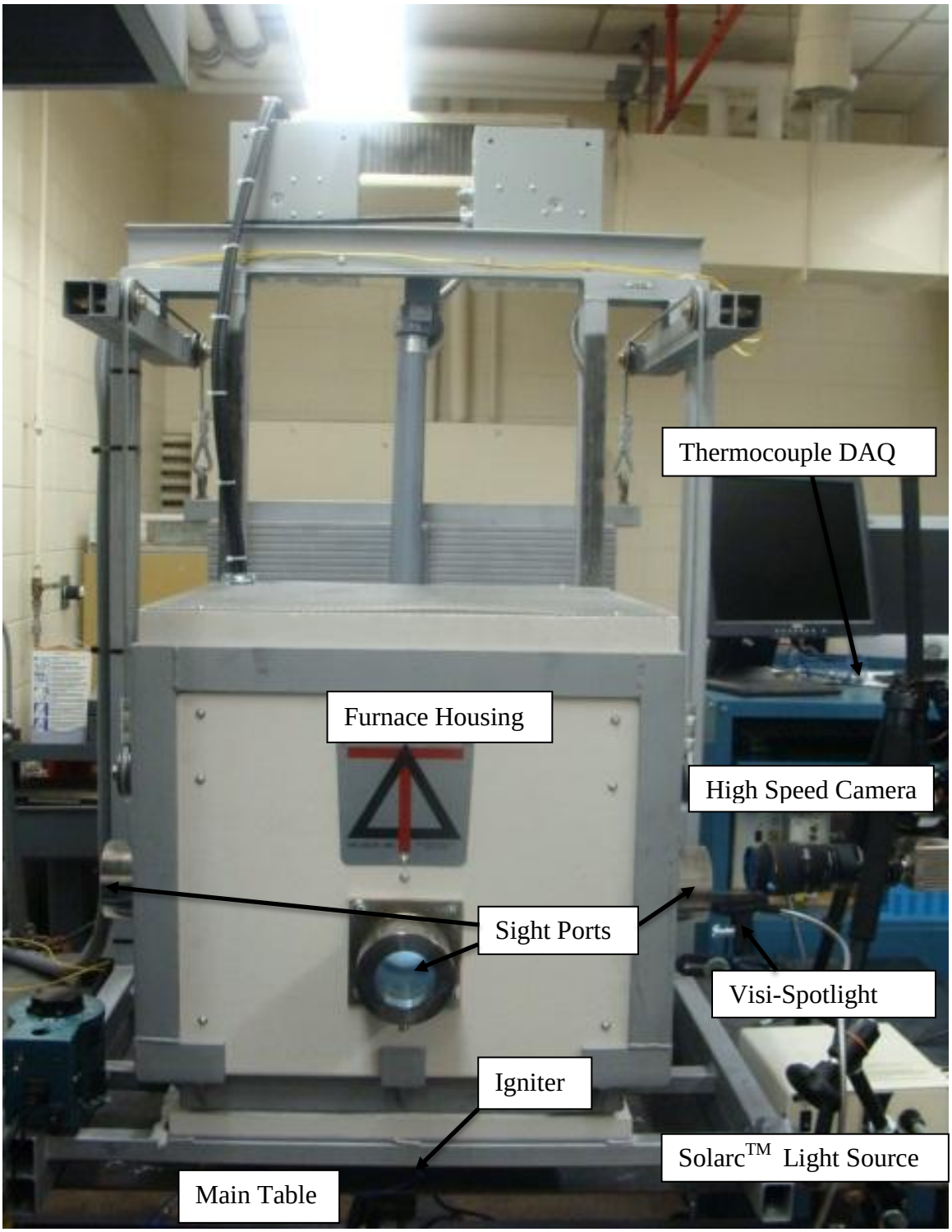

Fig. 3.1. Evaporation and combustion testing facility in test (lowered) position

The positioning of the furnace housing and the relative time count used in the experiments is shown in Fig. 3.2. As can be seen in the photos the time count starts as the bottom of the furnace passes the suspended droplet. The furnace was assumed to be constant temperature throughout and for that reason the droplet would enter the desired atmospheric conditions when the bottom reaches its horizontal plane. There is a short time period in which the droplet behavior cannot be visually captured during the process. The time between which the droplet disappears behind the furnace wall and when it reappears through the sight port is approximately one second.

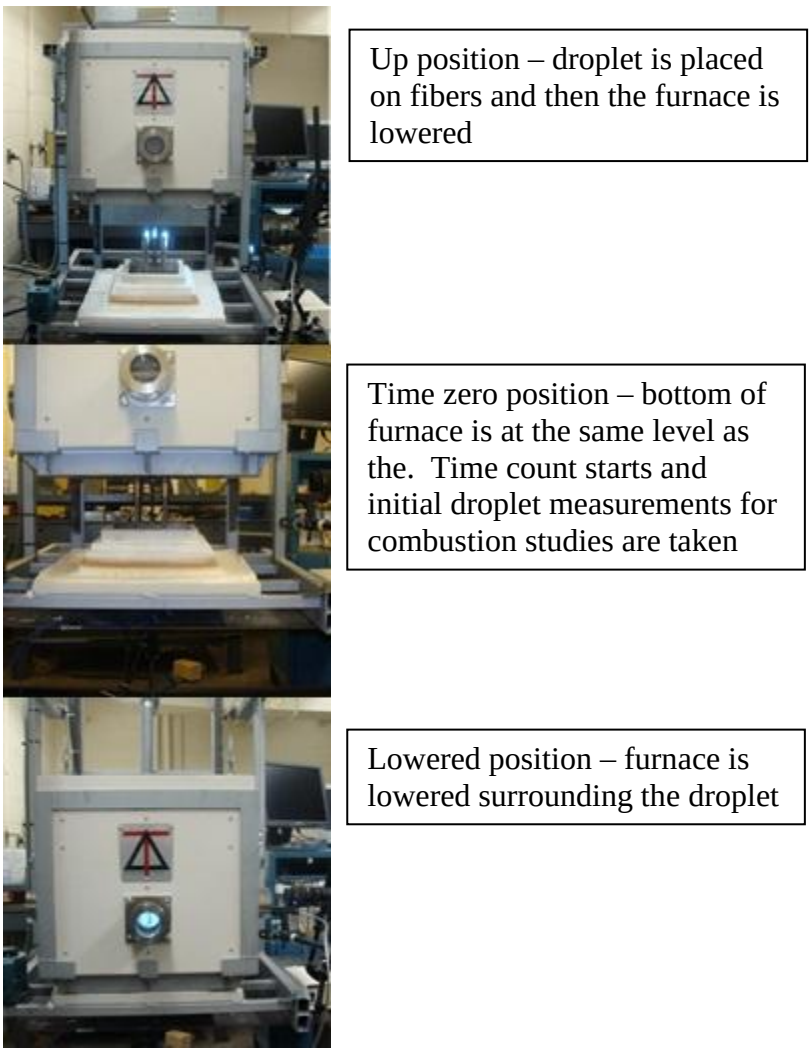

Fig. 3.2. Test facility time count

Fig. 3.3 shows an example of the video footage captured, for a droplet of Bu75 during the first, second, microexplosion and steady burning third stage of combustion. Video and strategically placed thermocouple data analysis is used to distinguish the three stages of combustion. The microexplosion phenomenon was also found to be more detailed with this configuration than any other research group reviewed. Using these methods a better understanding of the physical behavior can be analyzed.

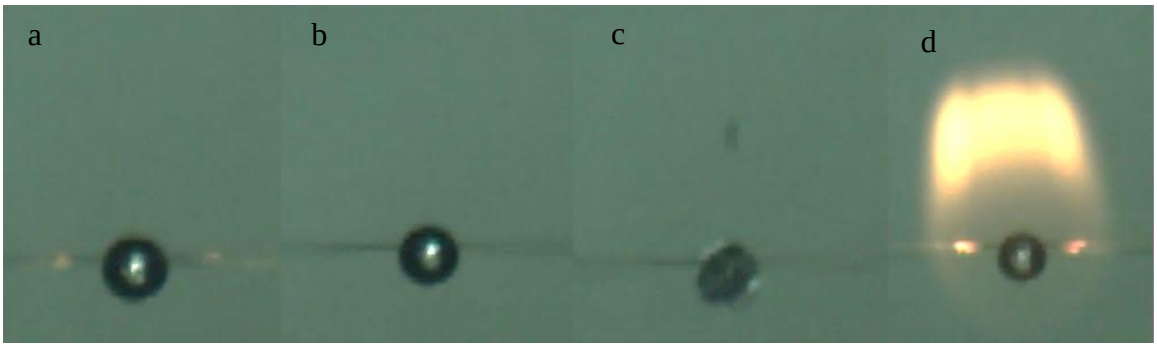

Fig. 3.3. Bu75 droplet video analysis at 200 fps f2.8 and 1000 µs shutter speed. a) First stage – butanol burning with nonluminous flame signified by glowing fibers; b) Second stage – flame shrinkage while heat is transferred inwards toward the droplet center signified by no glowing fibers and a temperature reduction in thermocouple data; c) Onset of third stage – microexplosion; d) Third stage – orange flame signifies soot formation and SBO is burning

The flame corresponding to the burning of butanol is thought to be blue. Capturing the blue flame was not possible using these techniques however the butanol flame may not be blue in actuality and may be nonluminous. Bae and Avedesian et al. did however capture a blue flame for JP8 fuel using their techniques which are described in [30].

The droplet supporting apparatus is shown in Fig. 3.4. Spherical fuel droplets, with minimal influence from the support device, which could be ignited using a hot wire source, were desired. Consequently the fuel droplets are suspended on the intersection of two ceramic microfibers with a nominal diameter of 11 µm which had a very low and almost negligible thermal conductivity (~0.14 W/m·K). The fibers are positioned such that they intersect perpendicular to each other at their center. The fibers are held in position by being pinched between high temperature silicon o-rings atop spring loaded brass collars and fixated steel collars surrounding the four steel posts. The steel collars

were fixated at a height which would position the droplet at the center of the furnace. The four 1.27 cm (0.5") steel posts were positioned 77.5 cm apart in a square configuration surrounding a center thru hole, on the 1.27 cm (0.5") steel base plate, which matches that of the one in the furnace bottom. A fifth post used to keep two Type K thermocouples in position for temperature measurements during experiments, was attached to the baseplate centered between two neighboring fiber holding posts. One of the thermocouples, with a bead diameter of ~0.45 mm, was positioned approximately 4.5 mm above the fiber intersection. The other thermocouple, with a bead diameter of 1.3 mm, positioned at the same vertical and horizontal position normal to the camera lens and approximately two diameters to the right of the fiber intersection relative to the camera. A picture of a droplet in position prior to being ignited in a combustion study is shown in Fig. 3.5. References to items and dimensions used for later analysis are shown in the figure.

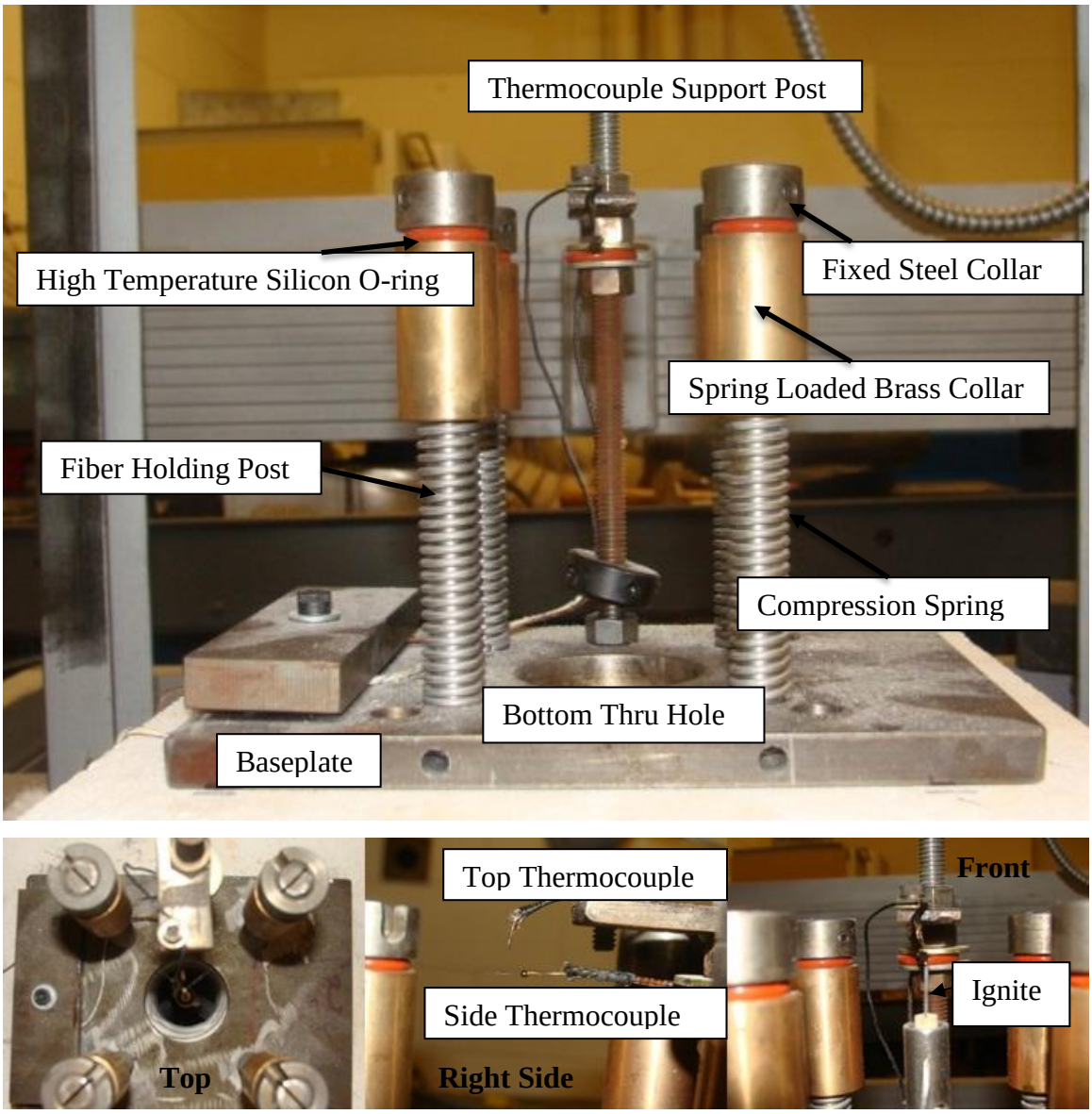

Fig 3.4. Droplet support apparatus

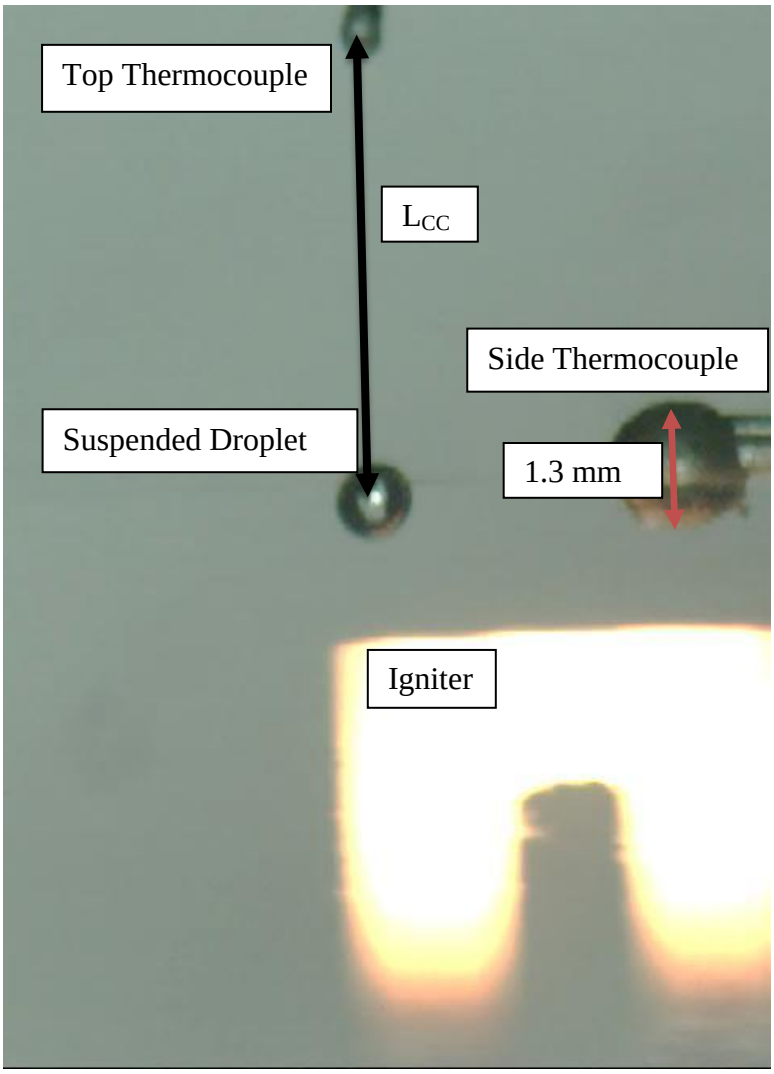

Fig. 3.5. Snapshot of droplet ignition during combustion study

3.2.2 Evaporation Methods

The convention for evaporation studies correlating droplet lifetime as a function of initial diameter and ambient temperature is a dimensionless diameter squared as a function of normalized time (referred to in literature as the d^2 – law). Consequently, this type of comparison was performed. The droplet diameter was measured as a function of time in ambient temperatures (T_∞) of 29, 100, 118, 165 and 225°C. The diameter was then squared and that value along with the time data were normalized by dividing by the initial

diameter squared. The data was used to produce plots of normalized $(D/D_0)^2$ vs. t/D_0^2 which were used for analysis.

Prior to the each test a temperature acquisition program written in LabVIEW was turned on to verify the temperature of the furnace throughout the test. A droplet was then placed on the intersection of the ceramic microfibers by a pipette. Consideration to make sure that the solutions were thoroughly mixed and that the pipette was clean before filling were taken. Once a droplet was suspended from the cross section of the fibers the high speed camera was triggered to start video recording and the furnace was lowered surrounding the droplet. The furnace was lowered by hand, taking approximately three seconds. The high speed camera recorded the lifetime of the droplet. The video data was then uploaded to the Xcitex ProAnalyst™ tracking software for analysis. Strategic image filtering and coloration adjustments were made to make the droplet appear as a white figure on a black background for tracking purposes. The 1-D tracking toolkit used a series of lines that sense intensity of color change in conjunction with a circle fit to measure the droplet diameter during vaporization. Figs. 3.6a and 3.6b shows a droplet in test position before the coloration and filtration changes were made and the same droplet being measured, using the methods described, respectively. The wire below the droplet in Fig. 3.6a is of known diameter and was used for calibration in the software.

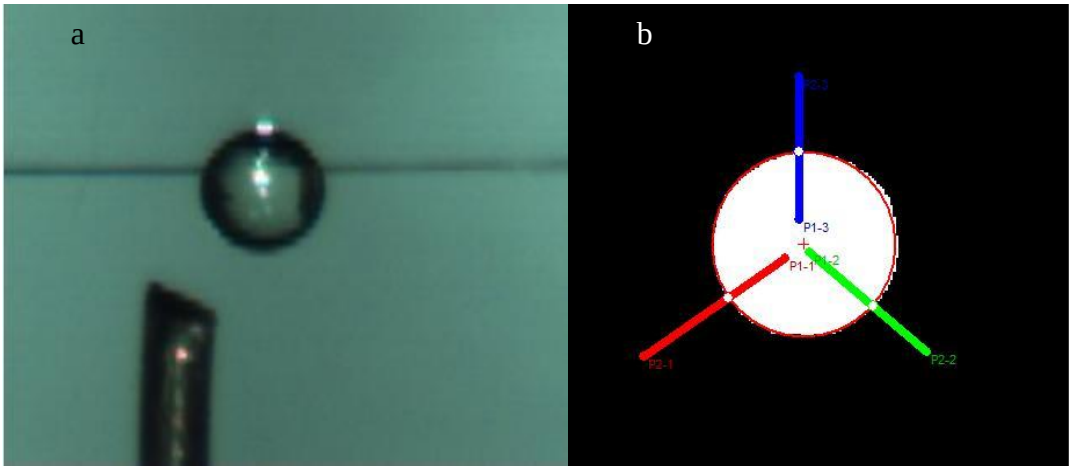

Fig. 3.6. a) Droplet in test position for evaporation study with calibration wire; b) Droplet being measured using Xcytex ProAnalyst™ software after image filtering and coloration adjustments were made

Because the tracking software needs similar lighting throughout a tracking process for accuracy the first focusable frame through the sight ports was considered time zero and the corresponding diameter was considered D_0 (The lighting when the furnace is up versus down is different making it impossible to keep the same filtering and coloration adjustments for both stages). At this point in the droplets lifetime it had been experiencing the elevated temperature for approximately 1 second which is the time it takes for the bottom of the furnace to cross the horizontal plane of the droplet and to reach the base of the furnace (Using Fig. 3.2 it is the time between the time zero stage and the lowered oven stage). The initial droplet swelling, described by Gogos et al., due to internal droplet heating is also neglected. The evaporation constants will be the same using this initial diameter however the final value for $(D/D_0)^2$ will be that of a droplet already in an environment for one second and will be larger than the theoretical value for $(D/D_0)^2_{final}$. The circle fit data for each frame and time was exported to Microsoft Excel, in order to plot $(D/D_0)^2$ vs. t/D_0^2 for each test.

Assumptions to be made for this procedure are:
-The furnace chamber is the same temperature (T_∞) throughout its interior
-The droplet mixtures are well mixed
-$D_0 \neq D_{0actual}$ but rather a diameter that has evaporated in an environment for 1 second
-No evaporation occurs in time frame between droplet placement and the introduction to the elevated temperature environment
-Droplet swelling due to elevated temperature is negligible

3.2.3 Combustion Methods

A basic combustion study was done on fuel droplets of pure butanol, soybean oil and mixtures of Bu75, Bu50, Bu40 and Bu25 in an effort to describe combustion behaviors of these droplets as a function of composition and temperature at ignition as well as to attempt to prove the feasibility of using the test facility for flashpoint testing. Pure SBO was burned using slightly different ignition techniques (i.e. holding the igniter in place longer) due to its high flashpoint. The testing facility was the same as used in the

evaporation studies incorporating droplet ignition. Evaporation rates and droplet size measurements can be used to estimate the droplet composition at the time of ignition. Video and thermocouple data results will be used to analyze the combustion behavior. Multiple tests were performed for each fuel mixture at an elevated temperature of 100°C. This temperature provides an environment which will bring the droplets to their in a suitable time period to ignite them before significant evaporation will occur. The two thermocouples positioned close to the droplet were used to estimate droplet temperature ($T_{ignition}$ via the side thermocouple) and to signify the onset of ignition and record the temperature rise above the droplet during combustion (T_1, T_2, and T_{final} via the top thermocouple). Video data captured via the high speed camera was analyzed using the ProAnalyst^{TM} software. The data rendered included initial diameter size (D_0), diameter at ignition ($D_{ignition)}$, diameter after the first stage (D_{fs}) and in some cases a final diameter (D_{final}) after an amount of time if a droplet happens to ignite but not burn completely. The video analysis also provided insight as to which of the fuels present in the mixture is actually burning during the combustion process. Pure butanol exhibits a nonluminous flame and pure SBO exhibits an orange flame when burned (signifying soot formation). The microexplosion and "three stage combustion" phenomena experienced with the burning of binary fuel mixtures were also analyzed using the video data.

Prior to each test a temperature acquisition program written in LabVIEW was turned on to begin acquiring temperature data from the two thermocouples. A temperature reading was recorded every ten milliseconds. A droplet was then placed on the intersection of the ceramic microfibers by a pipette. Consideration to make sure that the solutions were thoroughly mixed and that the pipette was clean before filling the pipette were taken. Once a droplet was placed on the cross section of the fibers the camera was triggered to start recording and the furnace was lowered around the droplet. When analyzing the data the first temperature rise signified time zero, or the time at which the bottom of the furnace housing reached the same horizontal plane as the fuel droplet and side thermocouple. The last frame in focus before the furnace blocked the camera from viewing was considered time zero and initial droplet diameter measurements were taken.

Since rapid data points representing droplet radius were not necessary for the combustion tests it was beneficial to manually measure the droplets using the ProAnalyst^{TM} software at the desired test times and was considered the most accurate for the D_0, $D_{ignition}$ and other droplet size measurements. At various times and thus various droplet temperatures the igniter was quickly (20 - 40 μs) brought close to the droplet at a distance of 1mm from the crosshairs (droplet diameter determines the distance from the droplet) and then retracted. A fixated collar on the igniter post kept the distance constant from test to test and desired timing could be achieved within ±0.25 seconds using this manual method. A solenoid triggered by a switch would give improved accuracy to ignition timing. The thermocouple above the droplet was used to signify ignition as well as to analyze temperatures during the three stage combustion process. The side thermocouple was used as a more accurate measurement of the actual temperature of the droplet at ignition since its time constant more resembled that of the droplet due to its larger bead diameter and horizontal position. The videos obtained provided the necessary geometrical data to make judgments on whether there was still butanol left in the droplet or not as well as the physical behavior of the droplets as they burned partially, completely, experienced a microexplosion or did not ignite at all. Flame color was also observed using video footage obtained allowing for insight as to what fuel was actually burning during the combustion process. This information will be used to clarify whether the gasification mechanism is diffusion dominant or not and to compare estimated ignition temperatures to flashpoint data collected previously from AURI. The controls in this experiment were the ignition times and temperatures while variables were the distance to the thermocouple beads and the initial droplet diameters which were normalized by using ratios of initial droplet diameters.

Assumptions to be made for this procedure are:

-The furnace chamber is the same temperature (T_∞) throughout its interior

-The droplet mixtures are well mixed

-$D_0 = D_{0actual}$

-No evaporation occurs in time frame between droplet placement and the bottom of the furnace reaching the same horizontal plane as the droplet
-Droplet swelling due to elevated temperature is negligible

4.0 Results and Discussion

4.1 Basic Fuel Properties

4.1.1 Properties of Pure Fuels

Properties of the pure fuels, at 25 °C are shown in Table 4.1. A number of the properties shown highlight the potential advantage of mixing butanol with SBO for use in combustion applications. Of particular interest is the viscosity and flash point temperature. Butanol has a significantly lower viscosity which when mixed with SBO will improve atomization thus lending to improved combustion characteristics. The substantially lower flash point temperature should promote ignition at about 40°C thus eliminating the need for preheating. Addition of butanol to SBO should also improve cold flow properties thus improving utilization of SBO in cold climates. The overall energy content of the mixture will not be adversely affected as butanol has a similar albeit slightly lower higher heating value. All property values listed in Table 4.1 have been measured in this work with the exception of the flash points, which were sent to the Agriculture Utilization Research Institute (AURI) to be measured via ASTM D93 closed cup standardized method.

Table 4.1

Basic properties of pure fuels at 25°C

Fuel Property at 25° C	1-Butanol	RBD soybean oil
Specific Gravity (ρ_m/ρ_{H2O})	0.806	0.919
Kinematic Viscosity (cSt)	3.04	53.46
High Heating Value (J/g)	33,939	36,952
Surface Tension (dyne/cm)	24.9	32.2
Flash Point (°C)	41*	217*
Plugging Point (°C)	< -56.2	-2
Cloud Point (°C)	< -50	-6.66
Pour Point (°C)	< -50	-10.33

* AURI – ASTM D93 (Pensky – Martins closed cup method)

4.1.2 Relative Density (Specific Gravity)

The effect of fluid composition and temperature on the relative density of the mixtures was analyzed. Fig. 4.1 shows a plot of specific gravity versus temperature for RBD soybean oil-butanol mixtures as well as the pure components. The average overall uncertainty for all the experimental measurements was ±0.003. As expected the plot shows a linear relationship with similar slopes for the pure fuels and blends.

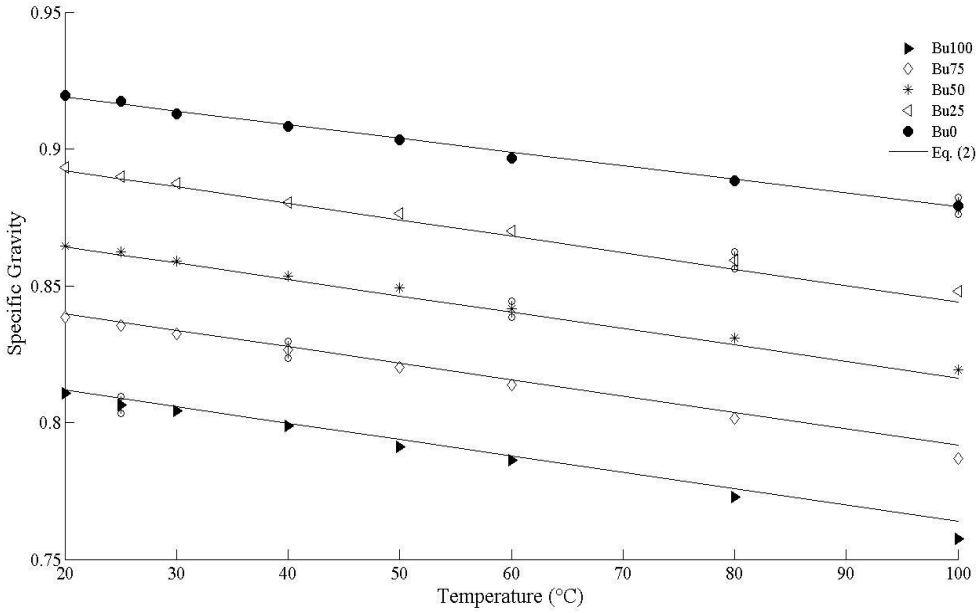

Fig. 4.1. Variation of blend specific gravity with temperature

Using linear regression the experimental data was fit to a line with high R^2 values, as can be seen in Table 4.2. It can also be concluded that density is directly proportional to the RBD soy oil content.

Table 4.2

Linear regression parameters for fuel densities relative to Eq. (2)

Fuel Blend	a	b	R^2
Bu0	-0.0005	0.9289	0.9943
Bu25	-0.0006	0.9041	0.9981
Bu50	-0.0006	0.8763	0.9985
Bu75	-0.0006	0.8517	0.9987
Bu100	-0.0006	0.8238	0.9968

Fig. 4.2 shows the effect of RBD soybean oil content on relative density at four different temperatures: 20, 40, 80 and 100°C.

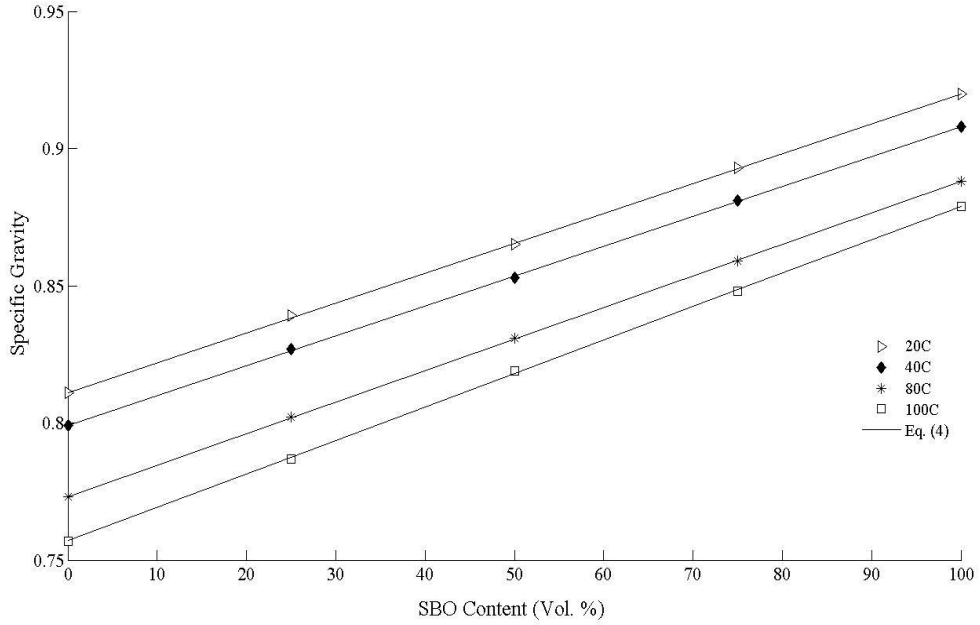

Fig. 4.2. Variation of specific gravity with blend composition

The AADs obtained using Kay's mixing rule for estimating relative densities of SBO-butanol mixtures as a function of composition are shown in Table 4.3. The estimated values fall within the ±0.003 error region and the AADs obtained were lower than those obtained by Benjumea et al. using palm oil biodiesel-diesel blends at similar temperatures [3].

Table 4.3

AAD values for density-composition relationship using Eq. (4)

Temperature (°C)	AAD (%)
20	0.012
40	0.012
80	0.012
100	0.001

4.1.3 Kinematic Viscosity

The temperature-kinematic viscosity relationship for all samples was analyzed and plotted in Fig. 4.3 with error bars representing the average measurement uncertainty associated with each test sample. The data shown in Fig. 4.3 followed an exponential relationship as expected. As the plot suggests the temperature-kinematic viscosity relationship becomes more linear with increasing butanol composition. As can be seen by comparing the Bu0 and Bu25 data, a small amount of butanol added to the mixture substantially shifts the viscosity towards that of pure butanol suggesting that the viscosity of the blends is closer to the viscosity of butanol than SBO.

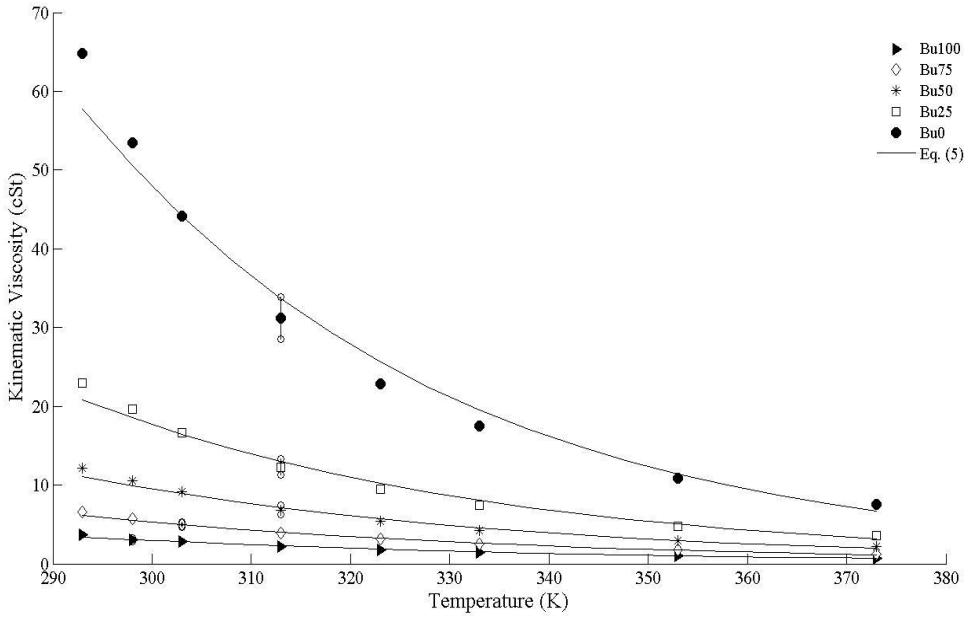

Fig. 4.3. Variation of blend kinematic viscosity with temperature

a, *b* and *c* for Eq. (5) was calculated for each mixture using the experimental data and the results are presented in Table 4.4. The lines representing the approximations using the Andrade equation are shown on the plot in Fig. 4.3. The high R^2 values and low AADs suggest that the kinematic viscosity of a certain blend can be predicted using Eq. (5) with an accuracy equal to or better than that of other research groups working with biodiesel-diesel blends [7], [27].

Table 4.4

Regression parameters of viscosity-temperature relationship for Eq. (5)

Fuel Blend	a	b	c	R^2	AAD (%)
Bu0	-14.1254	8372.735	-892287	0.9947	1.248
Bu25	-12.8644	7322.381	-780340	0.9946	0.154
Bu50	-12.3548	6797.054	-724366	0.9861	0.688
Bu75	-12.3465	6518.993	-694733	0.9846	0.802
Bu100	-12.1274	6148.244	-655222	0.9839	0.201

Composition-kinematic viscosity relationship trends are beneficial to estimate for mixtures based only on that of the pure components at certain temperatures, thus reducing the reliance on experimental data of mixtures. The Andrade equation can be used if viscosities of mixtures are known at three different temperatures, thus requiring some experimental data. A plot of experimental data for the kinematic viscosity versus fluid composition has been prepared at temperatures of 20, 40, 80 and 100°C and presented in Fig. 4.4 along with the Grunberg-Nissan approximation curves. Comparing the Grunberg-Nissan equation to the experimental data in this work the AAD values obtained were 4.54%, 5.10%, 4.38% and 4.72% corresponding to 20, 40, 80 and 100°C, respectfully. Isdale's method for predicting the interaction parameter was used utilizing the known chemical formula for 1-butanol and the more complicated chemical structure of RBD soybean oil from the fatty acid composition shown in Table 3.1.

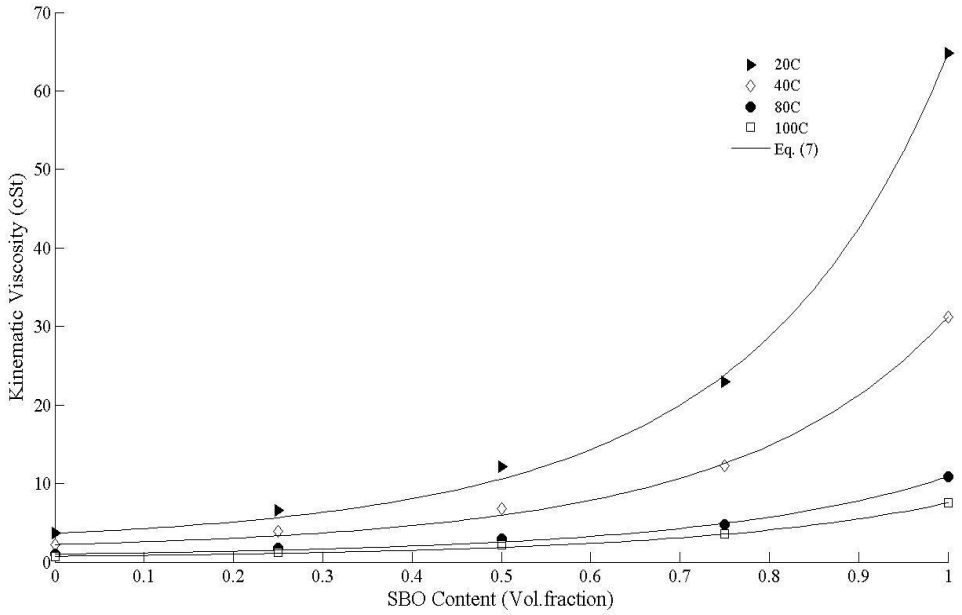

Fig. 4.4. Variation of kinematic viscosity with blend composition

The kinematic viscosity estimations using the Grunberg-Nissan equation and Isdale's method for estimating the interaction parameter prove to be nearly as accurate as Tat and Van Gerpen suggest they should be [21]. AAD values obtained using Eq. (7) and neglecting the interaction parameter $G_{SBO,Bu}$ proved to be substantially higher which emphasizes that it should not be neglected for SBO/butanol mixtures.

Other methods were explored to predict the kinematic viscosities of fuel mixtures. Enweremadu et al. suggests a second degree polynomial equation as a more accurate approach, however this yielded higher AAD values. Also, Poling et al. refers to the Method of Teja and Rice as an analogous form for liquid mixture viscosity which includes a reference to the two pure fluids, an acentric factor and parameter similar to G_{ij} in the Grunberg-Nissan equation. They state that either the Grunberg-Nissan equation or the Teja-Rice relation may be used for binary mixtures and that the Teja-Rice relation is more accurate for polar-polar mixtures and aqueous solution [21]. Since the binary mixtures discussed here are not aqueous and the mixture isn't strictly polar-polar the Grunberg-Nissan equation was chosen over the Teja-Rice relation.

4.1.4 Higher Heating Value

Higher heating values (HHVs) obtained from the calibrated bomb calorimeter were found to increase linearly with increasing SBO content. Fig. 4.5 shows the plot obtained from experimental data along with Kay's mixing rule. The average overall uncertainty, due mostly to precision error, was ±230 J/g and the AAD value obtained using Kay's mixing rule to estimate the HHV was 0.028%.

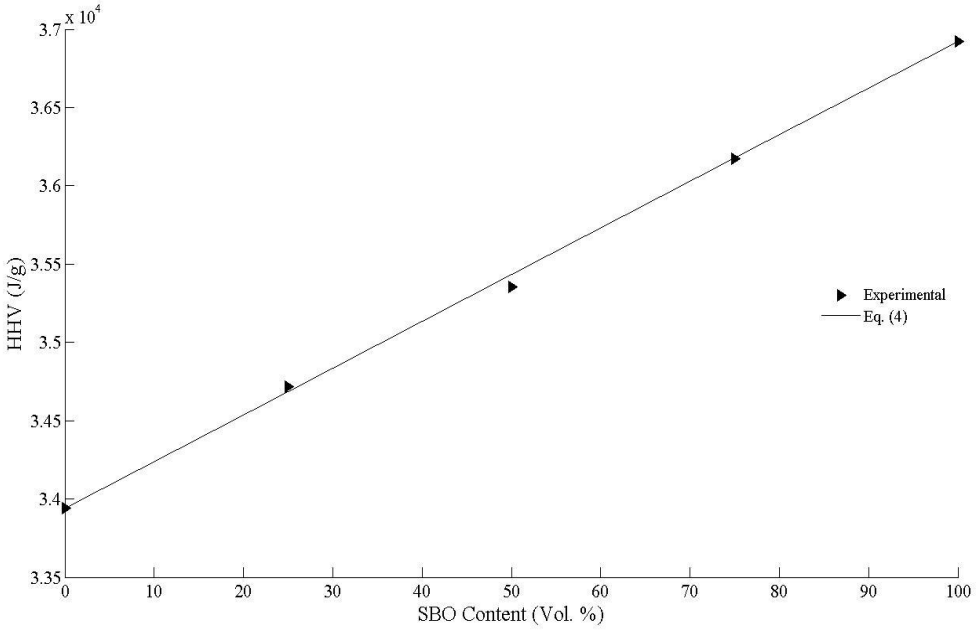

Fig. 4.5. Variation of higher heating value with blend composition

4.1.5 Surface Tension

The surface tension of all blends and pure components were measured and the average values were plotted against temperature. The resulting plot is shown in Fig. 4.6.

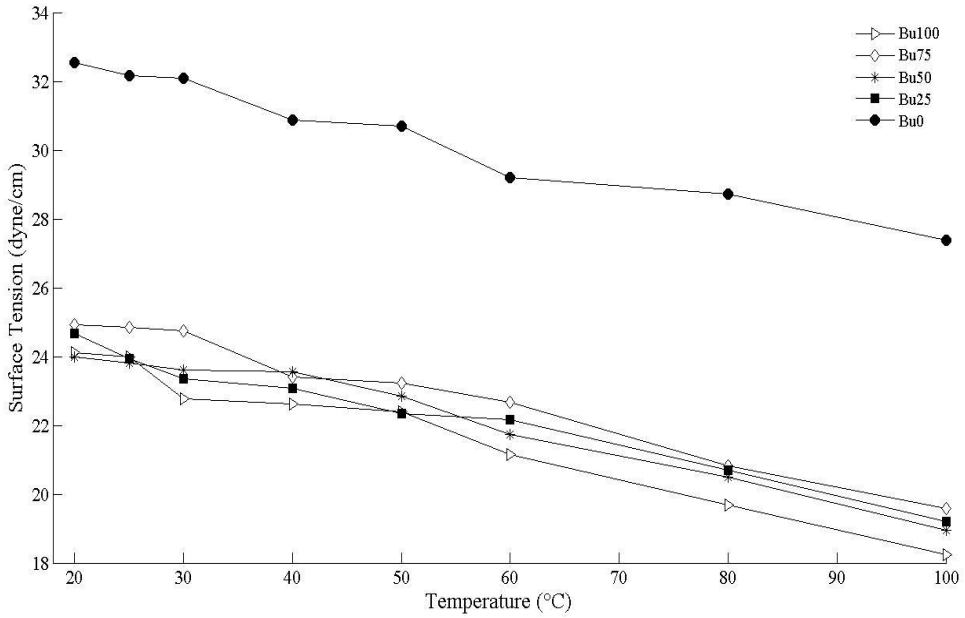

Fig. 4.6. Variation of blend surface tension with temperature

As can be seen in Fig. 4.6, the surface tension values of all blends vary monotonically with temperature. The surface tension decreases as temperature increases with similar slope for all test samples. Adding a small amount of butanol markedly changes the surface tension from pure SBO. Fig. 4.6 indicates that for all the mixtures tested the surface tension is nearly that of pure butanol. This is likely due the high molecular weight of SBO and the fact that the pure component with the lowest surface tension in a mixture (butanol) tends to concentrate on the surface causing its surface composition to be higher than that of the bulk mixture. Because SBO has a molecular weight nearly four times that of butanol the molar composition of SBO in a SBO/butanol mixture is much less than that of the composition by volume. Unlike viscosity and density, surface tension calculations are only done on a molar concentration basis thus reducing the SBOs contribution to any mixture. Poling et al. suggests that for most organic liquids the

surface tension-temperature relation can be represented by a linear equation like Eq. (2) [21]. Linear regression analysis was done for these blends and the results are shown in Table 4.5.

Table 4.5

Linear regression parameters of surface tension-temperature relationship for Eq. (2)

Fuel Blend	a	b	R^2
Bu0	-0.0653	33.764	0.9714
Bu25	-0.0626	25.597	0.9820
Bu50	-0.0642	25.626	0.9704
Bu75	-0.0693	26.538	0.9852
Bu100	-0.0724	25.534	0.9778

The surface tension of a mixture is not a simple function of the pure components because in a typical situation, the bulk composition is known but the surface composition is not. Estimations from Eqs. (10), (11), (12) and (14) were compared with experimental data from the mixtures at 20, 40, 80 and 100°C. The resulting AAD values are shown in Table 4.6 while a plot of the surface tension-composition experimental data is shown along with the most accurate mixing rule predictions (Eq. (14)) in Fig. 4.7.

Table 4.6

AAD Values for each surface tension prediction equation. The parachors [P_i] used for Equation 10 were obtained by a group contribution table and were 714.3 for SBO and 205.3 for butanol

Temperature	$AAD_{EQ.\ 10}$ (%)	$AAD_{EQ.\ 11}$ (%)	$AAD_{EQ.\ 12}$ (%)	$AAD_{EQ.\ 14}$ (%)
20 °C	9.14	8.98	3.49	1.64
40 °C	8.85	8.24	2.76	1.12
80 °C	9.54	9.59	2.66	0.94
100 °C	10.27	10.14	2.73	1.09

Table 4.6 shows that Eq. (14), derived from thermodynamics, is the most suitable method to predict surface tension values of SBO/butanol mixtures. AAD values at all temperature ranges were lower than that of any empirical approach. With the exception of the Bu25 mixture Eq. (14) was a very accurate prediction of surface tension values with AADs at all temperatures of 3.99%, 1.47% and 8.56% corresponding to the Bu75, Bu50 and Bu25 mixtures respectfully (AAD = 0 for pure components). The increasing AADs with increasing SBO composition suggest that butanol has a greater effect on surface tension than the SBO does which is visible in Fig. 4.6.

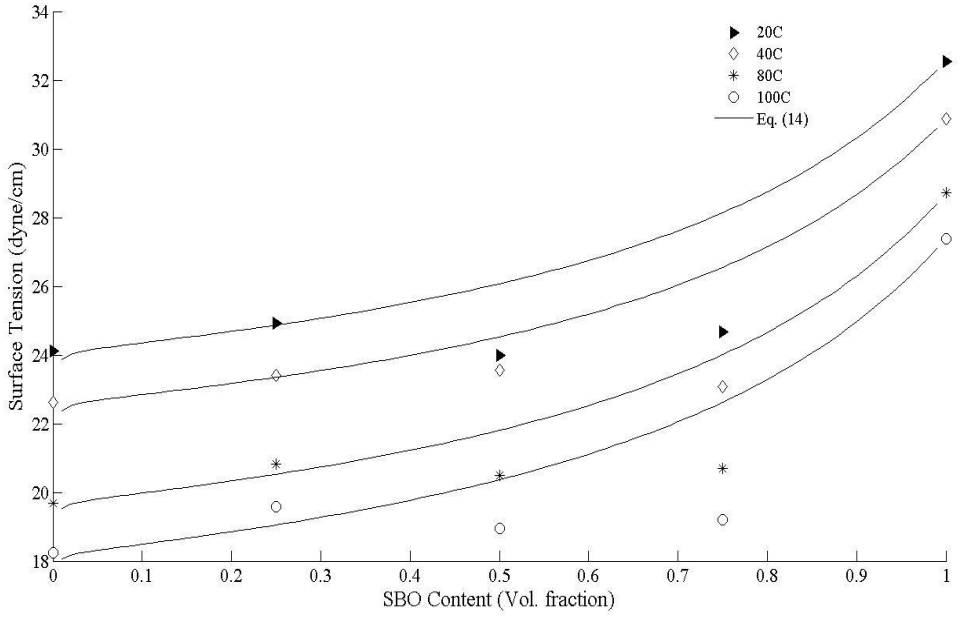

Fig. 4.7. Variation of surface tension with blend composition

4.1.6 Cold Flow Properties

Cloud point (CP), pour point (PP) and cold filter plugging point (CFPP) measurements of all test samples were determined in the lab with the exception of the CFPP of neat SBO which was obtained from literature [11]. The experimental results are presented in Table 4.7. As seen in Table 4.7, butanol reduces the CP of pure SBO by just over 2°C for Bu25. Increasing butanol content above 25% has nearly no additional impact. Dunn showed a similar trend with increasing butanol content in co-solvent blends of

SBO/methanol and SBO/No. 2 diesel/E95 mixtures [11]. Butanol content had a greater impact on PP. The mixture PP is reduced by 12°C from that of pure SBO for Bu50, and lowered by over 20°C for Bu75. Similar to the CP a small addition of butanol to SBO has an initial impact of lowering the CFPP by 20°C for Bu25. Additional increases in butanol composition however have a nearly negligible impact.

Table 4.7

Cold flow properties of blends and pure components

Fuel Blend	PP (°C)	CP (°C)	CFPP (°C)
Bu0	-10.33 ±1.53	-6.66 ±1.52	11*
Bu25	-12.33 ±1.54	-9 ±0.53	-10.33 ±1.53
Bu50	-22.5 ±1.41	-9.33 ±1.53	-12 ±1.54
Bu75	-33.33 ±1.66	-9.66 ±1.53	-12.66 ±1.54
Bu100	< -50	< -50	< -56

* Dunn 2002

4.2 Basic Fuel Evaporation

Fuel droplet lifetime for all mixtures and pure components were measured as a function of ambient temperature and initial droplet size using the methods described in section 3.2. A list of experiments performed including the initial composition, initial droplet diameter, ambient temperature, evaporation constant and corresponding R^2 values are presented in Table 4.8. The evaporation constant (K) is found by plotting a normalized diameter squared (d^2 – law) as a function of time and has units of mm^2/s. It is normalized by dividing both axes by the initial diameter squared as shown in Eq. (25).

$$K = -\frac{d}{dt}(D^2) = -\frac{d(D^2/D_0^2)}{d(t/D_0^2)} \quad (25)$$

Table 4.8

Summary of evaporation experiments performed

Fuel Blend	D_0 (mm)	T_∞ (°C)	K (mm^2/s)	R^2
Bu100	0.668	29	0.0028	0.9960
Bu100	0.683	100	0.0237	0.9914
Bu100	0.836	118	0.0413	0.9908
Bu100	0.674	165	0.0662	0.9913
Bu100	0.820	225	0.0928	0.9944
Bu75	0.804	29	0.0026	0.9922
Bu75	0.885	100	0.0281	0.9920
Bu75	0.805	118	0.0449	0.9920
Bu75	0.858	165	0.0616	0.9938
Bu75	0.952	225	0.0926	0.9931
Bu50	0.992	29	0.0029	0.9875
Bu50	0.971	100	0.0301	0.9766
Bu50	0.749	118	0.0404	0.9706
Bu50	0.918	165	0.0596	0.9780
Bu50	0.826	225	0.0925	0.9266
Bu0	1.075	285	0.0003	0.2312
Bu0	1.090	325	0.0015	0.6390
Bu0	0.945	350	0.0025	0.9635

4.2.1 Evaporation Rates as a Function of Composition

Poling et al. [21] suggests that in a binary mixture the pure component with the lower surface tension tends to concentrate at the surface of a mixture and a number of research groups [32-35], [42] suggest that in droplet combustion studies the more volatile pure component tends to diffuse towards the surface of the droplet. Consequently, in an effort to clarify these claims, it was desired to test if the evaporation rates were similar to that of pure butanol, which if found to be true, would suggest that there is constantly a layer of

pure liquid butanol at the droplet surface during vaporization at low temperatures. It could also clarify Matalon's suggestion that the mass diffusion outwards is faster than the rate of surface regression. At temperatures below which pure SBO will evaporate it is expected then that after sufficient time depending on the initial concentration and ambient temperature there will be a final liquid droplet consisting of pure SBO having a volume a fraction of the initial size equal to its contribution to the original mixture. Pure butanol was found to evaporate at room temperature while 100% SBO exhibited no significant evaporation at temperatures below 285°C. For example, according to this principle a droplet of Bu50 tested in an environment at 29°C < T_∞ < 285°C the droplet will evaporate until it has reached a volume 50% of the initial volume. Eq. (22) shows this

$$Vol_{final} = 0.5 * Vol_0 \tag{22}$$

Since evaporation rate results are presented using the d^2 – law concept it is convenient to transform Eq. (22) into diameters instead of volumes resulting in:

$$\frac{4}{3}\pi\left(\frac{D_{final}}{2}\right)^3 = (0.5) * \frac{4}{3}\pi\left(\frac{D_0}{2}\right)^3 \tag{23}$$

$$D_{final} = \sqrt[3]{0.5} * D_0 \tag{24}$$

Eq. (23) simplifies Eq. (24) and solves for what the final diameter should be as a function of the initial diameter. This equation can be used for any mixture by changing the fraction in the radical. For example, for a 25/75 – SBO/butanol mixture the number under the cubed root would be changed from 0.5 to 0.25. This was done, reorganized and then squared to present results in the commonly used form $(D/D_0)^2$. Table 4.9 shows final $(D/D_0)^2$ values for their corresponding mixtures. The experimental results allow for the analysis of geometrical properties and theoretical composition of the droplet at any instant of time assuming the only component experiencing vaporization is pure butanol. Fuel droplets of pure butanol, Bu75 and Bu50 with initial diameters ranging from 0.668-0.992 mm were tested at temperatures at or below 225° C. Droplets of pure SBO were

not observed to evaporate at temperatures below 285°C so ambient temperatures of 285, 325 and 350° C were used to test evaporation rates for pure SBO.

Table 4.9

Theoretical $(D/D_0)^2_{final}$ values for each mixture

Fuel Blend	$(D/D_0)^2_{final}$
Bu75	0.397
Bu50	0.630
Bu25	0.826

Table 4.8 shows that the evaporation constant of both mixtures resemble that of pure butanol for each ambient temperature. This can be observed visually in Fig. 4.8 which is a plot of the normalized diameter as a function of time for an ambient temperature of 29°C. Plots similar to plot shown in Fig. 4.8 have been produced for all test temperatures. They are shown in Fig. 4.9a, b, c and d. These plots can be used to show that, as expected, the mixed droplets have similar evaporation constants as that of pure butanol. If this is true there must always be butanol present on the surface of the droplet for this temperature range meaning that the butanol within the droplet is diffusing toward the droplet surface faster than the droplet is shrinking. This clarifies Matalon's suggestion that the mass diffusion rate outwards for the butanol would be faster than the rate of surface regression [29].

From the plots in Figs. 4.8 and 4.9 it is noticeable that the two mixtures exhibit normalized evaporation rates similar to that of pure butanol until a value of $(D/D_0)^2_{final}$ is reached that corresponds to the value listed in Table 4.9 and then stops evaporating. Since there is a lower initial concentration of butanol in a Bu50 blend the droplet will reach its $(D/D_0)^2_{final}$ value faster than that of a Bu75 droplet which can be observed from the plots in Figs. 4.9a, b, c and d. As explained in the methods section (section 3.2.2) the initial droplet diameter was recorded at the first frame of the furnace being in the lowered position resulting in the droplets being subject to the test conditions for 1 second before the measurement was taken. The time frames on the plots in Fig. 4.9 (x-axes) show the

criticalness of capturing the initial diameter before the 1 second delay between the furnace at the time zero position and the testing position especially at the higher temperatures. The fact that D_0 for the evaporation studies was measured after this one second time lapse explains the tendency for the droplets to not actually reach the $(D/D_0)^2_{final}$ theoretical value shown in Table 4.9. For example, in the 165° C case, if one were to use the initial diameter of the two droplets and its evaporation constant (Table 4.8 @ 165°C) to calculate how much of the droplet would have evaporated in that one second time period the result would be a reduction in diameter of 0.07 mm for the Bu50 droplet and 0.08 mm for the Bu75 droplet which would decrease the $(D/D_0)^2_{final}$ value to approximately 0.63 and 0.37 respectively. These are consistent with the theoretical value for that mixture shown in Table 4.9 with an accuracy of $(D/D_0)^2_{final} \pm 0.02$. It can also be noted that as the ambient temperature is reduced the $(D/D_0)^2_{final}$ value approaches the theoretical values shown in Table 4.9. This is to be expected because the evaporation constant is smaller at lower temperatures. None the less, at temperatures ranging from 29-225°C it is obvious from Table 4.8 and the plots provided in Figs. 4.8 and 4.9 that the droplets experience a vaporization rate similar to pure butanol and stop vaporizing at some point in time dependent on the initial droplet size and concentration. The size of the droplet remaining compares with good accuracy ($(D/D_0)^2_{final} \pm 0.02$) to the values listed in Table 4.9 suggesting that the liquid droplet remaining is purely the less volatile component, SBO. Expansion due to internal heating, which has been referred to as swelling in literature [31], [39], leading to inaccurate initial droplet size measurements as well as the possibility of error in volumetric mixing is likely to cause the small amount of difference between the predicted final droplet size and the experimentally measured final droplet size.

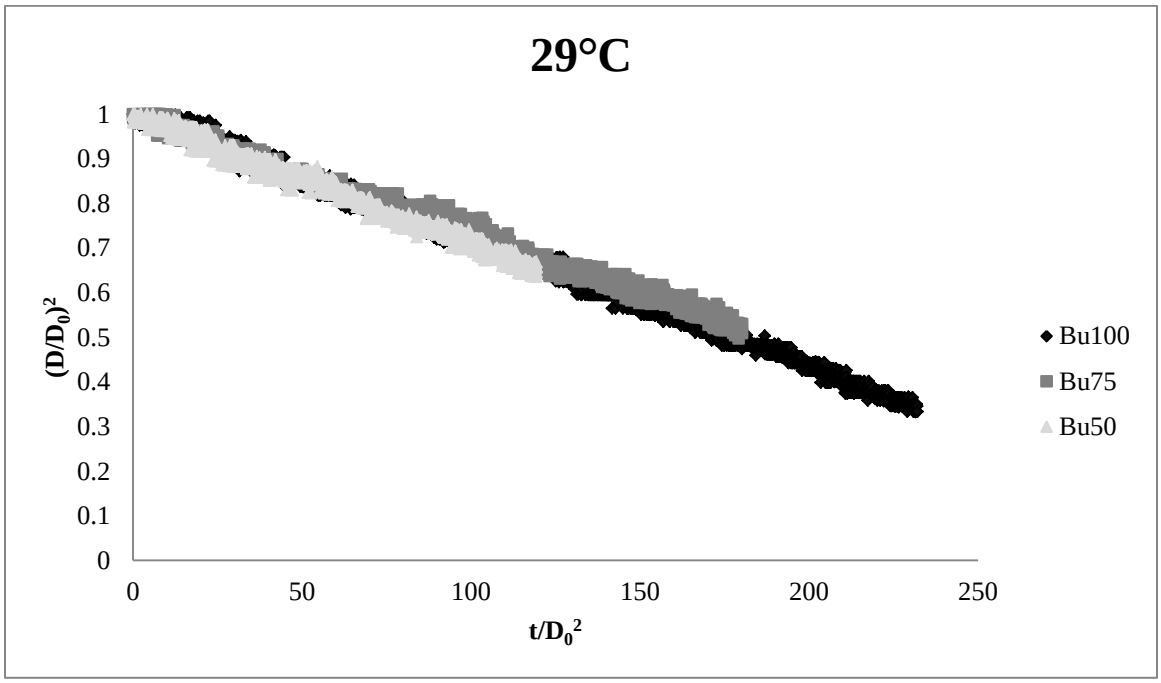

Fig. 4.8. Evaporation rates of all mixtures studied at room temperature (29°C)

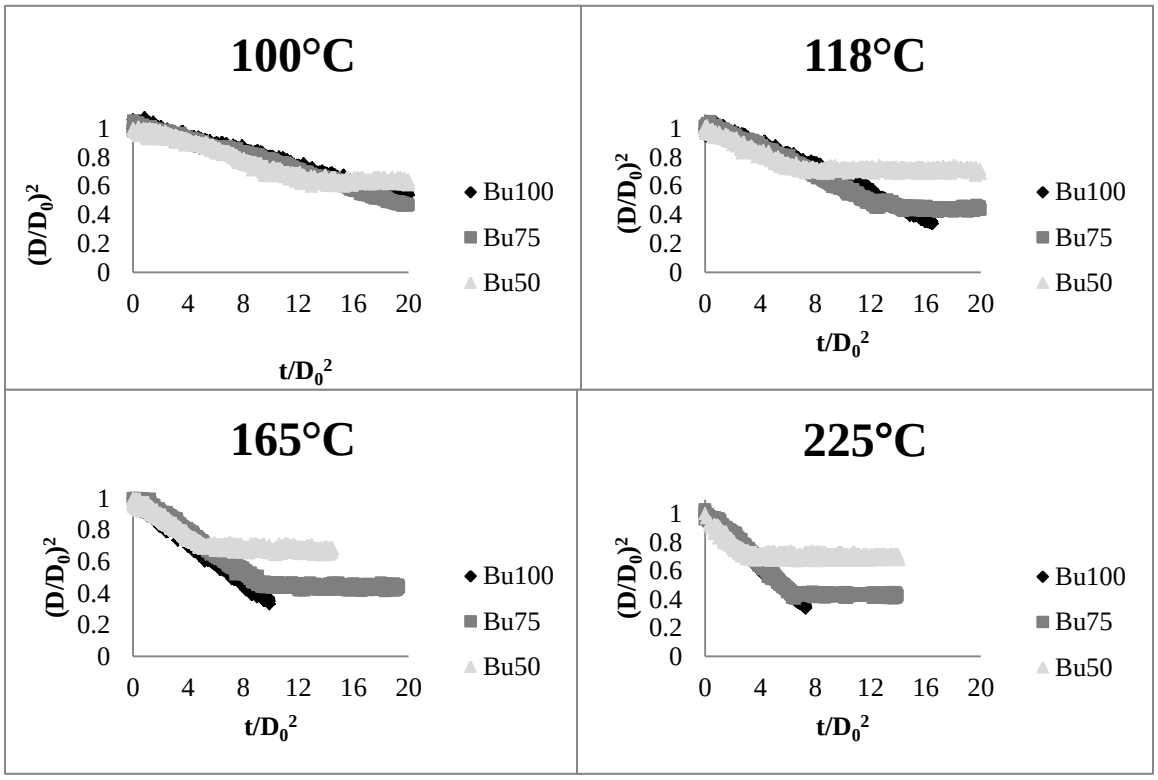

Fig. 4.9. Evaporation rates of all mixtures studied at 100°C, 118°C, 165°C and 225°C. The testing temperatures are shown as the plot titles

This confirms the suggestion that the component with the lowest surface tension and higher volatility (butanol) tends to diffuse toward the surface resulting in a higher concentration of butanol at the droplet surface during vaporization without combustion. This may explain the phenomenon that mixtures of such nature would experience flashpoints similar to pure butanol. Fig 4.10 has been prepared to show visually the diffusion process during the vaporization of a Bu75 droplet in low temperatures ($\leq$ 225°C). The butanol species is represented by the black areas and the SBO by red. As can be seen in Fig. 4.10 at the instant the droplet is formed the droplet is completely uniform, even at the surface and its composition is that of its initial mixture (4.10a). The butanol at the droplet surface begins to vaporize immediately and thus surface regression occurs. Instantaneously after droplet placement the droplet has formed a liquid layer of pure butanol at the surface due to the mass diffusion rate of butanol outwards (4.10b). The butanol at the surface continues to vaporize and the droplet shrinks at similar rates to that of a pure butanol droplet of the same size. The droplet continues to vaporize and

shrink while the mass diffusion of butanol to the surface is occurring (Fig 4.10c). The thickness of the liquid butanol at the droplet surface will depend on the surface regression rate and the mass diffusivity of butanol in SBO. This continues until the butanol in the mixture has been completely vaporized leaving a droplet of pure SBO with a droplet diameter corresponding to its initial concentration (Fig 4.10b). Using Table 4.9, a Bu75 droplet would have a final diameter of 63% its original size. This is shown to scale in Fig. 4.10.

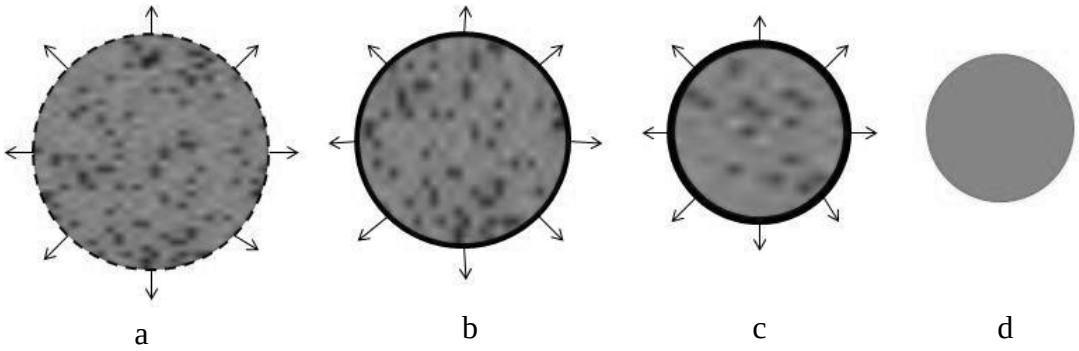

Fig. 4.10. Modeled Bu75 droplet during evaporation at low temperatures (≤ 225° C). Butanol is represented by black and SBO by grey a) Initial droplet at formation on the fibers. Droplet is uniform even at the surface; b) Droplet at the onset of evaporation. Butanol is beginning to concentrate at the surface; c) Droplet after a couple seconds of evaporation. Liquid butanol surface layer thickness depends on the surface regression rate and mass diffusion rate of butanol outwards; d) Final droplet left on the fibers consists of pure SBO and is 63% of initial size.

To compare with Makino and Law's suggestion that a Peclet number can be used to determine whether the gasification mechanism is diffusion-like or distillation-like the diffusivities of SBO into butanol and butanol into SBO have been calculated. A diffusion-like gasification mechanism is suggested from the experimental results so it would be most beneficial to use values in the diffusivity calculations that would result in a Peclet number value that is conservative on the distillation-like side. A higher Peclet number would suggest a diffusion-like gasification mechanism so values that would make the Peclet number as low as possible (i.e. high diffusivity) were used to prove that the mechanism is not distillation-like. Considering that diffusivities are temperature dependent the diffusivities were calculated for 573 K which, from Eq. 20, will increase

the diffusivity (lowering the Peclet number). Pure SBO, the less volatile component, does not have a boiling point but if a boiling point is assumed to be around 300° C (slightly higher than its smoke point) this means that the droplet surface temperature, and thus the interior temperature will never be above 300° C (573 K). This is because the surface temperature of a burning fuel is governed by the boiling point of the relevant fuel that is vaporizing during combustion. So even though 573 K is not reachable in the interior of the droplet during combustion, and definitely not during pure evaporation, it was used to calculate the diffusivities for a very conservative estimation leaning toward the distillation-like mechanism. The molecular volumes however were calculated at 100°C (373 K) because it is the highest temperature data for specific gravity available from this study (V = Molecular Weight/Specific Gravity). For the infinitely dilute case the $\mathcal{D}^{\circ}_{SBO\rightarrow butanol} = 0.101 \times 10^{-4}$ and $\mathcal{D}^{\circ}_{butanol\rightarrow SBO} = 0.499 \times 10^{-5}$. We are interested in the latter because we are trying to analyze the diffusion process of the butanol through the SBO toward the surface. There is significant proof provided by Poling et al. that the thermodynamic correction (ξ) used in Eq. (21) is a positive number less than one for binary mixtures suggesting that the diffusion coefficient based on any concentration ($\mathcal{D}_{butanol\rightarrow SBO}$) will be smaller than the diffusion coefficient for the infinitely dilute case ($\mathcal{D}^{\circ}_{butanol\rightarrow SBO}$). Consequently, using the infinitely dilute diffusivity is a conservative estimate for the diffusivity used in the Peclet number calculation. The regression rate defined by Makino and Law in Eq. (19) was of the magnitude > $3x10^{-3}$ for all droplets containing butanol at room temperature (room temperature provides the lowest regression rate further reducing the Peclet number). These conservative values lead to a resultant Peclet number of 60.12 (Eq. (20)) which is >>1 suggesting a diffusion-like gasification mechanism during evaporation as well with high confidence.

4.2.2 Evaporation Rates as a Function of Temperature

As expected the evaporation constant (K) increases with temperature. Fig. 4.11 plots the dimensionless diameter versus time at various temperatures for pure butanol to show this visually. Similar plots for the two mixtures studied are shown in Figs. 4.12 and 4.13. The mixed fuel plots show similar results and show that for all ambient temperatures the $(D/D_0)^2_{final}$ values are similar for each mixture. In fact, for the lowest elevated temperature (100° C) the $(D/D_0)^2_{final}$ is very close to the predicted value in Table 4.9. This is because the initial evaporation due to the one second between time zero and the initial droplet measurement had less of an effect.

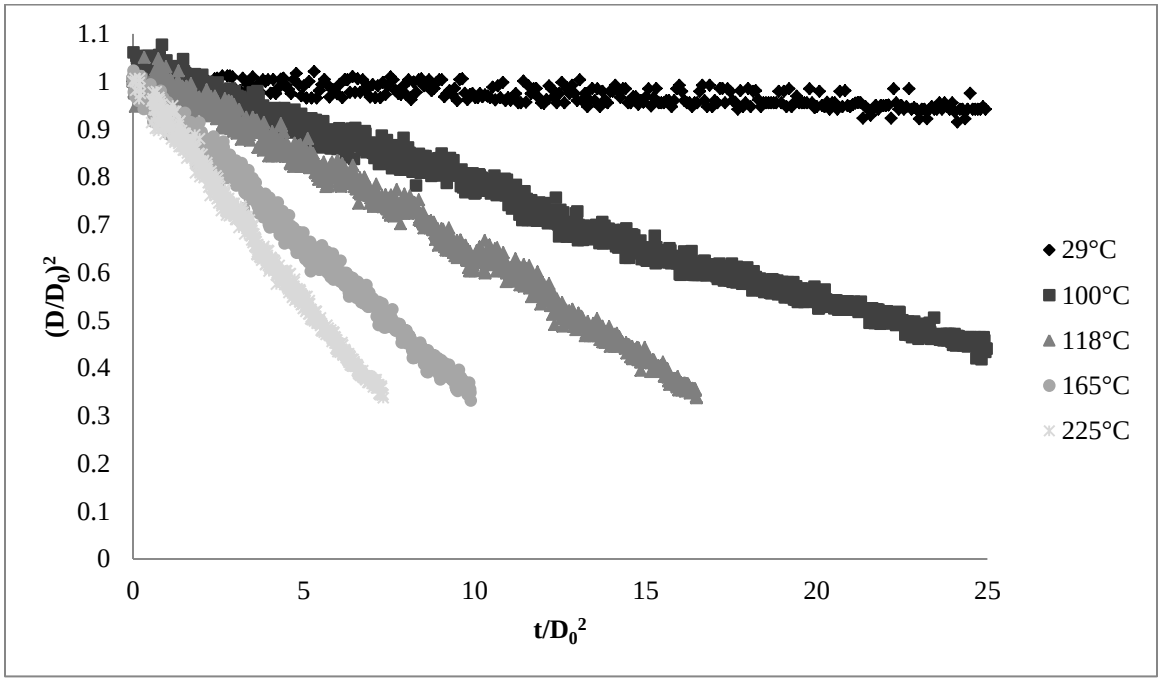

Fig. 4.11. Evaporation rates of pure butanol droplet plotted as the dimensionless diameter as a function of normalized time

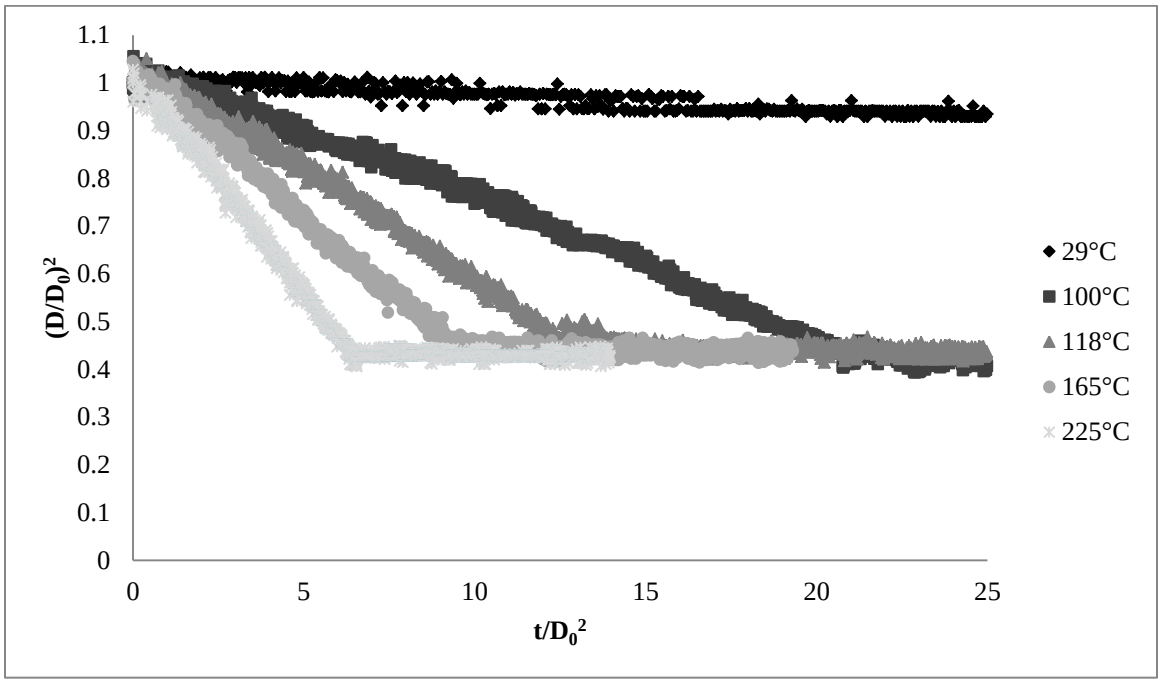

Fig. 4.12. Evaporation rates of Bu75 droplets plotted as the dimensionless diameter as a function of normalized time

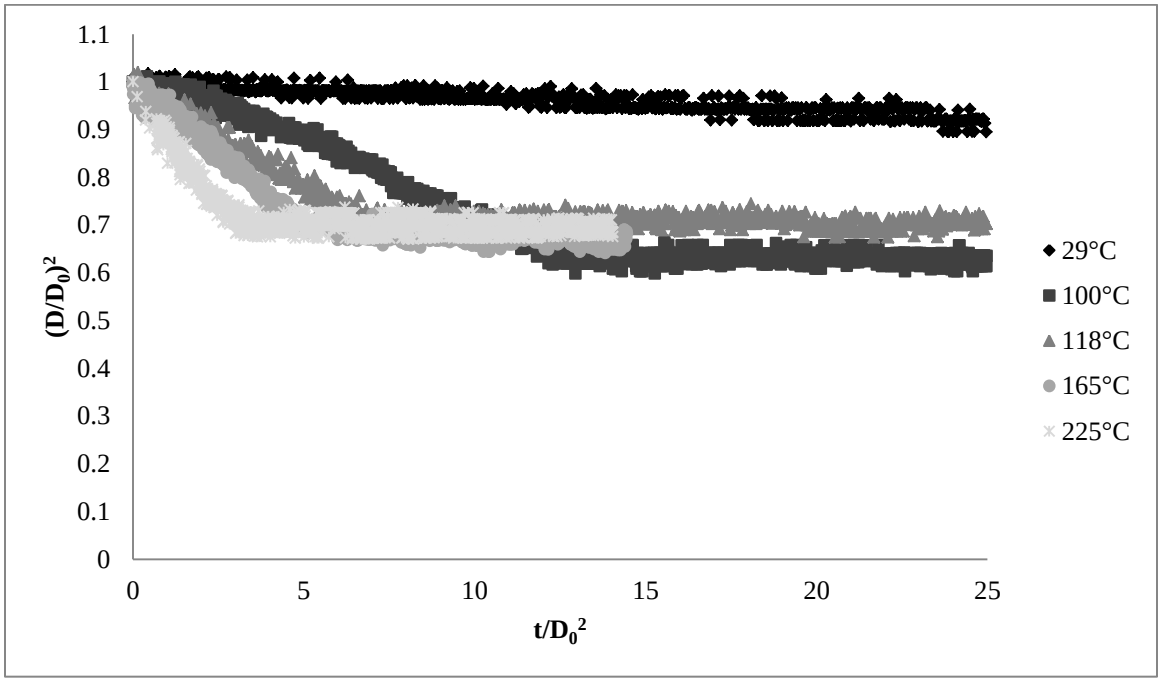

Fig. 4.13. Evaporation rates of Bu50 droplets plotted as the dimensionless diameter as a function of normalized time

Droplet evaporation rates coupled with combustion behavior data could essentially be used to describe what would be an ideal mixture concentration of SBO/butanol fuel blends in various applications where evaporation of fuel droplets prior to ignition may or may not be present. If the droplet evaporation rates can be assumed to be the same as pure butanol knowing it can help to suggest a relative composition of droplets in fuel sprays at the time of ignition in a combustion application.

4.3 Basic Fuel Combustion

4.3.1 Droplet Temperature Prediction

The flashpoint is very important when categorizing fuels for various applications because it represents the temperature a fuel will ignite at. Consequently, it was desired to estimate the fuel droplet temperature at ignition using our combustion facility and compare the results with flashpoint temperatures obtained using a standardized test method (ASTM D93 closed cup method). All samples were sent to the Agriculture Utilization Research Institute (AURI) for flashpoint measurements via ASTM D93. The results are shown in Table 4.10 for comparison with results obtained in this study. No previous research has attempted to use single fuel droplets to measure flashpoints.

From Table 4.10 it is apparent that all mixtures exhibit the same flashpoint and it is similar to that of pure butanol. The flashpoint temperature of pure SBO is almost five and a half times that of pure butanol making this an interesting phenomenon to investigate. Preheating is a possibility to make utilizing BDOs for alternative fuels a possibility, but is not very effective and it is costly. If the addition of butanol could eliminate this need by reducing a mixtures flashpoint to that of its own it would be a significant advantage. The temperature of the droplets in this study is dependent on the time they are subject to an elevated temperature and will be estimated using a thermocouple placed very close to the suspended droplet.

Table 4.10

Flashpoint measurements of relevant fuels via ASTM D93 Pensky-Martins closed cup method (as reported by AURI)

Fuel Blend	Flashpoint (°C)
Bu100	41
Bu75	40
Bu50	40
Bu25	40
Bu0	217

Since it is desirable to know, or at least estimate, what the actual droplet temperature is when ignition occurs during combustion tests (flashpoint temperature) it is important to see how a droplet heats in an elevated temperature environment. In an effort to prove that the thermocouple positioned to the right of the suspended fuel droplet (see Fig. 3.6) is useful to estimate droplet temperatures at ignition with good accuracy another evaporation study was performed. Droplets of SBO/butanol blends (25/75, 50/50, 75/25 by volume) were placed on a Type K thermocouple bead instead of the fibers and allowed to evaporate while temperature data was recorded for the thermocouple. The thermocouple bead was also subject to the elevated temperatures without any fuel present for a baseline heating curve for comparison. Temperature data collected from the thermocouple as a function of time in a 165° C environment for all mixtures is shown in Fig. 4.14. Temperature data corresponding to the thermocouple without any fuel suspended from the bead is also shown on the same plot. The plot shows that a droplet of SBO/butanol heats less quickly than that of a Type K thermocouple bead of similar diameters (i.e. exhibits a longer time constant) due to the higher heat capacity exhibited by the SBO/butanol liquid mixtures. Fig. 4.14 also shows that for the first ten seconds all mixtures heat at similar rates. A similar plot for T_∞ = 118°C is shown in Fig. 4.15. It also shows that the droplets heat more slowly but at similar rates for about the first 12 seconds for T_∞ = 118°C. Between one and four seconds the temperature of the droplet is between 2 and 7°C lower than that of the reference thermocouple respectfully. The

majority of combustion studies performed in this work were done in that time frame at 100°C. Since the deviation from droplet temperature to thermocouple bead temperature in the first four seconds shrinks as the ambient temperature is lowered (3-10 at 165°C to 2-7 at 118°C) it suggests an even smaller deviation from the thermocouple bead at 100°C justifying the thermocouples usefulness for estimating droplet temperature to within ±2°C for the faster ignition times and ±7°C for the longer ignition times.

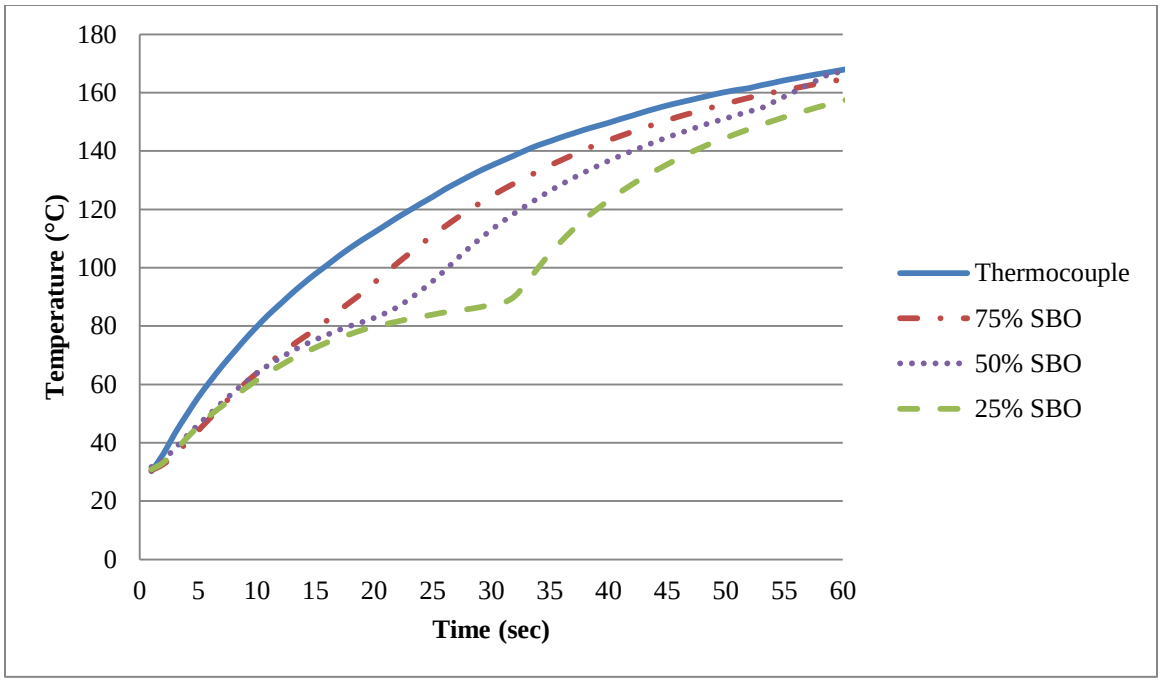

Fig. 4.14. Temperature profiles for all mixtures when hanging from a Type K thermocouple bead and baseline curve at T_∞ = 165°C

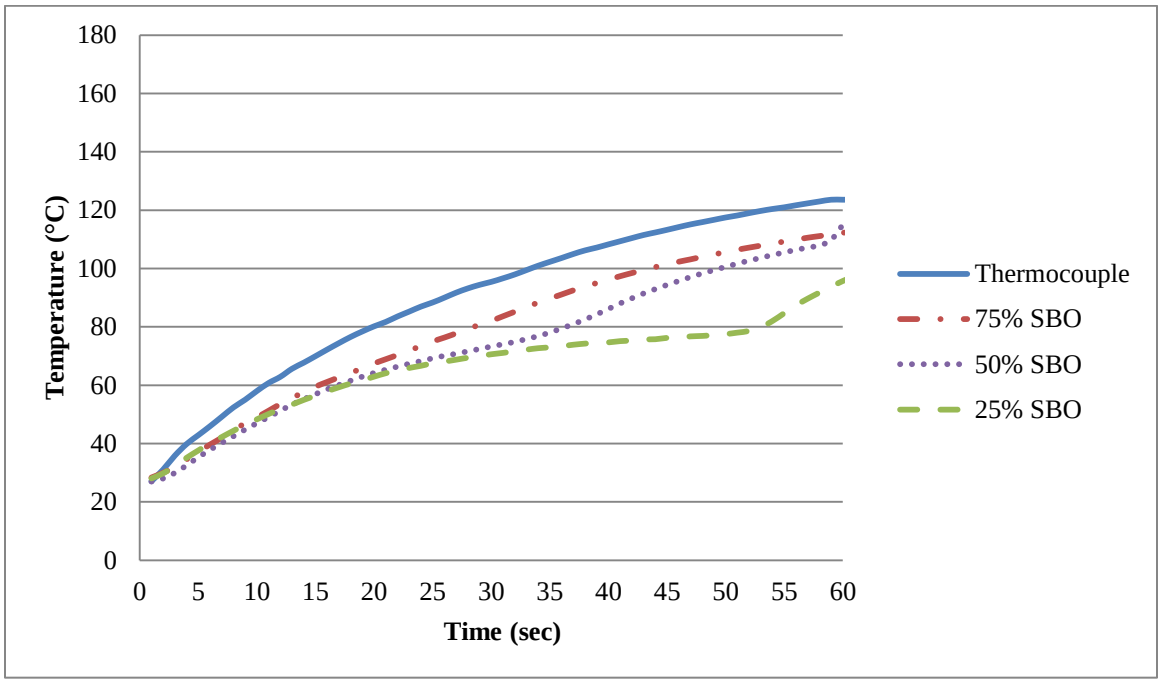

Fig. 4.15. Temperature profiles for all mixtures when hanging from a Type K thermocouple bead and baseline curve at T_∞ = 118°C

This is not an exact droplet temperature measurement but it is a fairly accurate estimate. Ignition of droplets of all initial concentrations was achieved at similar temperatures in this study which is in agreement with the flashpoint results obtained from AURI. Similarly to the model shown in Fig. 4.10 the ability for all mixtures to ignite at similar temperatures suggests that there is a liquid layer of vaporizing butanol at the surface of the droplet at the time of ignition.

4.3.2 Droplet Burning Behavior

A basic combustion study as described in section 3.2.3 was performed for mixtures of Bu75 and Bu50 fuel droplets as well as the pure components (Bu40 and Bu25 droplets were burned but not studied with as much detail). Experimental results indicated that the burning behavior was a function of the initial droplet size, relative composition and droplet temperature at the time of ignition. Initial concentration of the fuel droplets proved to be the most influential factor on their combustion behavior. The fuel droplets either: did not ignite, ignited but did not burn completely or ignited and burned

completely. As expected because of the large volatility difference between the two components and the diffusion-like gasification mechanism proposed in the previous section, all mixed droplets that burned completely exhibited a three stage combustion behavior including a microexplosion. The pure fuel droplets did not experience this phenomenon but rather burned steadily and did not boil or explode. Some of the droplets which did not burn completely burned steadily for a period of time followed by an extinction of the flame and left a liquid droplet of measurable diameter on the fibers. Others burned and exhibited a microexplosion followed by flame extinction and left a droplet on the fibers.

Data pertaining to unburned fuel was not found while reviewing literature from past research groups studying single mixed fuel droplets similar to SBO/butanol. This is obviously not a desirable combustion characteristic and the fuel properties need to be considered to investigate why the droplet did not burn completely. Consequently, measurements of droplet sizes and temperatures observed from the strategically placed thermocouples were recorded throughout the droplet lifetimes. This technique gave insight on the relevant concentrations of butanol present in the droplets throughout the combustion process as well as showed the effect the temperature rise resulting from the combustion process (temperatures observed from the thermocouple above the burning droplet) had on the droplets burning behavior. Diameter measurements were used to determine droplet size however swelling of the droplets due to thermal expansion was assumed to be negligible in the analysis. Most previous research groups do not account for thermal expansion and experimental results proved to be fairly accurate and semi-quantifiable neglecting its presence.

4.3.3 Pure Butanol

The pure butanol droplet combustion tests can be used to compare ignition temperatures to that of flashpoints obtained using the closed cup method. From Table 4.10 the flashpoint of the pure butanol used was 41° C so the droplets should not ignite below this temperature and should above this temperature. The furnace was set to 100° C so the time between the introduction to the elevated temperature (time zero) and the time of attempted ignition is the factor that governs the temperature of the fuel droplet. It should be noted that there is a dependence on the ambient temperature of the lab as well as the time to ignition. A higher ambient temperature would mean that the time it takes for the droplet as well as the thermocouples to reach 41° C is shortened. Since the droplet temperature is not known exactly an approximation is made by the thermocouple to the side of the droplet. From Fig. 4.15 it is shown that the droplet will actually heat slightly slower than that of the thermocouple. Ignition for all pure butanol droplets was attempted between times of 0.84 and 2.55 seconds which resulted in thermocouple temperature readings of 34.1 to 44.6°C. Table 4.11 shows a list of pure butanol combustion experiments performed including the initial diameter of the droplet, the diameter of the droplet at ignition, the temperature of the side thermocouple used as a reference (see Fig. 3.6), the time the droplet was in place prior to ignition (Ignition Time) and the temperature rise observed from the thermocouple above the droplet ($T_2 - T_1$). The temperature observed from the upper thermocouple is not a droplet surface temperature but rather a tool used to signify ignition as well as to show the temperature rise of the flame compared to the droplet size and in the case of the mixed droplets the three stage burning effect. Figs. 4.16 and 4.17 show examples of thermocouple data plots produced by droplets which did not ignite and did ignite respectively. A description of the test parameters is available in the captions.

Table 4.11

List of pure butanol experiments performed including droplet size data, temperature of the side reference thermocouple and temperature rise sensed by the top reference thermocouple when applicable

D_0 (mm)	$D_{ignition}$ (mm)	$T_{ignition}$ (° C)	Ignition Time (s)	T_2-T_1 (° C)
0.62	0.58	34.4	0.91	No ignition
0.72	0.71	34.4	1.25	No ignition
0.72	0.71	34.2	0.84	No ignition
0.78	0.76	34.6	0.87	No ignition
0.80	0.78	34.1	1.00	No ignition
0.69	0.65	41.6	2.06	189
0.71	0.70	38.1	1.67	205
0.79	0.77	36.7	1.32	286
0.81	0.79	34.7	1.58	346
0.84	0.78	44.6	2.55	315

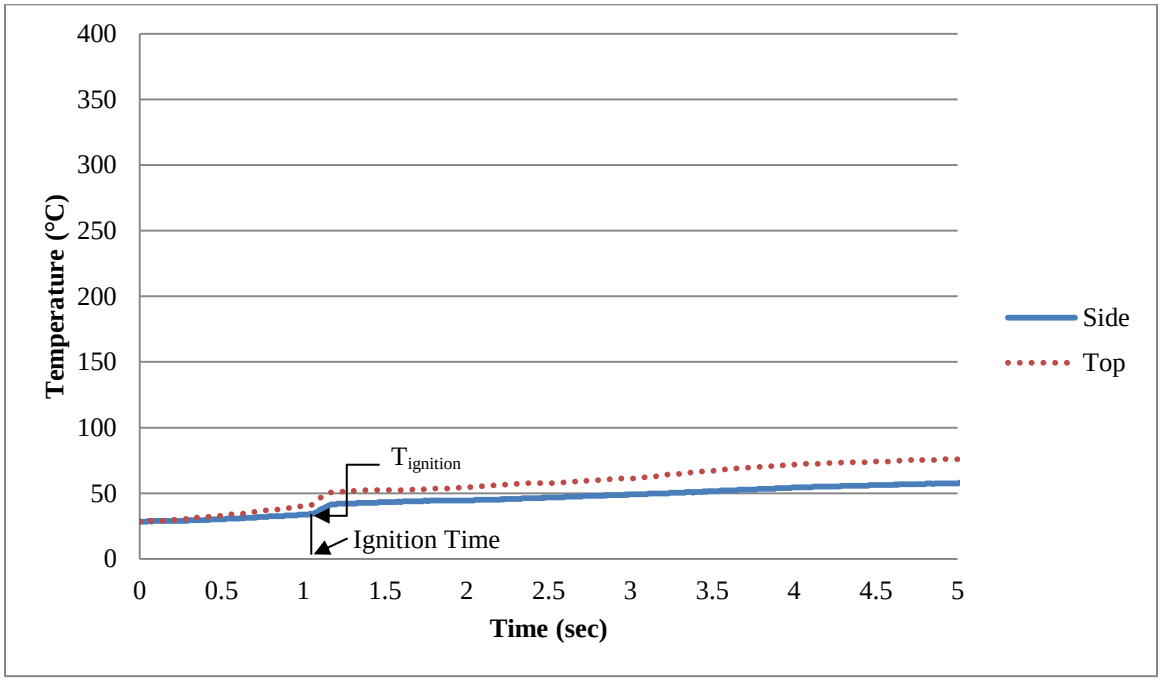

Fig. 4.16. Pure butanol droplet does not ignite at 1.00 second in 100°C ambient temperature; D_0 = 0.80 mm; $D_{ignition}$ = 0.78 mm; $T_{ignition}$ = 34.1°C

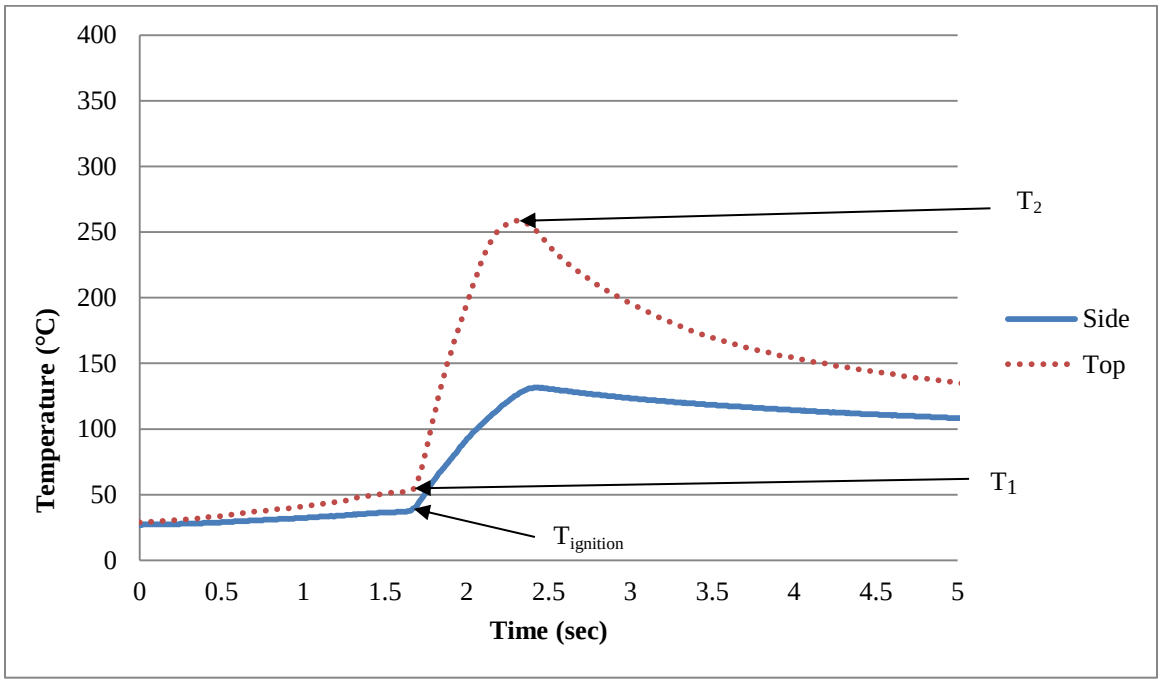

Fig. 4.17. Pure butanol droplet ignites at 1.67 seconds in 100°C ambient temperature; D_0 = 0.71 mm; $D_{ignition}$ = 0.70 mm; $T_{ignition}$ = 38.1°C

As can be seen from Fig. 4.16 there is a local temperature rise associated with the ignition process from the heating element even if ignition fails to occur. This temperature can only be quantified from data associated with droplets that did not ignite since it is masked by the combustion process of droplets that did ignite. For the five tests which ignition did not occur this temperature rise corresponding to the side thermocouple used as the ignition temperature reference was on average 7.4°C. Table 4.11 shows that no pure butanol fuel droplet was ignited when the reference thermocouple ($T_{ignition}$) was at or below 34.6°C and all trials were successful to ignite the droplets above this temperature. When the temperature rise from the igniter is added to this reference temperature it equals 42°C which is 1°C higher than the suggested flashpoint temperature of the pure butanol obtained using the ASTM D93 closed cup method. The agreement of the experimental results with that of the closed cup test results shows that this test method is feasible and with minor adjustments (i.e. a push pull solenoid like the one used in the Pan combustion facility) to better control the ignition process this facility could be a very accurate test method for flashpoint data of fuel mixtures. Multiple tests were also conducted at room

temperature which all failed to ignite pure butanol droplets. This is in agreement with flashpoint data obtained via ASTM D93 as well.

Table 4.11 also shows that the temperature rise (T_2-T_1) associated with the combustion process increases with the size of the droplet at *ignition*. This can be attributed to the fact that there is more liquid fuel to burn for larger droplets. Individual images abstracted from video analysis for the combustion of pure butanol are shown in Fig. 4.18. Video analysis showed that the flame exhibited during combustion of pure butanol droplets was nonluminous and was difficult to capture clarifying the need of thermocouples to signify the occurrence of ignition. The blue or clear flame also suggests no sooting from the combustion of pure butanol. There was also no soot left on the fibers after the droplet had completely burned. Estimates of flame size can be made by the faint glow on the ceramic fibers which result from heat at the edge of the flame shell.

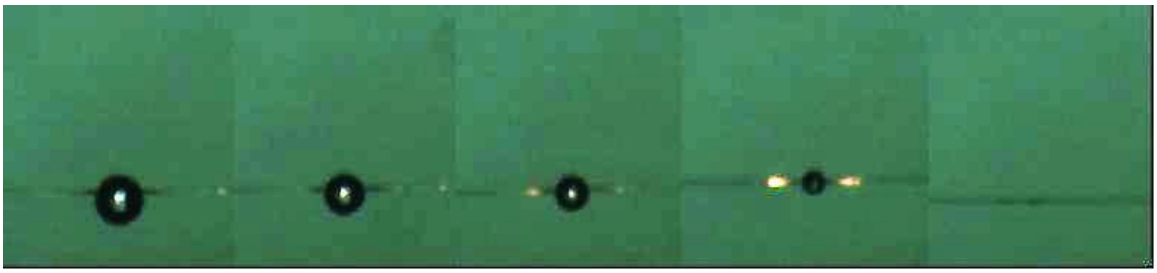

Fig. 4.18. Images from video analysis for the burning of pure butanol

4.3.4 Pure SBO

The combustion process of pure SBO was not studied in depth however it was ignited using the same process at $T_\infty > 300°C$ for comparison with the combustion process of the other fuels analyzed. Fig. 4.19. shows the bright orange flame exhibited by the burning of pure SBO which signifies soot formation. A small soot cloud and soot accumulation on the fibers was also observed at the end of the burning process. The combustion process of pure SBO was less steady than that of pure butanol. The flame observed was orange throughout the droplets lifetime and the flame exhibited a "puffing" type behavior as the droplet rapidly changed shapes and sizes. However, a microexplosion was not

observed. Fig 4.19 shows the pure SBO as it is burning for visual verification of the "puffing" behavior and the remaining soot left on the fibers.

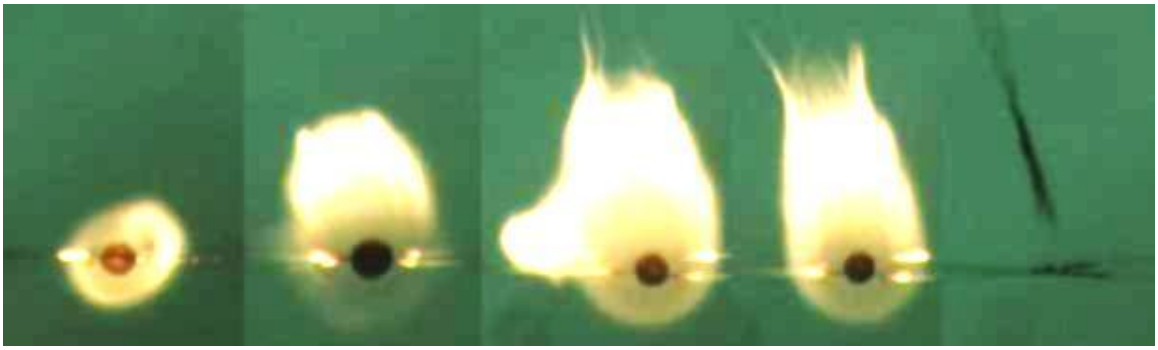

Fig. 4.19. Images from video analysis for the burning of pure SBO

4.3.5 Mixed Fuel

The combustion behavior of mixed fuel droplets of SBO and butanol are more interesting as well as more difficult to analyze and understand. The tendency to ignite or not was similar to pure butanol as suggested by the similar flashpoints shown in Table 4.10. Like pure butanol, mixed droplets ignited at any temperature at or above 34.1°C referenced from the side thermocouple and failed to ignite below 34°C with one exception where a droplet ignited when the thermocouple read 33.6°C. The similarity of ignition temperatures to pure butanol is consistent with results obtained via ASTM D93 closed cup method for these mixtures. However, there were cases in which the fuel droplet did not undergo a complete combustion but rather ignite, partially burn and the flame would extinguish leaving a liquid droplet behind. Consequently, there must be some other test method to classify these types of fuels as suitable for various applications. If incomplete combustion were to occur in a gas turbine engine unburned fuel would be left in the cylinders and exhaust systems resulting in possible damage to the engine and inefficiency of performance. Relative composition and droplet size data (two factors that govern the combustion process according to Lasheras et al. [37]) must be analyzed to attempt to predict when complete combustion of the fuel droplets will occur most frequently. In a spray combustion application atomization through a nozzle will result in numerous very small fuel droplets to be ignited by the gasification of the more volatile fuels however

analysis of single and larger fuel droplets could lead to an optimal, suggested range of blend composition for various applications. Droplet size measurements throughout the droplet combustion process are used to estimate the relative composition of the fuel droplets at the time of ignition and after the first burning stage. The tendency to experience microexplosions and the intensity of the microexplosions are also correlated with mixture compositions.

Complete combustion is referred to for droplets which ignited and burned completely leaving no liquid fuel behind on the fibers. For all mixtures of SBO and butanol which complete combustion occurred, a microexplosion and a three staged burning process, similar to that described by the Lasheras and Wang groups was observed [32], [34], [37]. The microexplosions however occurred at different times throughout the combustion process and at different intensities depending on the initial droplet concentration and size. Incomplete combustion was considered to have occurred if a droplet ignited and a liquid fuel droplet remained on the fibers due to flame extinction. Incomplete combustion was observed for some droplets of all mixtures. In some of these cases a microexplosion still occurred immediately before flame extinction and in others no microexplosion was observed. The tendency of a microexplosion to occur for these cases showed dependence on the initial droplet composition. There were also a few experiments which resulted in the droplet falling off the fibers during the microexplosion. Microexplosion intensity data was recorded from these experiments however they were not considered for whether complete or incomplete combustion occurred because video footage was unattainable after they had fallen.

Bu75 and Bu50 blends were studied more extensively for their burning behavior and tendency to produce microexplosions. After experiments were complete for the Bu75 and Bu50 blends and some post literature review was done it was believed that a 60/40 – SBO/butanol (Bu40) mixture would produce more intense microexplosions. Consequently some follow up experiments were done for that mixture. Bu25 droplets proved much harder to ignite because the low concentration of butanol present in the droplet had evaporated off before ignition could occur for most cases. However, it was

possible to ignite a few Bu25 droplets with very short ignition times so there were experimental tests, although fewer, to draw results from for comparison.

4.3.6 Mixed Fuel – Bu75

Multiple tests using droplets consisting of 25% SBO and 75% butanol by volume were done in an effort to investigate the principles that govern combustion behavior and the driving factors that cause a droplet to burn completely or not. The same process as used in the pure butanol experiments was used. The ignition time and temperature was however varied more in an effort to see if relative concentrations at the time of ignition could be used to justify this phenomenon. For example, if a droplet is in test position longer there is more time for the butanol to evaporate off lowering the relative concentration of butanol at the time of ignition. The results were investigated. Droplets with initial diameters ranging from 0.65 to 1.00 mm were used and ignition times varied from 0.96 seconds to 6.42 seconds. Twenty-one tests were performed with ignition times ranging from 0.96 to 3.25 seconds, fifteen of which ignited and did so at times above one second. The other six failed to ignite because they did not reach sufficient temperature to do so (i.e. the flashpoint of butanol). Thirteen tests were performed with ignition times between 4.56 and 6.43 seconds, all of which ignited. Droplets of mixed fuels which did not ignite are not included in the analysis but just used to show consistency in ignition temperatures (i.e. flashpoint) to pure butanol. As can be expected for longer ignition times the ignition temperature is higher. This temperature was found to be less of an influence on combustion behavior other than for use of flashpoint analysis. The relative concentration of the droplet at ignition was more of concern. The concentration, which can be estimated by the diameter measurement at ignition (assuming butanol is the only substance that has evaporated off prior to ignition) is a function of the initial diameter and the ignition time.

For the droplets which exhibited complete combustion the initial diameter, diameter at ignition, diameter prior to the third stage of combustion and the diameter of the droplet in its expanded bubble ($D_{explode}$) prior to the microexplosion were measured using the

Xcytex ProAnalyst^{TM} software. The time to ignition and ignition temperature observed from the side thermocouple were reported. The temperature at ignition (T_1) observed from the upper thermocouple (see Fig. 3.6) was recorded as well as the temperature rise associated with flame present during the first stage of combustion (T_2) observed from the same thermocouple. The final temperature rise produced by the complete combustion of the droplet (T_{final}) was also recorded so that the temperature rise during the first and third stages could be compared. Table 4.12 has been prepared to summarize all Bu75 tests performed which exhibited complete combustion.

Table 4.12

Summary of all Bu75 tests resulting in complete combustion. Diameters listed are in units of millimeters, temperatures in degrees Celsius and ignition time is in seconds

D_0	$D_{ignition}$	D_{fs}	$D_{explode}$	$T_{ignition}$	Ignition Time	T_1	T_2	T_{final}
0.75	0.72	0.52	0.82	42.0	2.12	52	216	245
0.75	0.60	0.50	0.66	62.3	4.56	82	189	273
0.77	0.71	0.55	0.67	45.0	2.29	56	243	305
0.78	0.67	0.49	0.78	60.8	4.57	80	216	272
0.80	0.77	0.58	0.74	40.4	2.20	54	198	256
0.82	0.81	0.57	0.84	43.0	2.13	50	250	328
0.86	***0.81***	***0.62***	***0.70***	***39.3***	***2.14***	***52***	***270***	***332***
0.86	0.78	0.64	0.70	65.7	6.42	89	270	342
0.87	0.77	0.59	0.74	57.2	5.30	81	289	326
0.9	0.84	0.59	1.00	35.4	2.20	52	368	462
0.94	0.84	0.66	0.94	56.4	5.10	76	308	367
1.00	0.93	0.69	0.95	58.3	4.90	79	358	394

Fig. 4.20 shows thermocouple data generated from a mixed fuel droplet for a case where complete combustion occurred. The plot corresponds to the test results reported in bold, italic font in Table 4.12. Corresponding images collected from video data recorded for the burning droplet is shown in Fig. 4.21. The numbers represent the time segment labeled on the temperature plot. Every test resulting in complete combustion had a

microexplosion after the second stage where flame shrinkage occurs. The flame shrinkage is signified by a near horizontal line or, in some cases, a decreasing temperature slope like shown in figure 4.20. The decrease in temperature can be expected because of the flame is shrinking while interior heating of the droplet occurs.

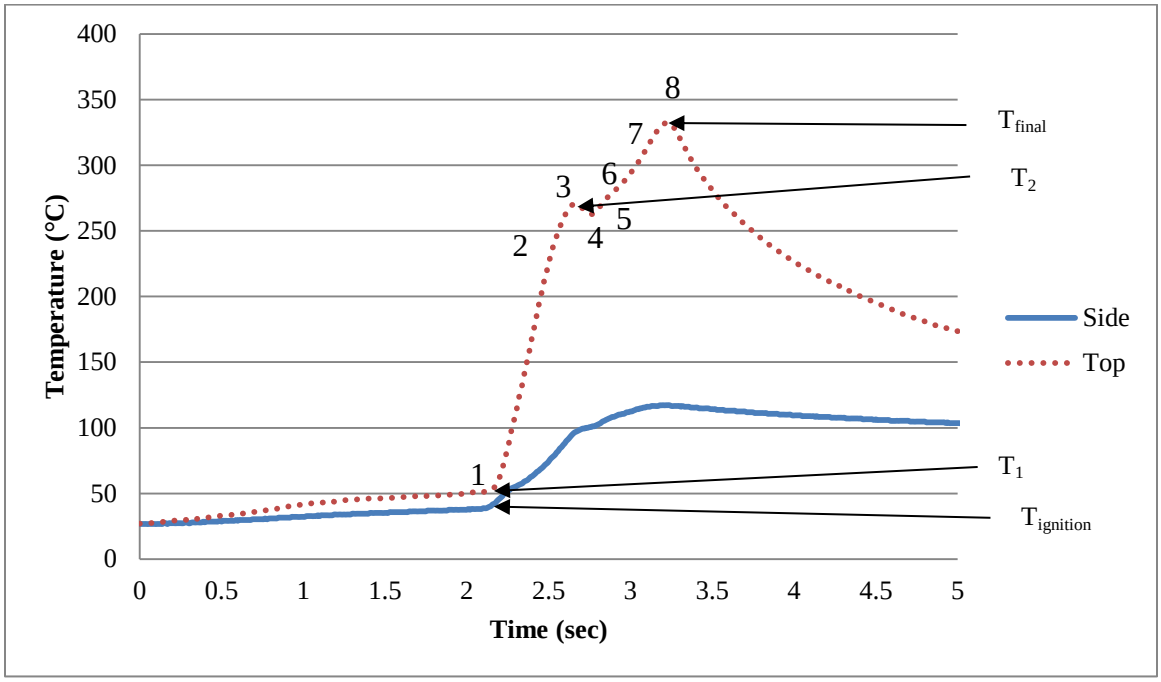

Fig 4.20. Bu75 droplet which ignites 2.14 seconds in 100°C ambient temperature and burns completely; D_0 = 0.86 mm; $D_{ignition}$ = 0.81 mm; D_{fs} = 0.62 mm; $D_{explode}$ = 0.70 mm; $T_{ignition}$ = 39.3°C

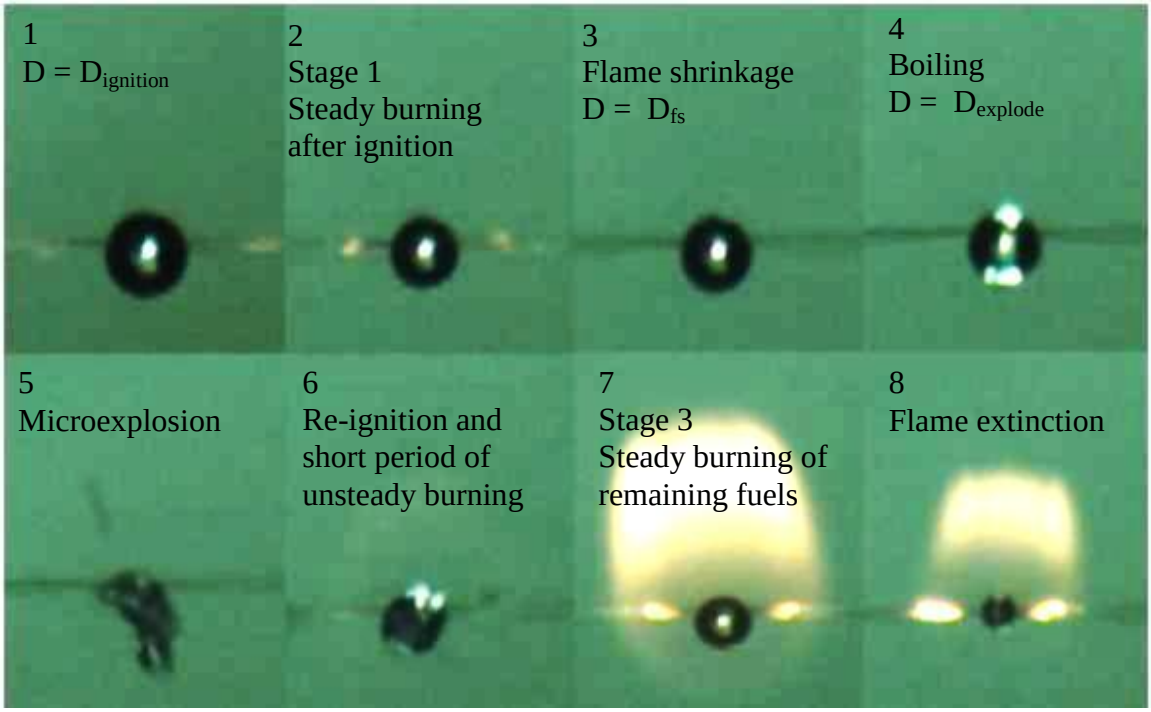

Fig 4.21. Images taken from video footage captured for the case of complete combustion correlating to Fig. 4.20

As expected the first stage of combustion is characterized by a nonluminous flame signifying no soot and is likely the pure butanol burning. After the microexplosion the rest of the combustion process is characterized by a distinguishable orange flame representing soot from the burning SBO. The plot in Fig. 4.20 is similar to the burning rates plots produced from Botera et al's studies (Fig. 2.3) where there is a steady first stage, a transition period where the droplet no longer shrinks signified by a near horizontal line, and then a steady third stage. The plots in this work use local temperature data via a close thermocouple rather than droplet diameters to show the staged burning effect. There is an initial period where the temperature rise ($T_2 - T_1$) is controlled by the butanol which on average is 60% of the total temperature rise ($T_{final} - T_1$). Then there is a period of flame shrinkage which can be seen from the temperature drop at the second stage and then a microexplosion followed by a second temperature rise associated with the co-burning of the SBO and remaining butanol. This is consistent with the suggestion from the Wang and Lasheras research groups that the droplet is ignited, burns the more volatile component while the surface temperature rises to the boiling point of the less

volatile component and then at flame shrinkage the heat is transferred towards the center of the droplet and if the droplet center reaches a temperature high enough to superheat the more volatile component a microexplosion occurs and a third combustion stage begins burning the remaining fuel. Neglecting expansion due to droplet heating, the measured droplet diameters at flame shrinkage suggest that there is still butanol present in the droplet at the time of the microexplosion. This is consistent with past research groups' suggestion of the diffusion limited gasification mechanism. Since the droplet diameters at flame shrinkage are such that the volume of droplet is greater than 25% (the initial concentration of SBO) that of its initial size it suggests that there is in fact butanol trapped within the surface when the microexplosion occurs. In other words, the mass diffusion rate of the butanol towards the surface is slower than that of the surface regression and thermal diffusion heating the interior of the droplet.

For droplets that experienced incomplete combustion and no microexplosion the diameter immediately after the flame was extinguished was measured. This was done to compare the droplet size to that of the initial to prove that liquid butanol was still present in the droplet. In some cases a final diameter was measured. This was done after a significant time period where the remaining droplet was allowed to further vaporize in the ambient environment after the droplet stopped burning. The final diameter correlated to a droplet volume very close to 25% the initial droplet volume suggesting the remaining fuel was purely liquid SBO. The measurements were in agreement with the $(D/D_0)^2_{final}$ explained in section 4.2.1 which would suggest a final volume corresponding to the initial concentration of SBO in the mixture. For a Bu75 droplet this value would be 0.397 (see Table 4.9).

Table 4.13 is similar to Table 4.12 but presents experimental results for the droplets which did not exhibit complete combustion or a microexplosion. Table 4.13 shows that on average T_2 is about 70° C lower than the cases which exhibited complete combustion. The ignition time and temperature do not seem to have an effect on the temperature at flame shrinkage (T_2). For the most part the droplets which had a larger diameter at ignition experienced a greater temperature rise during combustion. This can be expected

because for a larger droplet there should be more butanol present at the surface. For cases where complete combustion and incomplete combustion occurred there are a few overlapping droplet sizes. This means that both smaller and larger droplets resulted in both outcomes suggesting that the temperature rise during the first combustion stage is a major driving factor for whether the droplet will burn completely or not. It is helpful to restate that all droplets which burned completely exhibited a microexplosion. For the test results listed in Table 4.13 no microexplosions occurred which suggests that the droplets must experience a microexplosion to burn completely. If no microexplosion occurs there is no chance that the droplet will have complete combustion. It makes sense then that the temperature rise associated during the first combustion stage would be the most influential factor on whether the droplet will burn completely or not for the Bu75 blend. The interior of the droplet must reach a temperature where the butanol trapped inside is superheated to result in a microexplosion. A higher surface temperature after the first combustion stage would promote this. It is still a question as to what are all the aspects which govern the temperature rise of T_2. Since initial droplet size didn't prove to be the only factor it may have to do with the amount of butanol trapped within the surface of the droplet at flame shrinkage while the majority of the heat is being transferred toward the interior. The amount of butanol burned during the first combustion stage which provides the initial heat may also play a role. It has been suggested by Lasheras et al. the, during combustion, the interior of the droplet rapidly responds to the surface temperature variation. Consequently, for mixtures with low initial concentrations of the less volatile component the maximum surface temperature may be substantially depressed compared to a mixture with large initial concentrations of the less volatile component [37]. This would reduce the tendency for the interior to be superheated and is likely the reason so many Bu75 droplet tests did not experience a microexplosion and thus did not burn completely.

Table 4.13

Summary of all Bu75 tests resulting in incomplete combustion and no microexplosion. Diameters listed are in units of millimeters, temperatures in degrees Celsius and ignition time is in seconds

D_0	$D_{ignition}$	D_{fs}	D_{final}	$T_{ignition}$	Ignition Time	T_1	T_2	T_{final}
0.65	***0.61***	***0.43***	***0.42***	***39.0***	***2.14***	***56***	***142***	***NA***
0.68	0.63	0.48	0.42	50.3	3.25	67	176	NA
0.69	0.68	0.50	0.47	41.5	1.47	53	151	NA
0.73	0.66	0.50	0.49	55.4	5.30	67	198	NA
0.75	0.63	0.52	0.46	65.9	5.97	88	194	NA
0.77	0.72	0.53	NA	55.6	4.70	76	218	NA
0.78	0.75	0.54	NA	44.1	1.63	55	179	NA
0.78	0.72	0.55	0.49	59.1	4.80	79	225	NA
0.79	0.70	0.57	NA	59.5	5.10	81	235	NA
0.80	0.74	0.54	NA	59.3	5.40	79	233	NA
0.81	0.79	0.58	0.53	44.6	1.73	55	146	NA
0.81	0.77	0.57	0.49	33.6	1.00	42	264	NA
0.89	0.88	0.66	NA	42.9	1.95	54	216	NA
0.89	0.83	0.61	0.57	38.2	2.40	55	177	NA

Fig. 4.22 shows thermocouple data generated from a mixed fuel droplet for a case where incomplete combustion occurred. The plot corresponds to the test results reported in bold, italic font in Table 4.13. Corresponding images collected from video data recorded for the burning droplet is shown in Fig. 4.23. The numbers represent the time segment labeled on the temperature plot. From the plot in Fig. 4.22 it is apparent that there is no period where a horizontal line or slight decrease in temperature is observed. This suggests that there is no microexplosion. The images from the video data shown in Fig. 4.23 can also attest to this. From the temperature plot it is shown that the droplet ignites at about 40°C (similar to droplet test shown in Fig. 4.20) and burns steadily for a period of time and the stops burning. Fig. 4.23 shows that the flame is nonluminous throughout

the combustion process suggestion that only the butanol is burning. The temperature rise observed by the upper thermocouple is not as significant as that of the one observed for a case of complete combustion (Fig. 4.20). The initial droplet diameter and the droplet diameter at ignition in the case of incomplete combustion is smaller suggesting the volume of butanol contained in the droplet at ignition is also much smaller. Consequently, the smaller droplet will not produce as much heat in the first combustion stage as that of the larger droplet in the complete combustion case. There were however cases in which larger sized droplets experienced incomplete combustion and smaller droplets experienced complete combustion. The latter case however tended to be less likely.

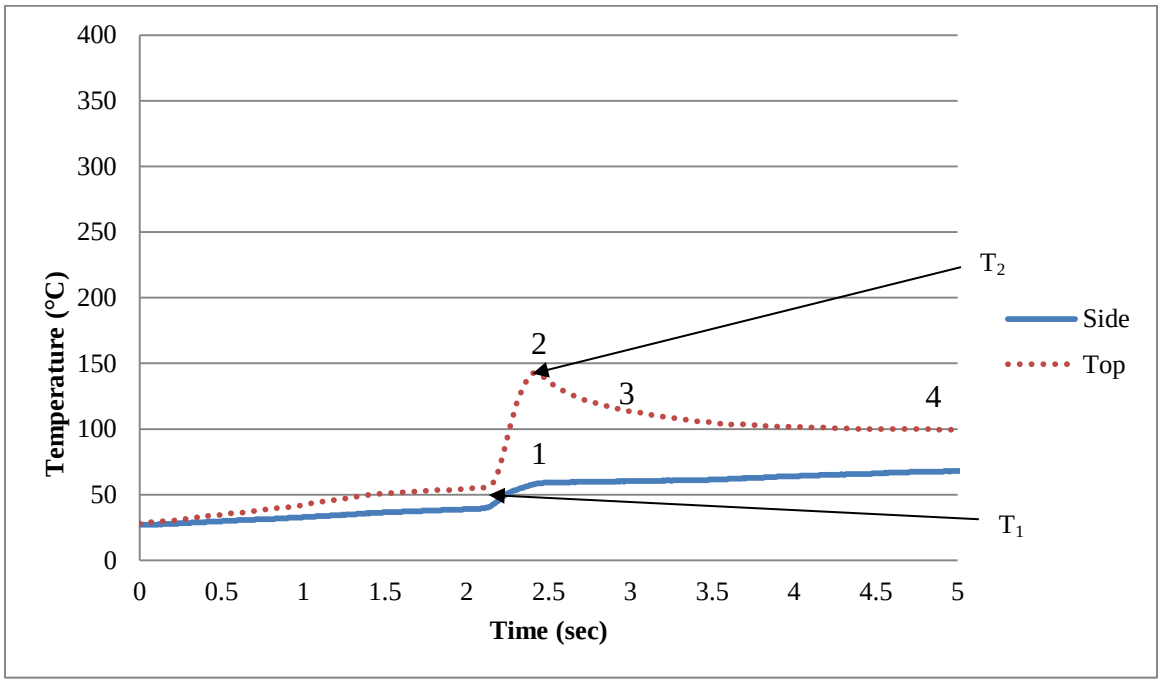

Fig. 4.22. Bu75 droplet which ignites at 2.14 seconds in 100°C ambient temperature but flame extinguishes and leaves a droplet on the fibers; D_0 = 0.65 mm; $D_{ignition}$ = 0.61mm; D_{fs} = 0.43 mm; D_{final} = 0.42 mm; $T_{ignition}$ = 39.0°C

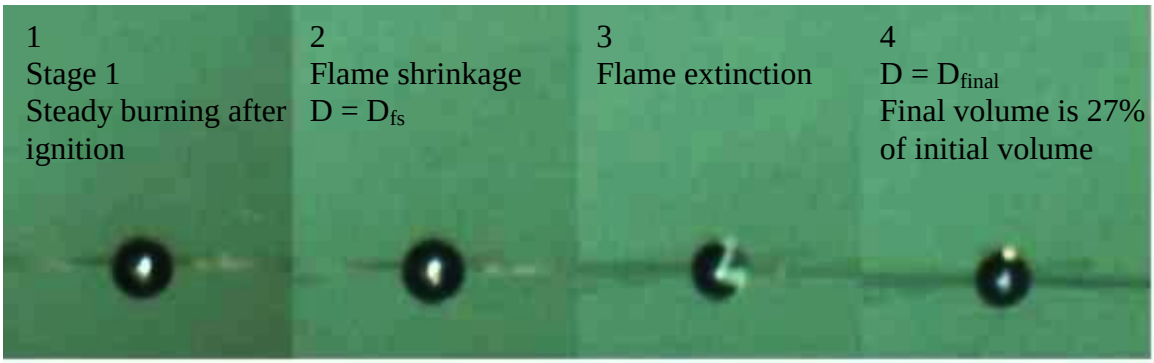

Fig 4.23. Images taken from video footage captured for the case shown in Fig. 4.22

In two Bu75 droplet tests the droplets ignited, burned steadily and then experienced a small microexplosion followed by flame extinction. In these tests a liquid fuel droplet was left on the fibers, one of which had a measurable volume less than 25% its original suggesting some SBO had been lost during the explosion. A table, similar to Tables 4.12 and 4.13, summarizing the results of these two tests is shown in Table 4.14.

Table 4.14

Summary of all Bu75 tests resulting in incomplete combustion and exhibiting a microexplosion. Diameters listed are in units of millimeters, temperatures in degrees Celsius and ignition time is in seconds

D_0	$D_{ignition}$	D_{fs}	$D_{explode}$	$T_{ignition}$	Ignition Time	T_1	T_2	T_{final}
0.83	***0.80***	***0.61***	***0.76***	***44.3***	***2.77***	***62***	***289***	***NA***
0.95	0.86	0.66	0.72	59.5	5.40	78	332	NA

Fig. 4.24 shows thermocouple data generated from an experiment where a microexplosion occurred but the flame still extinguished leaving liquid fuel on the fibers. The plot corresponds to the test results reported in bold, italic font in Table 4.14. Corresponding images collected from video data recorded for the burning droplet is shown in Fig. 4.25. The numbers represent the time segment labeled on the temperature plot. As can be seen from the temperature plot there was a period of steady burning during which the temperature rise observed by the upper thermocouple is quite significant. The temperature from the flame gets much higher than that of the test shown in Fig. 4.22. In fact the temperature rise (T_2-T_1) for both cases listed in Table 4.14 closely resembles that of the cases which experienced complete combustion. Somehow though, the flame was extinguished and the droplet stopped burning. The microexplosion phenomenon can be observed from the video data however is not apparent on the temperature plot. This is most likely because the flame had diminished at the time of microexplosion and never re-ignited.

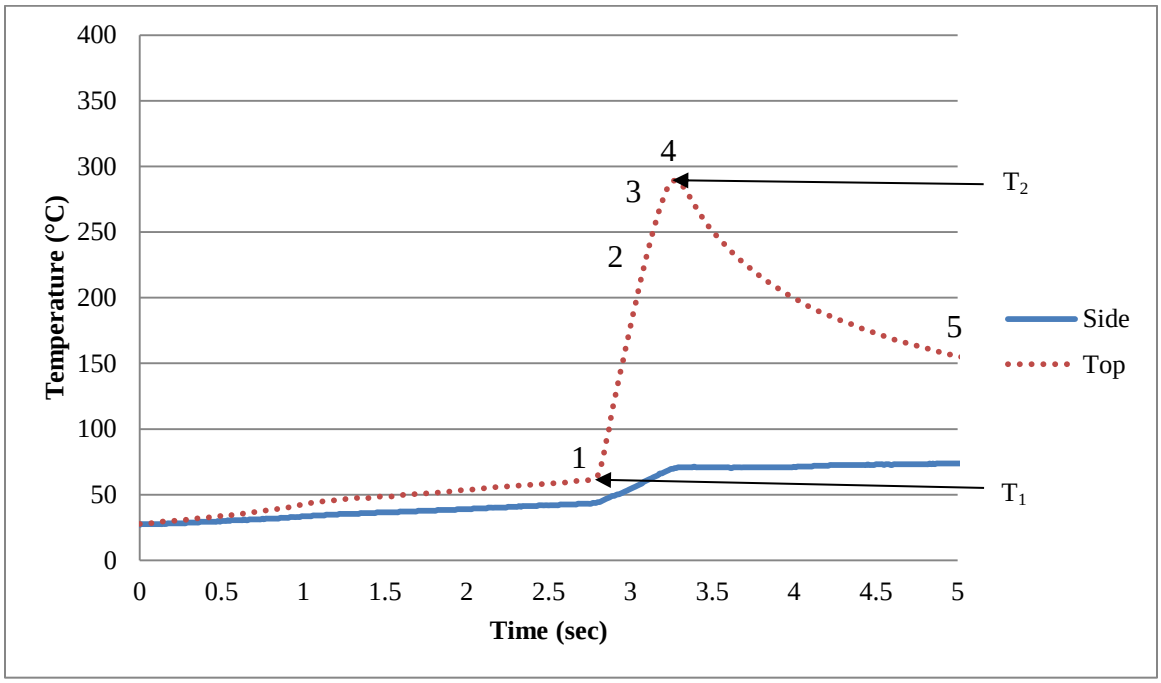

Fig 4.24. Bu75 droplet which ignites in 2.77 seconds and explodes in 100°C ambient temperature, explodes but flame extinguishes and leaves a droplet on the fibers; D_0 = 0.83 mm; $D_{ignition}$ = 0.80 mm; D_{fs} = 0.61 mm; $D_{explode}$ = 0.76 mm; $T_{ignition}$ = 44.3°C

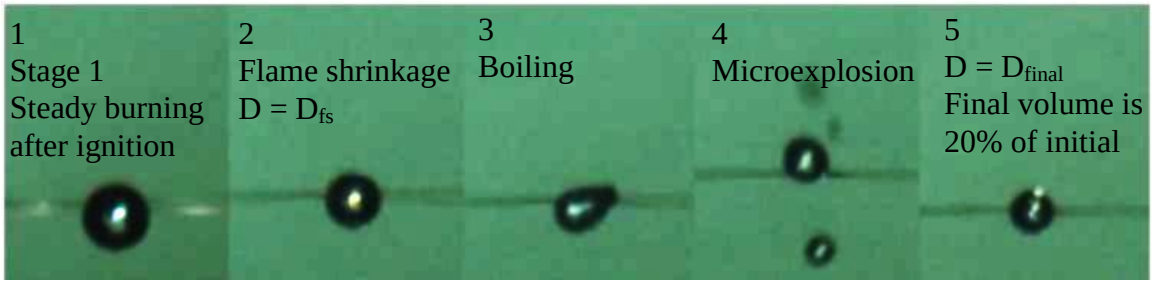

Fig. 4.25. Images taken from video footage captured for the case shown in Fig. 4.24

4.3.7 Mixed Fuel – Bu50

Tests were also performed using 50/50 - SBO/butanol fuel droplet mixtures at an ambient temperature of 100°C. The ignition behavior further reinforced that the flashpoints of SBO/butanol mixtures will resemble that of pure butanol as ignition occurred at similar temperatures as the Bu75 blend and pure butanol droplets. Sixteen tests were analyzed all of which experienced ignition with the side reference thermocouple reading at or above 36°C. Because of the lower content of butanol in the initial droplet the time to

ignition was not varied as much as in the Bu75 case. Experimental results proved that ignition was not possible for Bu50 after 5 seconds in 100°C ambient temperature suggesting that a significant amount of butanol had evaporated from the droplet and that ignition is then dependent on the flashpoint of pure SBO (greater than 100°C). Time to ignition for these tests ranged from 1.31 to 3.44 seconds and on average the ignition time was 1.99 seconds.

For the droplets which exhibited complete combustion the initial diameter (D_0) , diameter at ignition ($D_{ignition)}$, diameter prior to the third stage of combustion (flame shrinkage 'D_{fs}') and the diameter of the expanded bubble at the instant before the microexplosion ($D_{explode}$) were measured using the Xcytex ProAnalyst^{TM} software. The time to ignition and ignition temperature observed from the side thermocouple were reported. The temperature at ignition (T_1) observed from the upper thermocouple (see Fig. 3.5) was recorded as well as the temperature rise associated with flame present during the first stage of combustion (T_2) observed from the same thermocouple. The final temperature rise produced by the complete combustion of the droplet (T_{final}) was also recorded so that the temperature rise during the first and third stages could be compared. Table 4.15 has been prepared to summarize all Bu50 tests performed which exhibited complete combustion.

Table 4.15

Summary of all Bu50 tests resulting in incomplete combustion and exhibiting a microexplosion. Diameters listed are in units of millimeters, temperatures in degrees Celsius and ignition time is in seconds

D_0	$D_{ignition}$	D_{fs}	$D_{explode}$	$T_{ignition}$	Ignition Time	T_1	T_2	T_{final}
0.69	0.67	0.60	0.86	38.5	1.81	52	51	237
0.72	0.68	0.64	1.05	36.0	1.31	52	156	301
0.75	0.69	0.60	0.93	38.4	2.00	53	170	261
0.76	0.71	0.66	1.03	41.6	2.21	55	154	361
0.83	0.81	0.73	1.12	40.1	1.36	51	170	340
0.84	0.81	0.73	1.26	41.6	2.35	55	160	264
0.90	***0.85***	***0.80***	***1.20***	***42.6***	***1.60***	***55***	***203***	***338***

Fig. 4.26 shows thermocouple data generated from a mixed fuel droplet for a case where complete combustion occurred. The plot corresponds to the test results reported in bold, italic font in Table 4.15. Corresponding images collected from video data recorded for the burning droplet is shown in Fig. 4.27. The numbers represent the time segment labeled on the temperature plot. As expected, every Bu50 droplet test resulting in complete combustion exhibited a microexplosion after flame shrinkage. The flame shrinkage is signified by a near horizontal line at the point T_2 was measured. The temperature at the thermocouple stops rising at this point because the flame becomes smaller as the droplet interior heats.

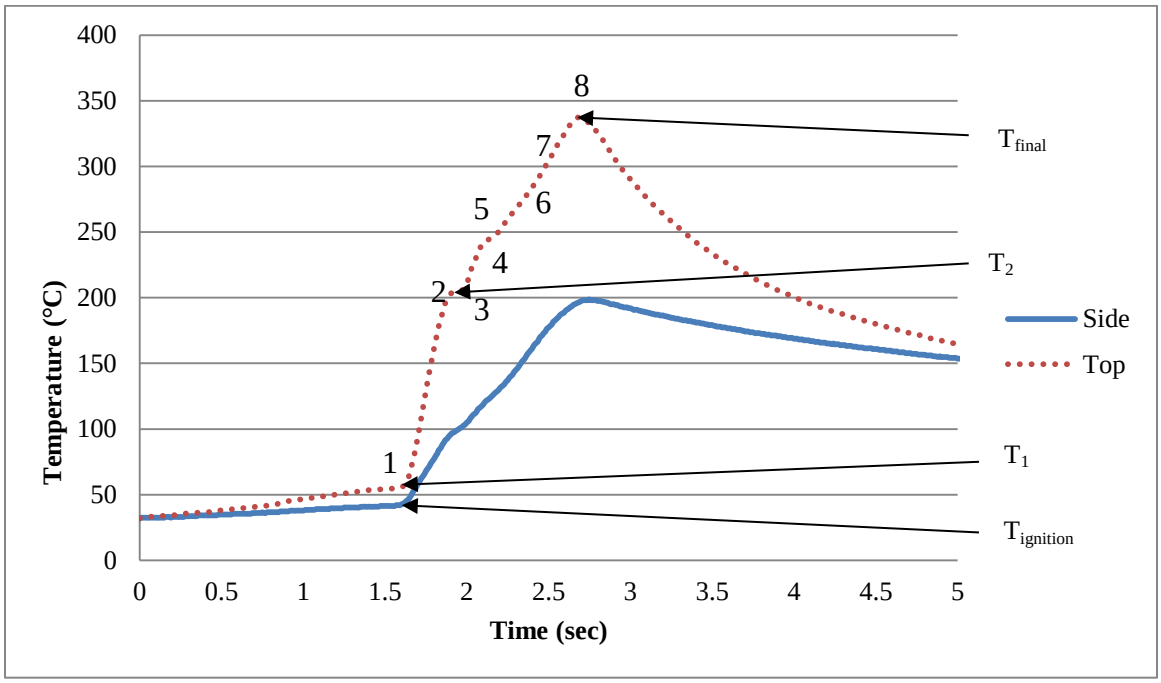

Fig. 4.26. Bu50 droplet which ignites in 1.60 seconds in 100°C ambient temperature and burns completely; D_0 = 0.90 mm; $D_{ignition}$ = 0.85 mm; D_{fs} = 0.80 mm; $D_{explode}$ = 1.2 mm; $T_{ignition}$ = 42.6°C

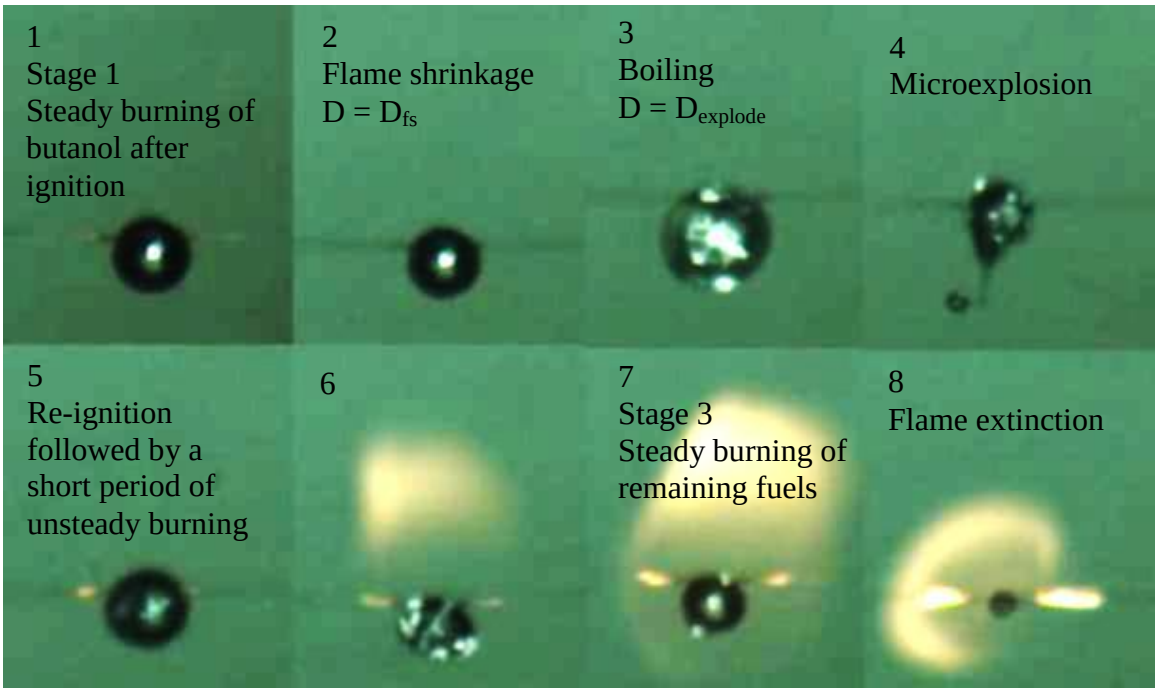

Fig. 4.27. Images taken from video footage captured for the case shown in Fig. 4.26

Similar to the Bu75 fuel droplets the first stage of combustion is characterized by a nonluminous flame signifying no soot and thus the burning of butanol. After the microexplosion the rest of the combustion process is characterized by a distinguishable orange flame representing soot formation from the burning SBO. Just like the burning rate plots produced from Botera et al's studies (Fig. 2.3) the microexplosion and transition period happen earlier in the droplets lifetime in comparison to a mixture with a higher concentration of butanol. The temperature rise collected from the top thermocouple was on average 40% of the overall temperature rise compared to 60% for the Bu75 mixture suggesting less burning must take place before the microexplosion occurs and that the explosion happens sooner in the combustion process. The unsteady burning at the onset of the third stage (i.e. when the microexplosion is occurring) is twice as long as that of the Bu75 case as well. This can be observed when comparing the time period after flame shrinkage to steady burning in the third stage in Fig. 4.20 (Bu75), where this period is approximately 13% of the total time from ignition to extinction, with Fig. 4.26 (Bu50) where this time period accounts for approximately 25% of the total burning time. The microexplosions also prove to be more violent for Bu50 than Bu75. This is evident from comparing the more unsteady transition period on the temperature profile graphs as well as comparing the size of the expanded bubbles prior to the explosion ($D_{explode}$) using Tables 4.12 and 4.15. On average, the size of the expanded droplet prior to the explosion compared to the initial droplet size is 34% larger for Bu50 droplets which exhibit complete combustion than that of Bu75 droplets. In the particular case of the experimental results shown in Figs. 4.26 and 4.27 it is almost as if there were two separate microexplosions. This was not necessarily the case but rather a long lasting microexplosion. The droplet diameters at flame shrinkage once again suggested that butanol was still present in the droplet prior to the microexplosion which is consistent with previous research findings.

In contrary to the Bu75 case, very few droplet tests did not exhibit a microexplosion. Only two of the sixteen tested samples ignited and did not experience a microexplosion. These two samples ignited with a nonluminous flame, burned for a short period and the

flame extinguished without exploding or re-igniting with an orange flame. It shows consistency that microexplosions are necessary for a third stage of combustion to occur for SBO/butanol fuel droplets. The test results for these two experiments are shown in Table 4.16. A diameter measurement was taken after the flame extinguished for both of these cases and the resultant volume calculated suggested that there was still butanol present in the droplet reinforcing the idea that some butanol is trapped within the droplet while combustion is occurring.

Table 4.16

Summary of all Bu50 tests resulting in incomplete combustion and no microexplosion. Diameters listed are in units of millimeters, temperatures in degrees Celsius and ignition time is in seconds

D_0	$D_{ignition}$	D_{fs}	D_{final}	$T_{ignition}$	Ignition Time	T_1	T_2	T_{final}
0.76	***0.74***	***0.71***	***0.61***	***41.3***	***1.75***	***54***	***161***	***NA***
0.80	0.77	0.67	NA	43.1	1.86	52	151	NA

Fig. 4.28 shows thermocouple data generated from one of these droplets. The plot corresponds to the test results reported in bold, italic font in Table 4.16. Corresponding images collected from video data recorded for the burning droplet is shown in Fig. 4.29. The numbers represent the time segment labeled on the temperature plot. The images from the video data in Fig. 4.29 and the lack of unsteady temperature rise in corresponding temperature plot (Fig. 4.28) show that no microexplosion occurred. From the temperature plot it is shown that the droplet ignites at about 40°C (similar to other droplet tests) and burns steadily for a period of time and the stops burning. Fig. 4.29 shows that the flame is nonluminous throughout the combustion process suggesting that only the butanol is burning. Video recording was prolonged so that a final diameter of one of these droplets could be measured about nine seconds after the flame was extinguished (sufficient time to evaporate all the butanol according to evaporation studies) and the volume calculated was equal to 52% of the initial volume. With no orange flame present during combustion this suggests that the butanol burned initially, there was still butanol present when the flame ceased and then the remaining butanol

evaporated from the droplet during that nine second period leaving pure, liquid SBO behind.

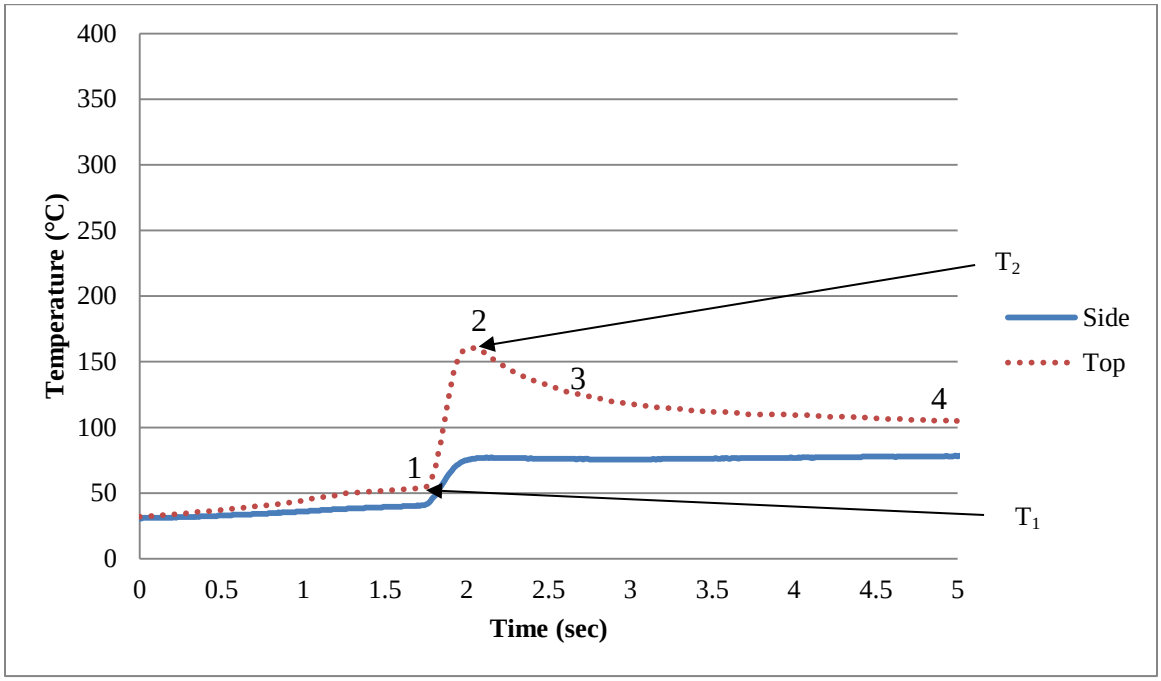

Fig. 4.28. Bu50 droplet which ignites in 1.75 seconds in 100°C ambient temperature and the flame extinguishes; D_0 = 0.76 mm; $D_{ignition}$ = 0.74 mm; D_{fs} = 0.71 mm; D_{final} = 0.61 mm $T_{ignition}$ = 41.3°C

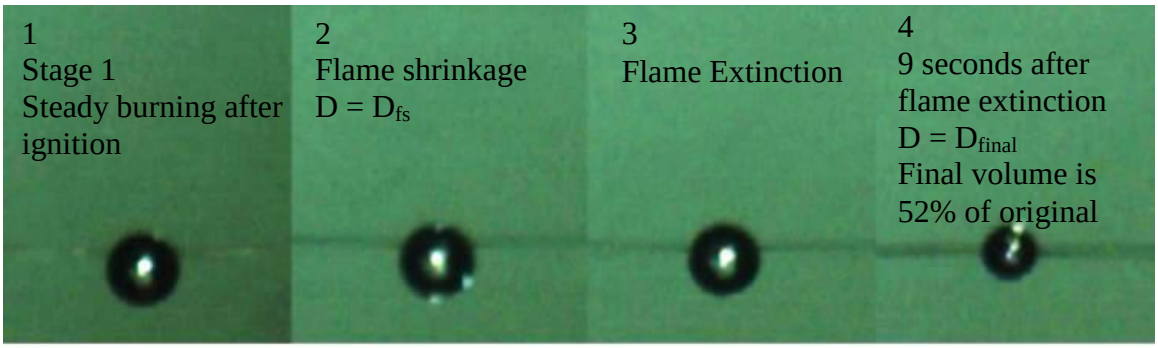

Fig. 4.29. Images taken from video footage captured for the case shown in Fig. 4.28

Similar sized droplets to the one analyzed in Fig. 2.28 and 4.29 with similar ignition times have proved to result in complete combustion. Consequently, initial droplet size and the ignition time do not seem to be the determining factor for whether the droplet will burn completely. However, microexplosions must occur for complete combustion.

There are no cases for either of the discussed mixture ratios where a complete combustion of the fuel droplet has occurred without exhibiting a microexplosion. Because of this and the suggestion by the Lasheras and Botera research groups that microexplosions could improve atomization it is of interest to focus on the cause of microexplosions as well as the cause of incomplete combustion. The occurrence of microexplosions for single mixed fuel droplets with high volatility differentials seems to be more dependent on the initial concentrations than droplet size and ignition time. The Bu50 mixed droplets proved to be more prone to have microexplosions during combustions than the Bu75 mixtures.

Seven of the sixteen tests resulted in the droplets boiling and exploding prior to leaving a fuel droplet on the fibers without an ignition in the third stage of combustion. A summary of all the test results exhibiting this behavior is provided in Table 4.17. The initial diameters and the ignition times are similar to the other droplet tests using the Bu50 blend. The volume of the remaining droplets, after the microexplosion had occurred were also measured to be smaller than or equal to 50% of the initial volume suggesting that some SBO was lost in the occurrence of the explosion. Video footage provided evidence (nonluminous flame) that the SBO was not burned in the first stage prior to the microexplosion.

Table 4.17

Summary of all Bu50 tests resulting in incomplete combustion and exhibiting a microexplosion. Diameters listed are in units of millimeters, temperatures in degrees Celsius and ignition time is in seconds

D_0	$D_{ignition}$	D_{fs}	$D_{explode}$	$T_{ignition}$	Ignition Time	T_1	T_2	T_{final}
0.74	0.70	0.66	1.01	40.7	1.35	52	139	139
0.79	0.75	0.69	1.04	39.3	1.93	49	137	178
0.82	0.78	0.71	0.73	41.2	1.51	53	158	158
0.82	0.76	0.74	0.92	46.3	2.53	61	164	183
0.83	0.78	0.68	1.38	49.6	3.44	66	153	181
0.87	0.85	0.77	0.83	47.0	2.23	54	169	184
0.90	***0.86***	***0.80***	***1.24***	***45.7***	***2.54***	***60***	***144***	***180***

Fig. 4.30 shows thermocouple data generated from one of these droplets. The plot corresponds to the test results reported in bold, italic font in Table 4.17. Corresponding images collected from video data recorded for the burning droplet is shown in Fig. 4.31. The numbers represent the time segment labeled on the temperature plot.

As can be seen from the temperature plot and the video images in Figs. 4.30 and 4.31 the droplet starts to burn similarly to one resulting in a complete combustion. The first burning stage exhibits a nonluminous flame until flame shrinkage occurs. The droplet then swells and explodes in a similar manner to the droplet analyzed in Fig. 4.26 (Bu50 which undergoes complete combustion). The boiling and explosions are more violent and occur at an earlier period in the droplets lifetime than that of a Bu75 droplet. The temperature plot shows that heat was actually released and sensed by the upper thermocouple during the explosion. The amount of heat released during the explosion is more than in similar cases (explosion and incomplete combustion) for the Bu75 mixtures as well. Actually no heat was shown to be sensed by the upper thermocouple for the Bu75 cases of microexplosion and incomplete combustion. In five of the seven tests listed in Table 4.17 a temperature rise was sensed during the explosion. This further

suggests more violent microexplosions for the droplets of equal initial concentrations which is consistent with the Lasheras group's findings.

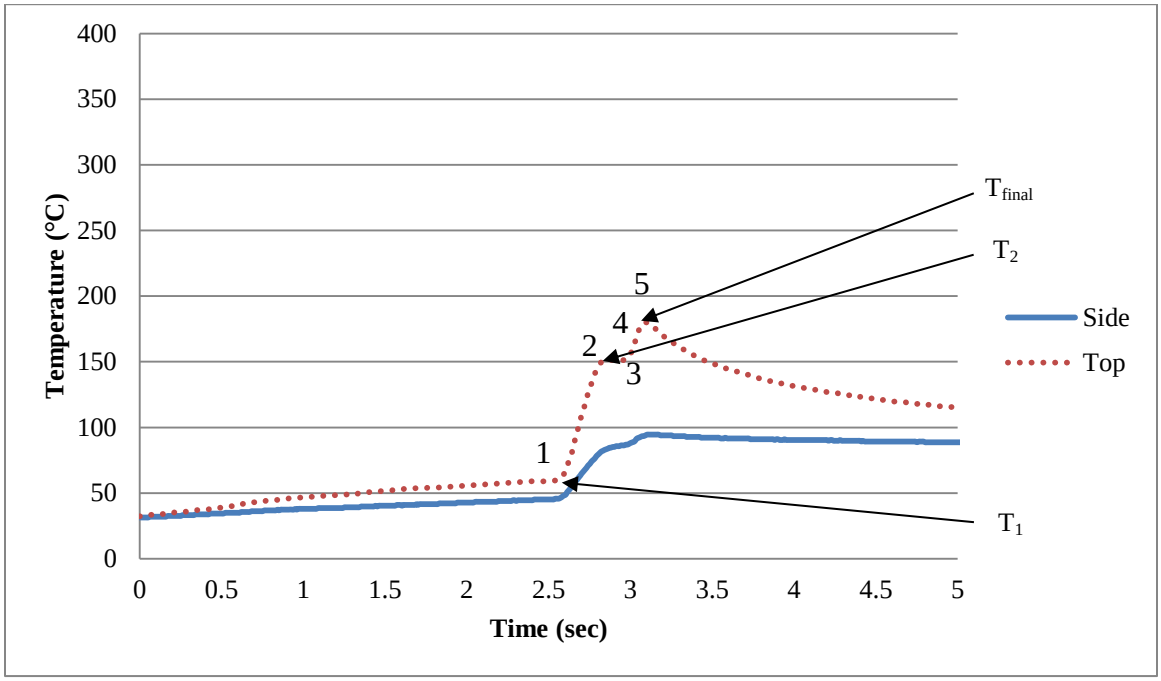

Fig. 4.30. Bu50 droplet which ignites in 2.54 seconds in 100°C ambient temperature, explodes and leaves a fuel droplet behind; D_0 = 0.90 mm; $D_{ignition}$ = 0.86 mm; D_{fs} = 0.80 mm; $D_{explode}$ = 1.24 mm; D_{final} = 0.70 mm; $T_{ignition}$ = 45.7°C

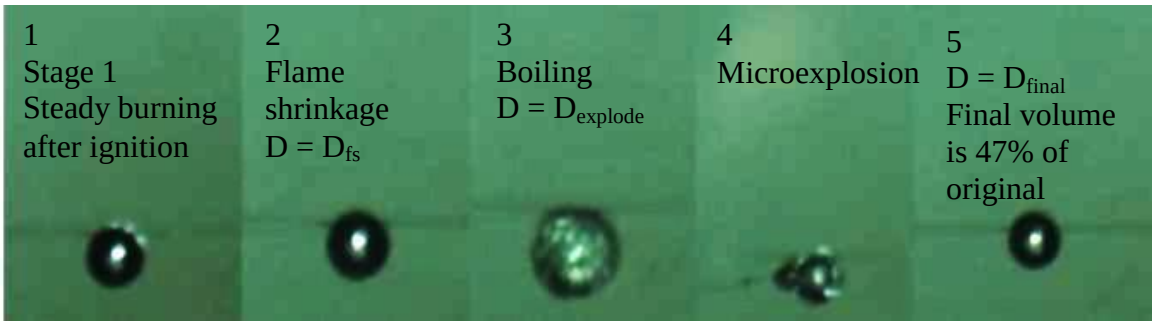

Fig. 4.31. Images taken from video footage captured for the case shown in Fig. 4.30

In this study it was not possible to assume that the droplets which experienced microexplosions and did not re-ignite in the third stage would have done so in a spray combustion application. It makes sense that in past research the incomplete combustion phenomena did not occur because most research groups were using auto ignition to ignite

the droplets which provides much more energy throughout the droplet lifetime to make sure the less volatile component could be ignited. Groups which used spark or hot wire ignition techniques were not using fuel mixtures with candidate properties to produce microexplosions (i.e. not significant volatility differentials). This is a viable reason that their fuel droplets would always exhibit complete combustion. The process used here may be more accurate for categorizing a fuel mixture based on combustion behavior because it better represents ignition at the flashpoint of the fuel. It also allows for the study of the combustion behaviors dependence primarily on the droplet properties. This is because the droplet is ignited in an ambient temperature below the boiling point of the more volatile fuel and the igniter is removed immediately resulting in complete dependence of the droplet properties on its burning behavior. Whether the droplet will burn completely, or not and whether a microexplosion will occur depends solely on the temperature the droplet reaches during the combustion process and the relative concentrations throughout the droplets lifetime.

4.3.8 Mixed Fuel – Bu40

Experimental results show that droplet mixtures of components with high volatility differences have a tendency to experience microexplosions and at a greater intensity when the initial concentrations of the pure components are nearly equal. It has been suggested by Lasheras et al. that slightly lower than equivalent concentration of the more volatile component (~40%) produce even more intense explosions than a 50/50 mixture for some fuel mixtures [37]. Also, experts have suggested that microexplosions could actually have a beneficial effect on combustion for atomization applications because the fuel components are broken up better mixing them with the oxidizing gases in a combustion chamber [35], [37]. Because of these reasons it was desired to look more in depth into the microexplosion phenomenon and perform additional experiments using Bu40 droplets.

Similar combustion tests to the 25/75 and 50/50 - SBO/butanol were performed on multiple Bu40 droplets. Ignition of the droplets was achieved at similar ignition times

and temperatures suggesting that the fuel mixture has the same flashpoint as the other mixtures and pure butanol. As expected the occurrence of microexplosions was nearly as often as that of the Bu50 droplets. However the microexplosions were more violent causing many of the droplets to explode and fall off the fibers. Fifteen single droplet tests were performed using the Bu40 mixture eight of which exploded and fell off the fibers. This was not nearly as common for the other mixtures. Droplet size analysis for microexplosion comparison could be done on these droplets however, whether the droplets would have undergone complete combustion or not remained unknown. Three droplets burned completely, four tests resulted in incomplete combustion (liquid fuel left on the fibers), two without a microexplosion and two tests which did exhibit microexplosions. It was expected that the droplets which fell off the fibers would have undergone complete combustion and there was some video evidence that an orange flame was present when the droplet was falling but these tests were not considered for comparison with the other fuel droplets for complete/incomplete combustion analysis. They were however used for comparison on whether microexplosions occurred or not.

A summary of the test results for the three Bu40 experiments which resulted in complete combustion provided in Table 4.18. The droplets were of similar size to the other mixtures studied and ignited at similar ignition times.

Table 4.18

Summary of all Bu40 tests resulting in complete combustion. Diameters listed are in units of millimeters, temperatures in degrees Celsius and ignition time is in seconds

D_0	$D_{ignition}$	D_{fs}	$D_{explode}$	$T_{ignition}$	Ignition Time	T_1	T_2	T_{final}
0.68	0.67	0.64	0.69	35.7	1.29	49	70	157
0.76	***0.73***	***0.72***	***1.02***	***44.9***	***1.65***	***56***	***93***	***253***
0.77	0.76	0.75	0.96	42.5	1.05	47	80	250

Fig. 4.32 shows thermocouple data generated from one of these experiments. The plot corresponds to the test results reported in bold, italic font in Table 4.18. Corresponding images collected from video data recorded for the burning droplet are shown in Fig. 4.33.

The numbers represent the time segment labeled on the temperature plot. As can be seen from the temperature plot the transition period (flame shrinkage) and the microexplosion happens much sooner in the droplets lifetime than the other mixtures. This means that less fuel (butanol) is burned in the first stage. The temperature rise sensed by the upper thermocouple in the first stage is on average 14% of the total temperature rise associated with the combustion process. This is much lower than the previous two mixtures discussed. This could imply that there is actually more butanol left in the droplet at the time of the microexplosion making the microexplosion more intense. The microexplosion lasts longer and is even more violent than that of 50/50 mixtures as hypothesized. This is in agreement with Lasheras et al's data for n-Paraffin/ethanol mixtures. The video images show that the droplets burn in a three staged manner like the other mixtures.

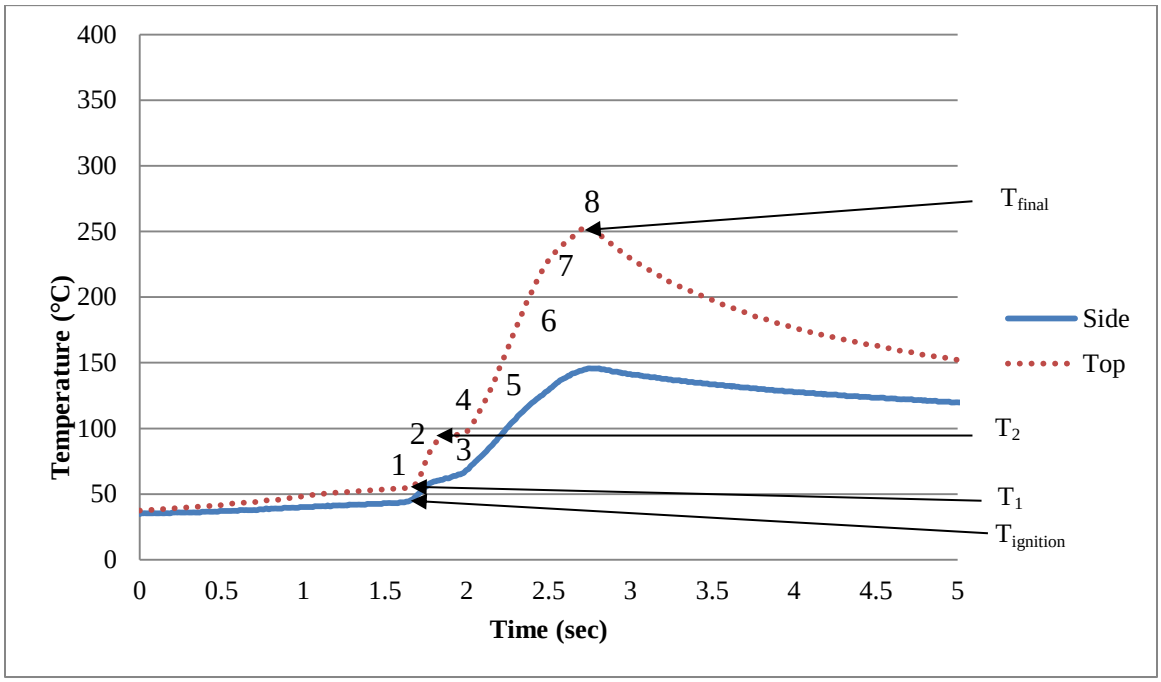

Fig. 4.32. Bu40 droplet which ignites in 1.65 seconds in 100°C ambient temperature and burns completely; D_0 = 0.76 mm; $D_{ignition}$ = 0.73 mm; D_{fs} = 0.72 mm; $D_{explode}$ = 1.02 mm; $T_{ignition}$= 44.9°C

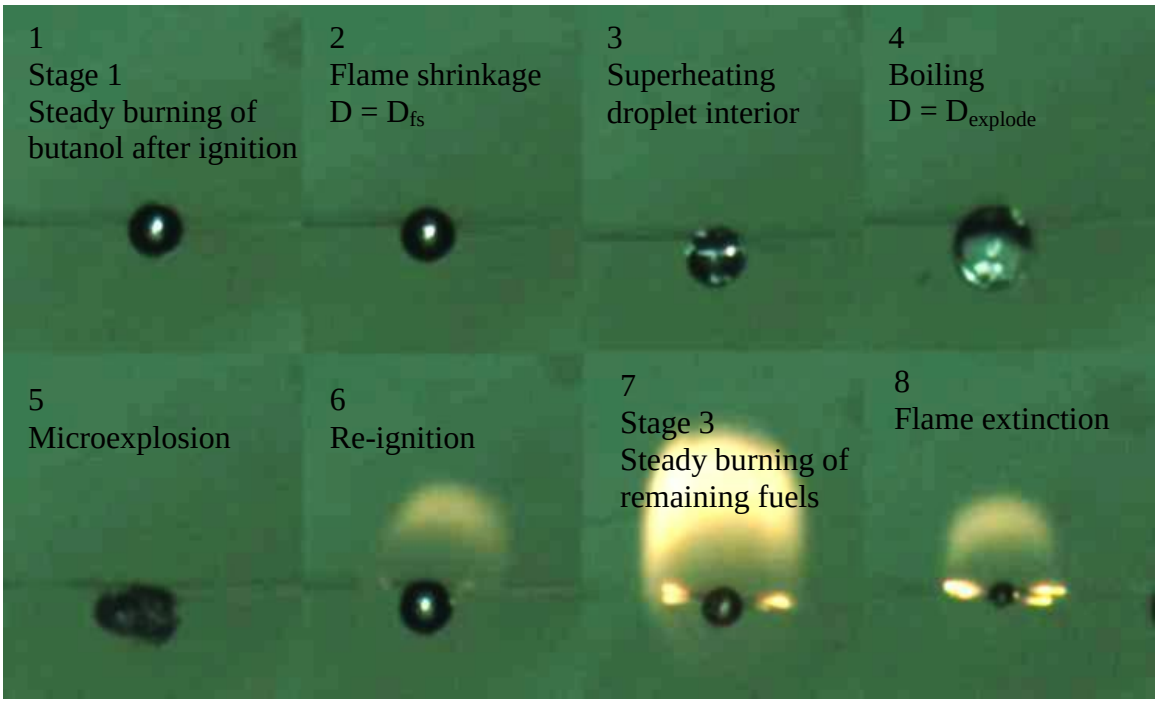

Fig. 4.33. Images taken from video footage captured for the case shown in Fig. 4.32

Table 4.19 presents a summary of the experimental results for the two tests which did not exhibit a microexplosion and left a liquid droplet on the fibers after the flame was extinguished. The droplets are much larger than the droplets which burned completely suggesting that the initial diameter may be the most influential factor for this mixture on whether or not complete combustion will occur.

Table 4.19

Summary of all Bu40 tests resulting in incomplete combustion and no microexplosion. Diameters listed are in units of millimeters, temperatures in degrees Celsius and ignition time is in seconds

D_0	$D_{ignition}$	D_{fs}	D_{final}	$T_{ignition}$	Ignition Time	T_1	T_2	T_{final}
0.90	0.89	0.87	NA	44.8	1.60	57	110	NA
1.02	***0.98***	***0.96***	***0.87***	***44.8***	***2.00***	***57***	***134***	***NA***

A similar temperature profile plot to the one in Fig. 4.32 has been prepared. It is shown in Fig. 4.34 and the data corresponds to the droplet results reported in bold, italic font in

Table 4.19. Video data for the same test is shown in Fig. 4.35. The numbers representing the time segment in the combustion process on the temperature plot correspond to the numbered video images. From the video data it is apparent that only butanol burns before the flame is extinguished because there is no orange flame throughout the combustion process. It is also apparent from the temperature plot that the temperature rise due to the burning of the fuel sensed by the upper thermocouple is much higher than the temperature rise ($T_2 - T_1$) during the first burning stage in the cases of complete combustion. That means the temperature at the surface of the droplet prior to flame extinction was at least that of the surface temperature at flame shrinkage for a droplet which burned completely. This means that the initial droplet size must have affected the combustion process and the interior of the droplet was not able to be superheated resulting in no microexplosion. Either the surface layer of pure SBO was too thick for sufficient heat transfer to the inside of the droplet to occur or there was not enough butanol trapped within the surface to cause homogeneous nucleation and burst the droplet. The latter does not seem to be the case because comparing the droplet diameter at flame shrinkage with the initial diameter suggests that the droplet still consists of about 30% butanol by volume. Like the other mixtures, for one experiment resulting in incomplete combustion and no microexplosion, video footage was prolonged after flame extinction to take a final diameter measurement. This measurement was taken about six seconds after flame extinction which is sufficient time to evaporate the amount of butanol which would have been remaining in the droplets. The final diameter was measured and the volume calculated was 62% of the initial volume which suggests since no microexplosion or orange colored flame was present during the combustion process that the final liquid droplet was pure SBO.

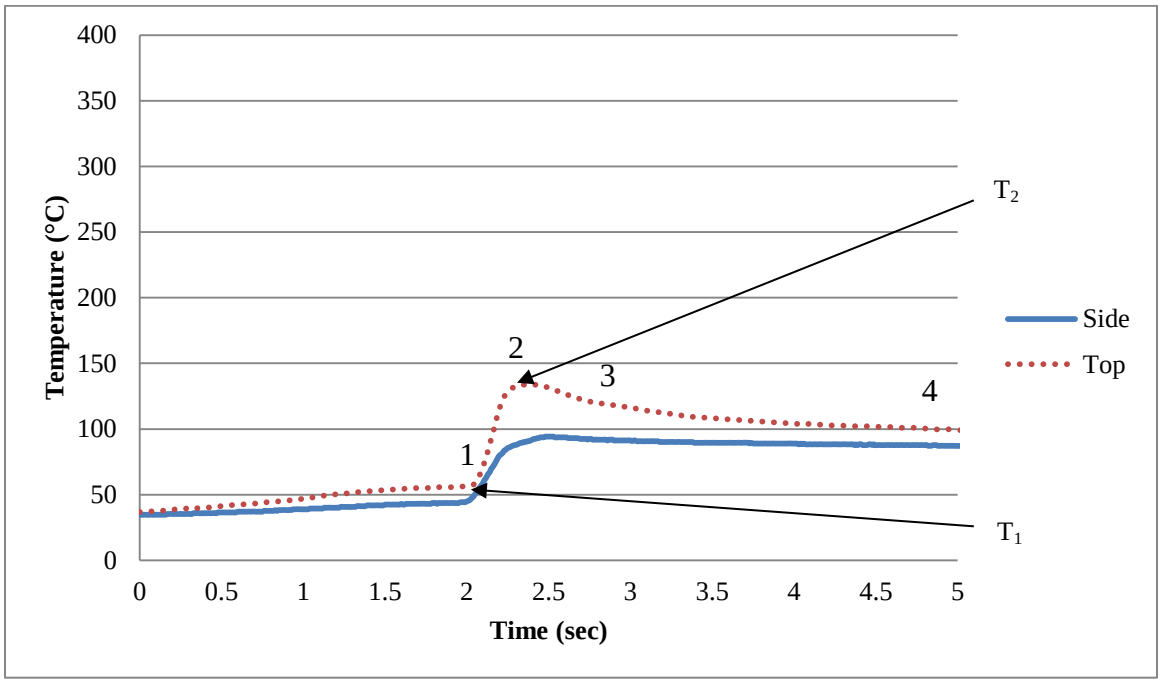

Fig. 4.34. Bu40 droplet which ignites in 2.00 seconds in 100°C ambient temperature and leaves a fuel droplet behind with no explosion; D_0 = 1.02 mm; $D_{ignition}$ = 0.98 mm; D_{fs} = 0.96 mm; D_{final} = 0.87 mm; $T_{ignition}$ = 44.8°C

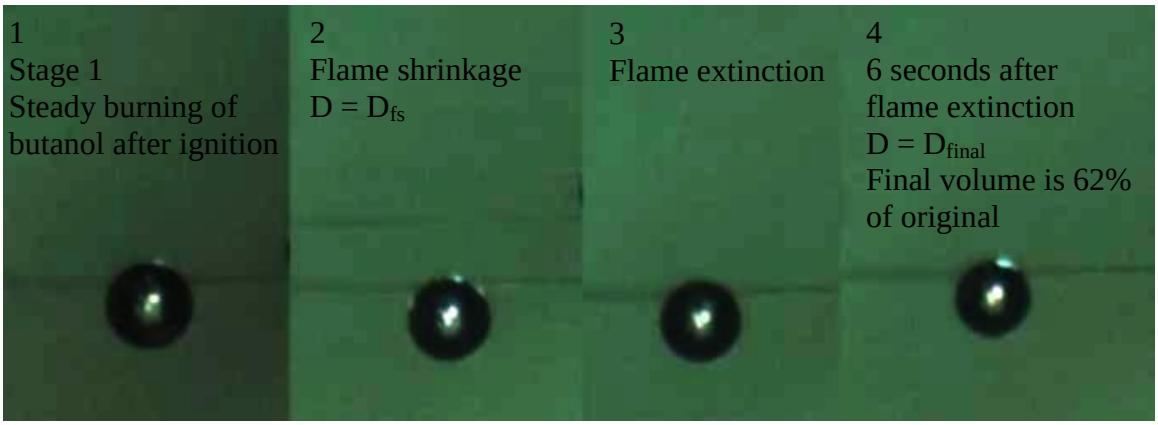

Fig. 4.35. Images taken from video footage captured for the case shown in Fig. 4.34

Table 4.20 presents a summary of the experimental results for the two tests which did exhibit a microexplosion but did not re-ignite and burn completely. There is one very large droplet and one that is of similar size to the droplets which burned completely listed in Table 4.18. The large droplet exploding contradicts the statement that the large diameter prevents the superheating of the inside of the droplet. However, droplet size

data suggests for the larger droplet that significantly more butanol had burned during the initial burning stage than those which didn't exhibit a microexplosion. This suggests that maybe the prolonged flame surrounding the droplet provided sufficient heat to superheat the interior. It is still important to try to understand why the droplets did not re-ignite. Experimental results showed that these two particular tests resulted in the most violent microexplosions (if violence is defined as the size of the bubble before the explosion compared to the initial size). These two droplets expanded over 260% of their original volume prior to the microexplosion compared to an average of 180% for the droplets which re-ignited and burned completely. The microexplosion could have resulted in an energy loss so great that the third burning stage was not possible. Alternatively, all the remaining butanol, which would re-ignite at a lower temperature and help to ignite the SBO, was ejected during the violent explosion of the droplet.

Table 4.20

Summary of all Bu40 tests resulting in incomplete combustion exhibiting a microexplosion. Diameters listed are in units of millimeters, temperatures in degrees Celsius and ignition time is in seconds

D_0	$D_{ignition}$	D_{fs}	$D_{explode}$	$T_{ignition}$	Ignition Time	T_1	T_2	T_{final}
0.72	***0.70***	***0.68***	***1.32***	***37.4***	***1.25***	***52***	***85***	***110***
1.13	1.11	1.07	1.56	45.2	1.25	53	132	246

A temperature profile plot for the test results reported in bold, italic font in Table 4.20 has been prepared and is shown in Fig. 4.36. Corresponding video images with labeled time segments are shown in Fig. 4.37. From the temperature plot a microexplosion is evident and there is a temperature rise associated with it. The video images show how large the droplet expanded before bursting. It then boiled again but never exploded and the flame was extinguished leaving liquid fuel on the fibers.

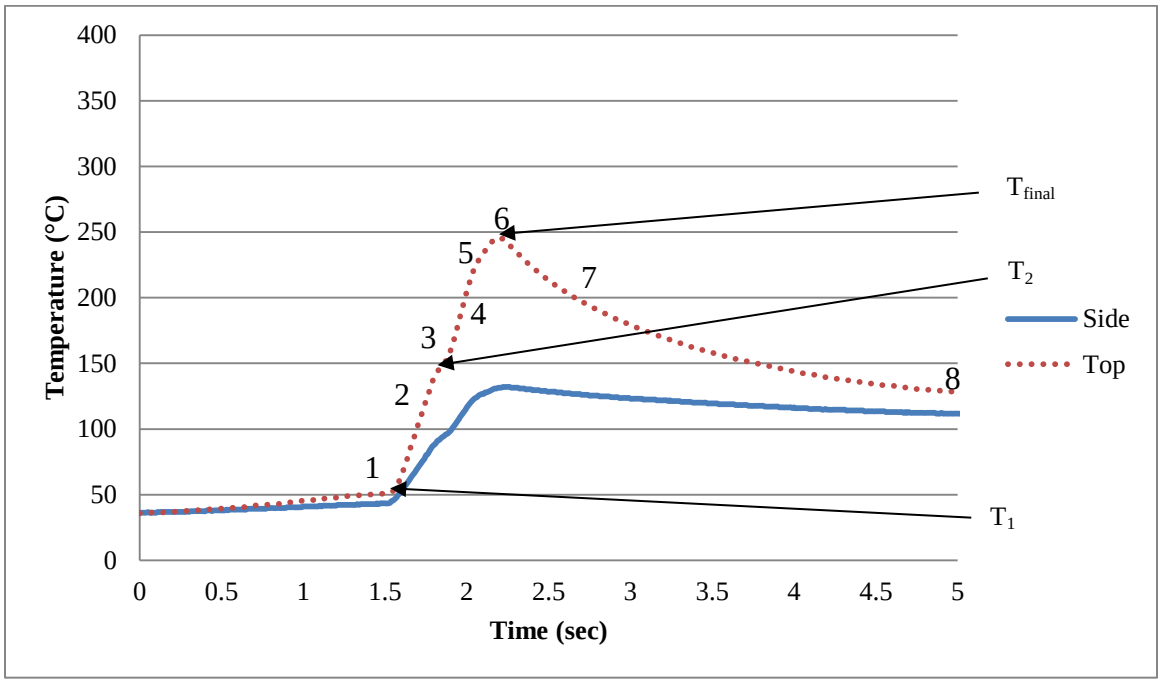

Fig. 4.36. Bu40 droplet which ignites in 1.25 seconds in a 100°C ambient temperature, explodes and leaves a fuel droplet behind; D_0 = 0.72 mm; $D_{ignition}$ = 0.70 mm; D_{fs} = 0.68 mm; $D_{explode}$ = 1.32 mm; $T_{ignition}$ = 37.4°C

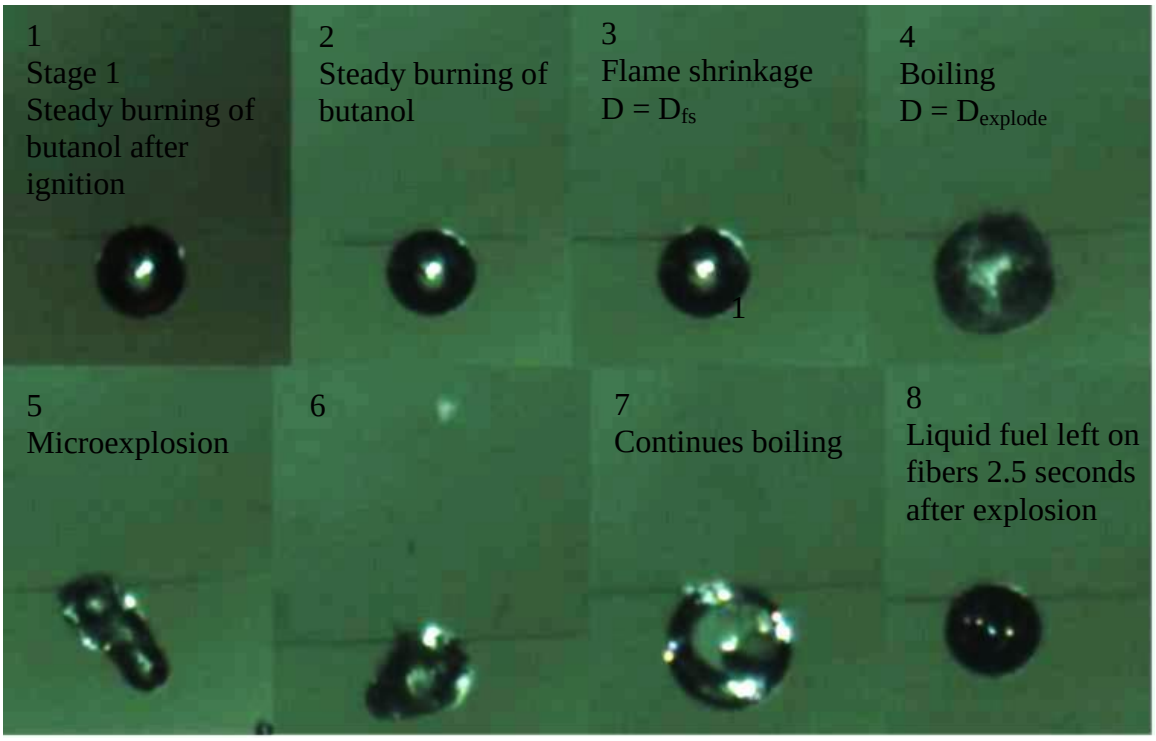

Fig. 4.37. Images taken from video footage captured for the case shown in Fig. 4.36

4.3.9 Mixed Fuel – Bu25

Combustion studies were also done for droplets consisting of 75% SBO and 25% butanol (Bu25) for completeness. From past research it was expected that this mixture would produce microexplosions less intensive as the Bu50 and Bu40 mixtures and even sooner in the droplets lifetime. The Bu25 droplets proved harder to ignite and produced microexplosions less frequently than any of the other mixtures studied. None of the tests resulted in complete combustion. Eight droplet tests were studied, seven of which did not exhibit a microexplosion. The test which did have an explosion occur fell from the fibers. This test was only used for explosion intensity analysis since all relevant measurements could be taken prior to it falling. The seven droplets tested which did not explode were on average larger than the droplets of the other mixtures studied. Unintentionally, larger droplets seemed to be formed for this mixture using a pipette. The droplets were ignited at similar ignition times however ignition was only achieved at times less than two seconds. This suggests that if left in the elevated temperature for too long (> 2 seconds) a sufficient amount of butanol will evaporate from the surface making ignition in a 100° C atmosphere impossible.

Table 4.21 lists the test results for the seven tests which did not burn completely or have a microexplosion. As mentioned there were no cases of complete combustion for this mixture.

Table 4.21

Summary of all Bu25 tests resulting in incomplete combustion and no microexplosion. Diameters listed are in units of millimeters, temperatures in degrees Celsius and ignition time is in seconds

D_0	$D_{ignition}$	D_{fs}	D_{final}	$T_{ignition}$	Ignition Time	T_1	T_2	T_{final}
0.84	0.81	0.79	NA	43.2	1.90	54	74	NA
0.84	0.82	0.81	NA	41.7	1.54	52	60	NA
0.89	***0.88***	***0.86***	***NA***	***42.6***	***1.63***	***53***	***65***	***NA***
0.94	0.92	0.91	NA	40.6	1.54	51	66	NA
0.97	0.95	0.95	NA	42.7	1.18	51	59	NA
1.00	0.98	0.98	NA	46.0	1.8	54	73	NA
1.02	1.01	0.99	NA	42.8	1.86	51	70	NA

A temperature profile plot generated from the thermocouples on the test reported in bold, italic font in Table 4.21 is shown in Fig. 4.38. Plots from all tests are very similar. It was nearly impossible to see the burning droplet with the camera so video data is really not of interest for the Bu25 mixture. A slight temperature rise sensed by the upper thermocouple signified that the droplet had ignited. From the plot it is apparent that the temperature rise is very small compared with the other mixtures tested. The temperature read by the thermocouples continues to rise after flame extinction because the burning of the fuel fails to increase the temperature above the ambient temperature (100° C). This is likely the reason that the droplets did not explode or burn completely. From the diameter measurements at flame shrinkage (same as flame extinction in this case) in Table 4.21 it proves that butanol is still present in the droplets at the time the droplets cease to burn just like the other mixtures. However the low initial content of butanol results in an insufficient amount of it at the droplet surface at the time of ignition. Because of this the temperature of the droplet cannot get hot enough to superheat the interior, explode and re-ignite.

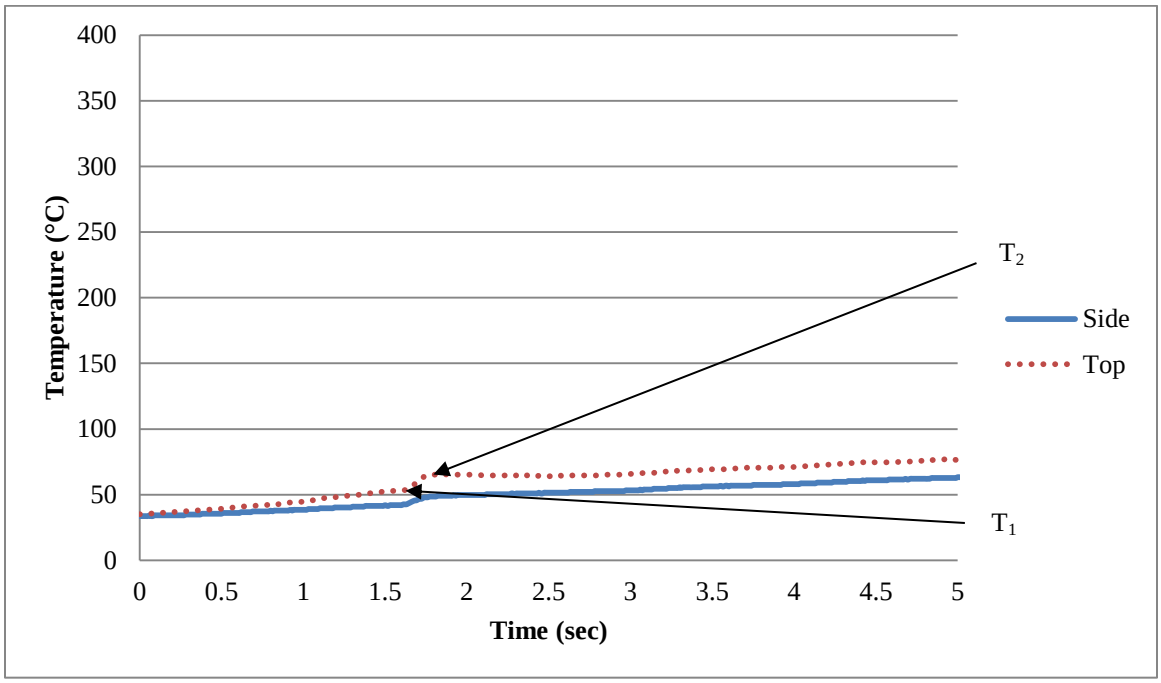

Fig. 4.38. Bu25 droplet which ignites in 1.63 seconds in a 100°C ambient temperature leaves a fuel droplet behind with no microexplosion; D_0 = 0.89 mm; $D_{ignition}$ = 0.88 mm; D_{fs} = 0.86 mm; $T_{ignition}$ = 42.6°C

4.3.10 Mixed Fuel – Comparison

When comparing SBO/butanol fuel mixtures for suitability in combustion applications there are many aspects to consider. Since the interest in this study is for its suitability for mostly atomization or spray combustion applications this study uses single fuel droplets to study combustion behavior. Single larger droplets can give insight to what the numerous smaller droplets in a spray combustion situation will behave like. First and foremost, since incomplete combustion was found to occur, it was necessary to compare the frequency of its occurrence between the mixtures of different concentrations. Experimental results proved this to be more common for the Bu75 and Bu25 blends. Since experts suggest that the microexplosions can benefit a combustion process by improving atomization it was necessary to compare the tendency that a microexplosion would occur for the different mixtures. It was also beneficial to compare the intensity of the microexplosions because more intense microexplosions lead to better breaking up of the fuel. Every droplet which burned completely exhibited a microexplosion. So

microexplosions are necessary for complete combustion to occur. It could also be theorized that droplets that did not burn completely would have a better chance of doing so if a microexplosion occurred in a spray combustion application where it would be surrounded by other burning droplets. The same thing could also be assumed for fuel droplets which fell off the fibers due to intensive microexplosions. Consequently, the best fuel mixture would be one that experiences microexplosions most often and most violently. This would however have some dependence on economic and environmental value as in most situations there are cost-quality tradeoffs.

Table 4.22 has been prepared to sum up the experimental results shown in the previous sections. Table 4.22 provides information on how many total experimental tests were analyzed for each mixture and how frequently different outcomes occurred. The number of tests analyzed includes all droplets which ignited including tests which fell off the fibers. The table provides the frequency of droplet tests which resulted in complete combustion (CC), incomplete combustion with no microexplosion (IC), incomplete combustion with a microexplosion (MEIC) and disruptive microexplosions which caused the droplets to fall off the fibers (DME). It can be observed from the table that microexplosions are much more common for mixtures of near equal concentration. It can also be observed that if one were to assume that microexplosions are beneficial to combustion that the mixtures of nearly equal concentration would be far more effective in a spray combustion application. If one were to assume the droplets which fell during a microexplosion would have ignited, the Bu40 blend would have resulted in complete combustion much more frequently than its nearest competitor (16% more often than the Bu50 blend).

Table 4.22

Summarization table providing total tests examined and frequency of responses for each mixture. Frequency data represents how often each outcome occurs compared to how many total tests were analyzed for that mixture

Fuel Blend	CC	IC	MEIC	DME	Total Tests Analyzed
Bu75	0.43	0.50	0.07	-	28
Bu50	0.39	0.11	0.39	0.11	18
Bu40	0.13	0.20	0.20	0.53	15
Bu25	-	0.88	0.12	-	8

The causes of the microexplosions and the droplets to burn completely must be investigated. Understanding that it is the diffusion rate limited gasification mechanism that causes the staged burning and superheating of the inside of the droplet may help to understand the dependence of initial parameters to produce the explosion. In all combustion cases the droplet size at flame shrinkage suggests that butanol was still present further clarifying the diffusion limited gasification mechanism. This means that the relevant concentration of butanol can be calculated at the time of ignition and after the first burning stage. It can be calculated by comparing the volume of the droplet at these times to that of the original volume and assuming the only species that has gasified is butanol. If it is not possible to take a diameter measurement the evaporation rate of pure butanol can be used to estimate the droplet size at ignition in various ambient temperatures. This means that in a spray combustion application if the diameter of the droplets leaving the nozzle is known and the time the droplets are in the combustion chamber prior to ignition a droplet size and relative concentration at ignition can be estimated. This is helpful because different amounts of fuel are burned during the first stage for each mixture. Knowing the concentration and volume of butanol at ignition one can estimate how much will burn during the first stage and how much will be remaining instantaneously before the microexplosion. Since superheating of the butanol is required for a microexplosion to occur more butanol remaining in the droplet may promote microexplosions.

To compare the tendency of microexplosion to occur for the different mixtures the plot shown in Fig. 4.39 has been prepared. The amount of tests which resulted in microexplosions over the total tests analyzed has been plotted for each mixture. Tests resulting in any microexplosion including ones that burned completely, left fuel on the fibers or fell off the fibers are accounted for. Diameter measurements could still be made at the time of the microexplosions for the tests which the droplets fell making it accurate to use these tests. The plot suggests that the odds of microexplosions occurring are best for droplets of nearly equal concentrations. The Bu40 blend results in microexplosions nearly as often as the Bu50 blend.

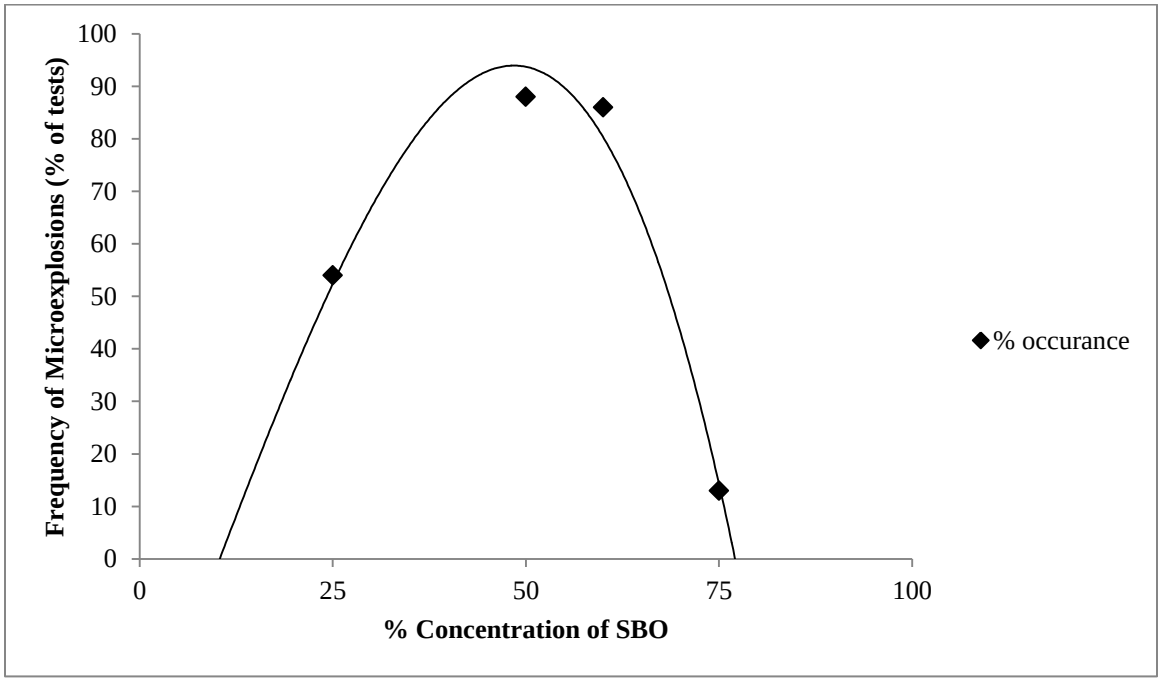

Fig 4.39. Plot of tendency for microexplosions to occur versus initial concentration of SBO in the mixture

A plot comparing the intensity as defined by Wang et al. in previous research ($(D_{explode}/D_0)^2$) has been prepared and is shown in Fig. 4.40. The plot shows that the Bu40 mixture has the most intense microexplosions. This is likely the reason they fall off the fibers during the explosion more often than the other mixtures.

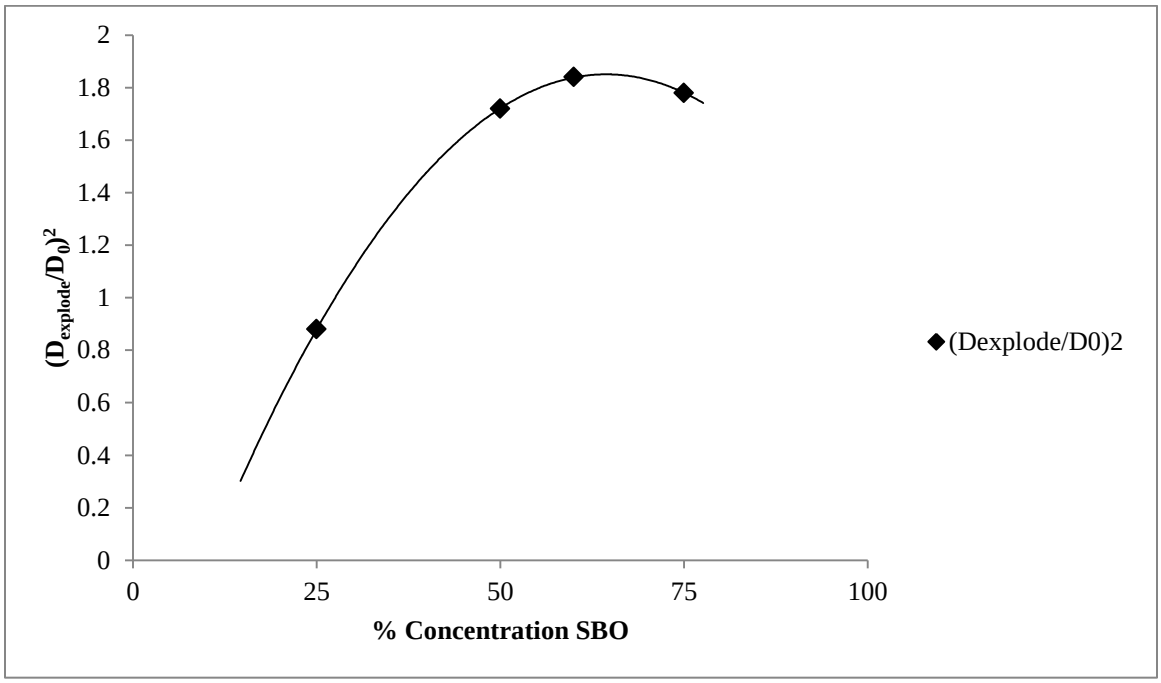

Fig. 4.40. Plot of microexplosion intensity versus initial concentration of SBO in the mixture

The tendency for microexplosions to occur may depend on how much butanol is remaining in the droplet at the time of flame shrinkage. To investigate this, droplet diameters at ignition and at flame shrinkage were examined. Since butanol is the only species that has gasified up to the point of flame shrinkage an estimation of how much butanol is remaining in the droplet at ignition and flame shrinkage can be made. This can be done by calculating the volume at these two time segments and subtracting the initial volume of pure SBO that was in the droplet assuming it to be the same. A plot has been prepared comparing average concentration of butanol lost ($\%Bu_{loss}$) during the first stage over the concentration at ignition ($\%Bu_{ignition}$) for each mixture. The concentration at ignition is always slightly lower than the initial concentration due to evaporation prior to ignition. The evaporated fuel does not impact the burning so that is why the instantaneous concentration at ignition is used. The plot is shown in Fig. 4.41. What the plot means is that for a case with more butanol initially in the mixture more fuel is burned in the first stage and less butanol is remaining in the droplet at flame shrinkage. For the case of the Bu40 mixture there was very little butanol burned in the first stage resulting in

most of the butanol present in the initial droplet still remaining at the time of flame shrinkage prior to the microexplosion. This could explain the more violent microexplosions and the higher tendency for them to occur. Having little butanol remaining in the droplet at the time of flame shrinkage like the Bu75 case may explain why microexplosions occur less frequently. There may not be a sufficient amount of the volatile component (butanol) to boil and burst the droplet. The Bu25 mixture was the closest to the Bu40 mixture as far as the amount of butanol in the droplet at flame shrinkage but the initial amount of butanol proved to be insufficient to heat the droplet to a temperature where superheat of the interior was possible. There was also insufficient data for Bu25 microexplosions to consider the results accurate.

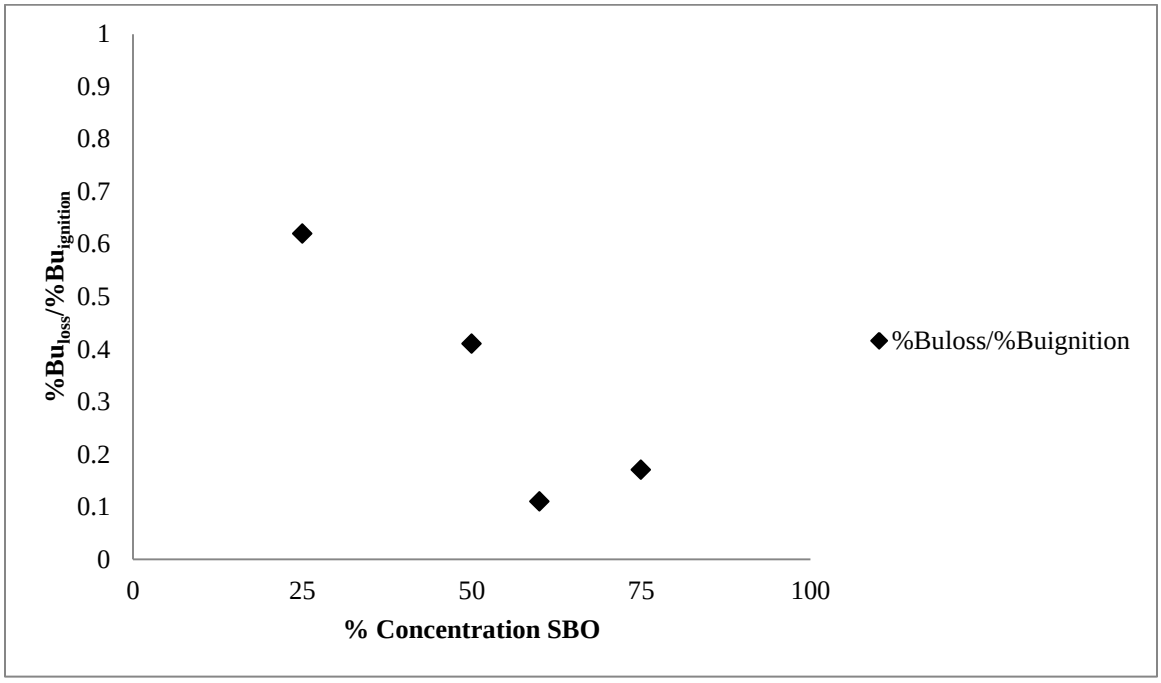

Fig. 4.41. Plot of concentration of butanol burned in the first stage over the concentration present at ignition versus the initial concentration of SBO in the mixture

The interior of the droplet must be superheated to a temperature where homogeneous nucleation of the more volatile component is possible for microexplosions to occur. Consequently the heating at the droplet surface plays an important role. Fig. 4.42 models how the droplet is being heated throughout its lifetime during combustion. The strait

arrows outward represent gasification and heat lost to the atmosphere. The curved arrows inward represent heat from the surface thermally diffusing towards the droplet interior. The black represents the butanol component while the grey shade represents SBO.

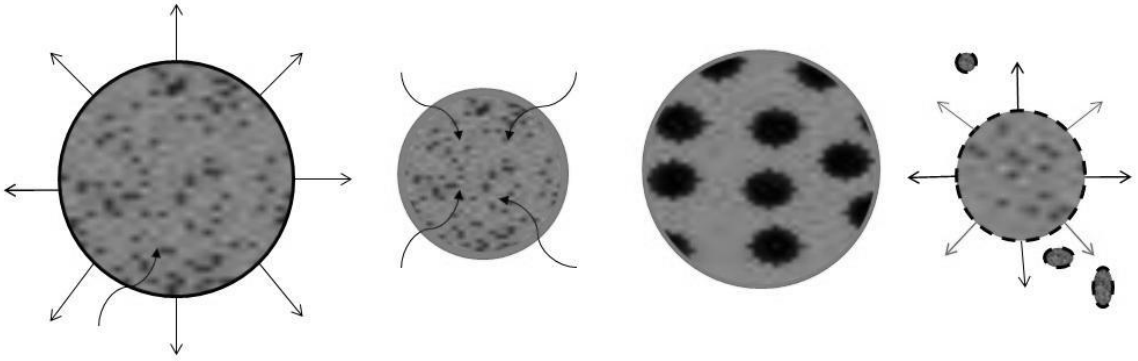

Droplet in the first burning stage. The steady burning of the pure butanol cause the surface temperature and heating of the droplet to depend on the lower boiling point of butanol.	Flame shrinkage and internal heating. A layer of pure SBO exists at the surface causing the surface temperature to rise towards its boiling point. Thermal diffusion towards the droplet interior begins to superheat the butanol trapped inside.	The remaining butanol has been superheated and begins to form bubbles. The droplet expands before it bursts.	Microexplosion and re-ignition of the droplet. Co-burning of the SBO and remaining butanol.

Fig. 4.42. Model of SBO/butanol droplet undergoing combustion

As is suggested in previous research it is suspected that during the first stage for all mixtures the droplet surface temperature is governed by the boiling point of the more volatile component (butanol). This would imply that the droplet surface temperature is the same for all mixtures during the first stage. For Bu75 droplets then, the first burning stage lasts longer burning more butanol before flame shrinkage. This explains why mixtures where flame shrinkage and internal heating occurs sooner would be more likely to experience microexplosions. Also, the lower initial concentration of the less volatile component (SBO) may cause the maximum droplet surface temperature to be lower than that of droplets with higher initial concentrations of SBO. This would reduce the

tendency for microexplosions to occur. Experimental results show that when more butanol is present in the interior of the droplet at the time of the microexplosion the intensity and frequency of the microexplosions tend to increase. It also may explain why droplet size had more of an influence for the Bu75 mixtures than the others. Larger droplets have more butanol in the initial droplet. They also burn longer and produce more heat from the flame. This could increase the maximum surface temperature and make homogeneous nucleation more likely to occur. For the other mixtures which have near equal concentrations significantly more butanol is present at the time of flame shrinkage. The surface temperature would be similar to the Bu75 droplets so there is still sufficient heat produced by the initial flame to superheat the interior. For the Bu25 droplets there just simply is not enough butanol burned in the first stage to superheat the remaining butanol.

Bu75 droplets proved to be more dependent on initial droplet size as well as the temperature rise ($T_2 - T_1$) than the other mixtures as to whether a microexplosion and complete combustion would occur. This makes sense because a greater temperature rise is associated with larger droplets. Plots of temperature rise multiplied by the distance from the droplet center to the thermocouple bead center (see Fig. 3.5 in the experimental methods section) versus the concentration of butanol lost during the first stage over the concentration of butanol at the time of ignition was produced. The plots include data for all mixtures except Bu25 due to lack of sufficient experimental data. The temperature rise is divided by the initial diameter to normalize the data. These are important plots because they show visually how much butanol is burned compared to the initial amount in each droplet as well as the dependence on the temperature rise associated with combustion on the occurrence of complete combustion and microexplosions. The data on these plots were averaged and placed on one plot to show the variation between mixture compositions. This plot is shown in Fig. 4.43. As a reminder, the temperature reported by the thermocouple is not a measurement of droplet temperature so it is inaccurate to use for quantifiable information, as far as droplet temperature, in characterizing combustion

behavior. The droplet size as well as placement was also not consistent which alters accuracy of the upper thermocouple data.

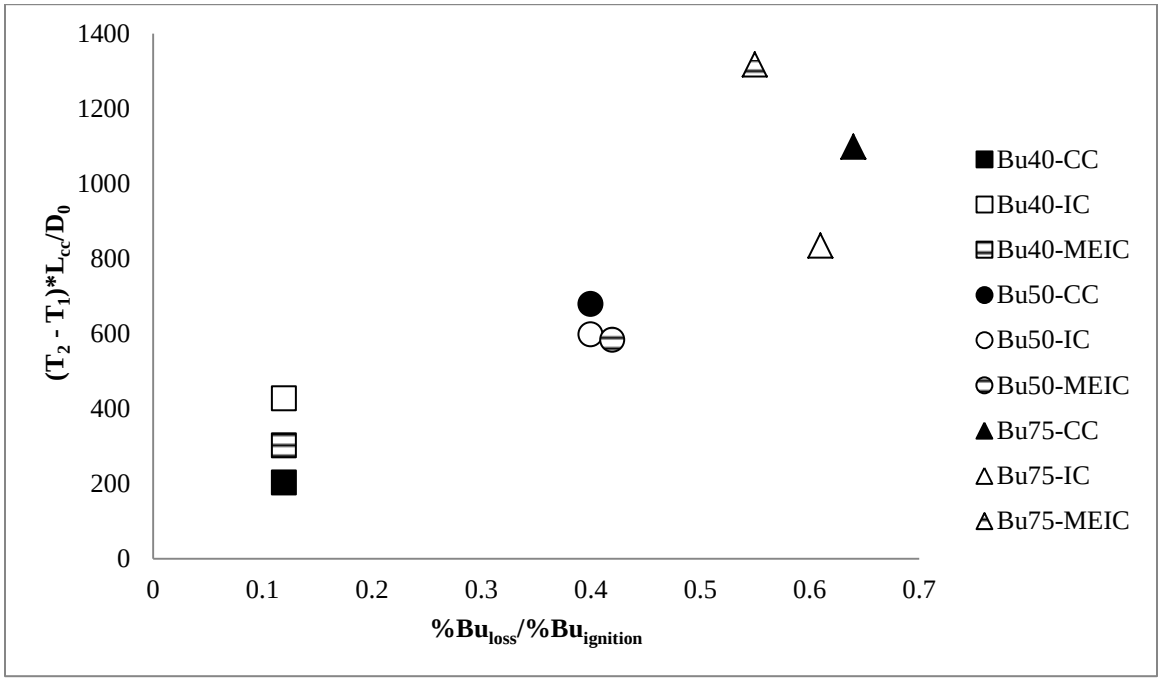

Fig. 4.43. Plot of concentration lost during first burning stage over the concentration at ignition versus the normalized temperature rise as observed by the upper thermocouple during combustion for relevant mixtures

On the plot in Fig. 4.43 complete combustion cases are represented by CC, incomplete combustion with no microexplosion IC and incomplete combustion with a microexplosion MEIC. The plot shows that for mixtures with high concentrations of butanol it is fairly dependent on the temperature rise during combustion as to whether or not complete combustion will occur. The greater the normalized temperature rise the greater the tendency for the droplet to burn completely or at least explode. This is the case for the 50/50 mixture as well however the difference in the normalized temperature rise is much smaller suggesting that the droplet is less dependent on that. For the Bu40 blend the normalized temperature rise seems to be not important at all as to whether the droplet will explode or burn completely. The behavior is actually flipped and the droplets proved to burn completely at temperature rises below which they did not. They exploded with a lower temperature rise as well. Just heating the interior of the droplet

past the boiling point of the more volatile component (i.e. the cause of microexplosions) has proved insufficient to result in complete combustion. It has been shown experimentally that microexplosions can occur and the flame will still extinguish leaving a droplet of liquid fuel behind however in an atomization situation it is likely that these broken up droplets would ignite due to the temperature rise associated with the many burning droplets in the surrounding them.

This research method allows for the study of incomplete combustion which would be unfavorable in any application. Incomplete combustion of single mixed fuel droplets is not reported in previous literature and thus the parameters which govern its occurrence cannot be reviewed. This work was not able to quantify an exact concentration ratio which would produce complete and effective combustion 100% of the time because incomplete combustion occurred for all mixtures studied. A better controlled igniting mechanism controlled by a timer and solenoid could control the test better to achieve more accurate relative concentrations of the droplet at ignition. However, it was shown that the Bu75 mixture was more dependent on the droplet size at ignition and the temperature rise resulting from the burning droplet than the droplets with near equal concentrations. This suggests that altering the initial concentration of the fuel would be more effective on producing microexplosions rather than attempting to design a combustion chamber which would govern fuel droplets' concentration levels using evaporation times and pre-heating temperatures. One could assume an ideal concentration if it is true that microexplosions would benefit combustion during atomization since microexplosions have proved to be more common as the volumetric concentrations get closer to each other. One could suggest that the highest concentration of pure SBO that would produce a microexplosion 100% of the time would be the most ideal mixture because of the cost and availability of SBO versus that of butanol. On the other hand SBO produces more soot than pure butanol which affects mechanical parts and emissions so one would maybe suggest it would be the highest concentration of butanol which would produce microexplosions 100% of the time would be more suitable for some applications. Judging from passed researchers results and the results found in

this work the range of concentration ratios which would likely produce microexplosions most often would be between 60/40 and 50/50 – SBO/butanol. This would provide a fuel droplet which requires less burning during the first stage and the microexplosions would likely be most violent resulting in better breaking up of the fuel. The ignition mechanism which would likely be the most effective for this mixture would be one where there is minimal evaporation between the time the fuel leaves the nozzle and ignition because this would provide a relative concentration at ignition closest to the initial concentration. A nozzle which would produce the best results would be that of an externally mixed type or one which the fuels are mixed just before the nozzle exit. This would likely cause more droplet collisions which according to Wang et al. promotes the microexplosion phenomenon compared to a situation where the droplet is premixed and uniform close to the tip of the nozzle [34].

4.4 Economic and Environmental Impacts

4.4.1 SBO/butanol Blends: The Optimal Blend Ratio

Using the experimental results from the property testing and evaporation and combustion studies the economic and environmental effects of utilizing an optimal mixture of SBO/butanol as an alternative fuel source for various applications can be analyzed. Combustion studies showed agreement with flashpoint results obtained via ASTM D93 showing that any amount of butanol at a concentration greater than 25% by volume added to SBO will reduce the mixtures flashpoint to that of pure butanol (~ 41°C). This means, as far as ignition temperature alone, that any mixture of SBO/butanol with butanol concentrations above 25% would be as suitable as pure butanol as an alternative fuel source for combustion applications. Combustion studies also revealed that mixtures of nearly equal concentrations (i.e. Bu50 and Bu40) were most optimal when considering burning behavior like complete combustion and the occurrence of microexplosions. Basic property testing showed that increasing the amount of butanol past 50% by volume only had effects on the pour point when considering cold flow properties. The cloud point and cold filter plugging point were not significantly changed with increasing

butanol past 50% concentration by volume. The property testing also provided evidence that the HHV of the fuel mixture increased with SBO content. Viscosity and specific gravity decreased with increasing butanol however the change was not very significant at 40°C (flashpoint of butanol) when comparing the Bu75 and Bu50 mixtures. Surface tension, which affects atomization, was lowered to nearly that of pure butanol for all mixtures. Multiple online sources claim that butanol costs about $4 per gallon. The cost of pure SBO in 2011 was also $4 per gallon [49]. Pure SBO is commercially produced on a large scale however butanol is currently not, but is expected to be in the near future. For these reasons it is believed that, assuming these fuel costs, an optimal fuel concentration range would be between 50 and 60 percent SBO (between Bu50 and Bu40). Since butanol is cleaner burning and the cost of the two fuels are assumed to be equal the economic comparison will be done using a Bu50 blend. The cost per gallon will be $4.

4.4.2 Transesterification vs. Simple Mixing

The transesterification process required to make biodiesel from neat BDOs like soybean oil is energy consuming and costly. The conversion process alone accounts for 87% of the total energy required in the production of biodiesel from the ground up [57]. Consequently, it is interesting to compare the effect which replacing biodiesel with the simple mixed SBO/butanol fuel blend would have on the economy. It is likely that the SBO/butanol blend is a better candidate for use in gas turbine engines than in diesel engines which is biodiesels primary use. However, the concept of simple mixing can be compared with the biodiesel production process to show its cost effectiveness.

In 2010, 222 million gallons (28 trillion Btus) of biodiesel were consumed in the U.S. Since soybean oil accounts for about half of the feedstocks used to produce biodiesel about 850 million pounds of soybean oil would have been consumed assuming 100% conversion efficiency and that the other feedstocks have similar densities. Because of the lower energy density of Bu50 compared to soybean oil biodiesel more Bu50 (about 260 million gallons) would be required to provide the 28 trillion Btus of energy consumed. In

2010 the cost of biodiesel was $5 per gallon versus $4 for the pure SBO and the estimated Bu50 fuel price. The cost does not account for biodiesel tax credits assuming that, possibly, there would be similar tax credits for the use of Bu50. The histogram in Fig. 4.44 compares the annual usage of each fuel, as well as the annual cost correlating to the total usage at $5 for biodiesel and $4 for Bu50. Biodiesel is more costly because of the transesterification process used during production. In a 2005 Bioresource Technology Journal article which modeled the production of biodiesel [58] it was estimated that 88% of production costs are attributed to the feedstock (SBO) while 12% account for the rest of the process. The production cost of biodiesel was estimated to be $2 per gallon in the same article based on 2005 feedstock prices. The recovery and sale of glycerol generated during production was included in the analysis which reduced production costs by 6%. Using these estimations about $53 million would have been saved on the production process associated to the making of biodiesel in 2010. The plot in Fig. 4.44 shows a reduction in annual cost of about $72 million. Since soybean oil prices have been rising since 2005 this number seems like an accurate estimation. There was also significantly less biodiesel produced and consumed in 2005 compared to 2010. Even though more soybean oil must be used if the Bu50 blend were to replace biodiesel the consumption of pure SBO would still be well below the amount of soybean oil stored in the U.S. annually (2 to 3 million pounds). This avoids competition with food sources and promotes the utilization of stored fuel which cost money and other resources to store.

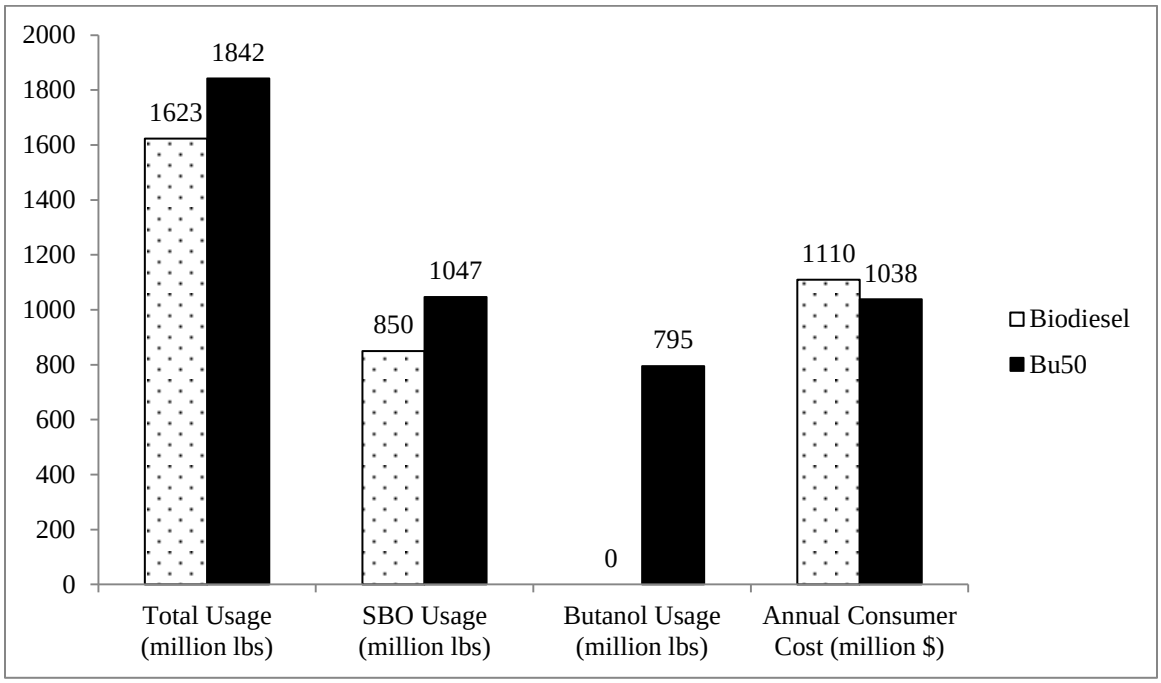

Fig. 4.44. Histogram comparing a scenario where current biodiesel is replaced by Bu50. Fuel utilization and consumer costs are reported

4.4.3 Ethanol vs. Butanol: Which is a Better Renewable Fuel Source

The physical properties of butanol make it a potentially better renewable alternative fuel source than ethanol. Ethanol, an alcohol like butanol, could essentially have been used in this study in place of butanol and may have produced similar results. Ethanol is the most widely used renewable fuel source currently in the U.S. and since butanol could be a potential replacement in the future it is worth investigating the topic.

The physical properties of butanol prove to be superior to ethanol when considering their use in gasoline engines (gas turbines, car motors, etc.). Butanol has a higher energy content than ethanol and has the same range of volatility as gasoline which it is infinitely miscible with [20], [50]. This means that butanol could essentially be mixed with gasoline at any concentrations up to 100% without engine modification [20]. For example, a man named David Ramey drove a 1992 Buick Park Avenue across the U.S. on 100% butanol without any engine modifications. Ramey claimed that the use of butanol in his ’92 Buick improved torque properties and mileage and reduced

hydrocarbon emissions by 95% compared to gasoline [59]. In contrast, standard car engines can combust fuel up to 15% ethanol without modification and the flexible fuel vehicles can combust up to 85% ethanol [50]. Butanol is also a non-corrosive fuel and is knock resistant. Butanol is non-corrosive because it is not miscible with water. Ethanol on the other hand is and can be contaminated with it. As a result ethanol has to be stored in separate tanks at petroleum distribution centers and mixed just prior to transportation. Ethanol also has less versatility in transportation methods than butanol as it cannot be transported in pipelines because of its moisture problem [50]. Currently ethanol is primarily produced by fermentation from corn starch and sugars (corn ethanol). Corn ethanol competes with food production and has substantial life cycle CO_2 emissions compared to ethanol (or butanol) produced from nonfood feedstocks like switchgrass. Butanol can be produced from a larger variety of biomass sources than ethanol and the facilities currently being used to produce ethanol can be converted to butanol fermentation at minimal cost [50]. NO_x emissions would also be reduced from burning butanol instead of ethanol because it has a lower oxygen content.

There are however disadvantages to the use of butanol as an alternative source over ethanol. The main disadvantage is that butanol fermentation has a much lower chemical yield than ethanol. This means that more feedstock is needed to produce equivalent amounts of butanol which in turn increases fuel costs. Butanol has a similar octane rating to gasoline but ethanol has a much higher octane rating which means that fuel blenders can buy a cheaper low octane fuel to blend with it. A third disadvantage is that currently butanol is not recognized as a biofuel in the U.S. so it may not be able to receive the same subsidies as ethanol.

The current tax incentives and mandates placed on the use of ethanol help to offset production costs and stimulate the expansion of the industry. The physical properties butanol and environmental impacts its utilization could have suggest that butanol is a better alternative fuel source than ethanol especially for the transportation sector which ethanol is predominately used for. A few drawbacks make it less desirable. There are currently studies on methods which would increase butanol yields. David Ramey –

president of ButylFuel LLC - currently has a patented method for the production of butanol (ButylFuel™) which he claims outputs yields equal to ethanol production [59]. Ramey plans to produce 10 million gallons of butanol per year using the ButylFuel™ production method. It is also likely that tax incentives would be put in place if butanol production became more efficient and cost effective [59]. Higher scale commercial production of butanol is targeted for the next two to three years [20].

4.4.4 SBO/butanol Blends as an Alternative Source of Aviation Fuel

Currently, the low energy content of light alcohols like butanol prevents their viability as a replacement for aviation fuels as a pure component. However, butanol trails only two renewable energy sources in energy density in comparison with that of jet fuel (Jet A). Biodiesel and Fischer-Tropsch synthetic fuels (FT synthetic) are closer in gravimetric and volumetric energy densities than butanol to conventional jet fuel. However energy density can be increased with the addition of soybean oil to butanol. From bomb calorimeter results the addition of 50% by volume (i.e. Bu50) increases the HHV by approximately 1.5 MJ/kg (equivalent to 1.28 MJ/Liter) over pure butanol. The effect on the LHV would be similar to that of the HHV. A recent article by Chung Law provided a plot like the one shown in Fig. 4.45 comparing energy densities of various alternative aviation fuels to the currently used Jet A fuel [20]. A projected data point for the Bu50 fuel is added to the plot to show the improvement in energy densities when SBO is added to the butanol.

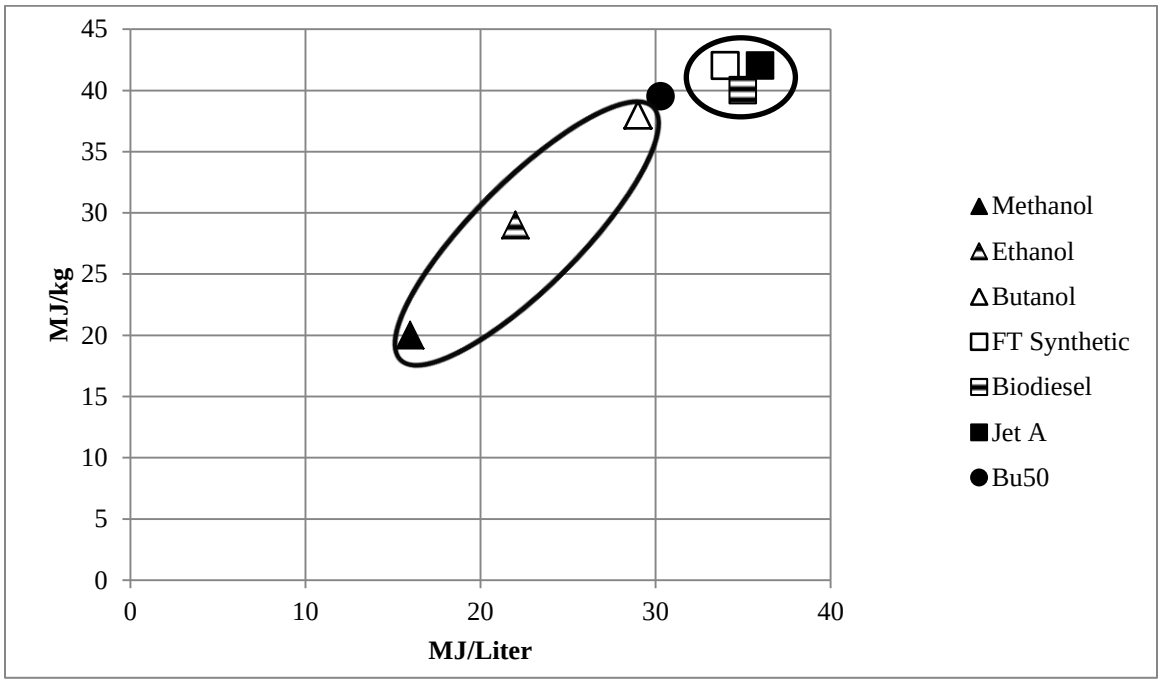

Fig. 4.45. Gravimetric and volumetric energy densities of various alternative aviation fuels including the currently used Jet A fuel and the Bu50 fuel

With an energy density close to that of Jet A, Bu50 is worthy of being analyzed as an alternative fuel source for aviation fuel. Blending the SBO/butanol mixtures with conventional jet fuels could be an even better and more realistic, compromised solution. Gas turbines like the ones used to power jets require viscosities below 5.5 cSt at 40°C for some fuel grades and even lower for others [60]. The viscosity of Bu50 is slightly higher at about 6 cSt at 40°C. Bu75 is below the standardized requirement however there would be less impact on the energy density with lower concentrations of SBO. Mixing with Jet A or other conventional aviation fuels seems to be the most feasible solution. In 2010 aviation fuel was used to provide 2,973 Btus (16.5 billion gallons) of energy in the transportation sector. The histogram in Fig. 4.46 compares annual fuel utilization and consumer costs for a scenario where a Bu50 would provide half of that energy. In other words the SBO/butanol fuel would be mixed with conventional aviation fuel at a concentration such that the energy consumption demand is met. As a result of the lower energy density of Bu50 more total fuel is expected to be utilized. It is reported that the

$36 billion were spent by the consumer on aviation fuel in 2010 which equates to $2.18 per gallon versus $4.00 per gallon for Bu50.

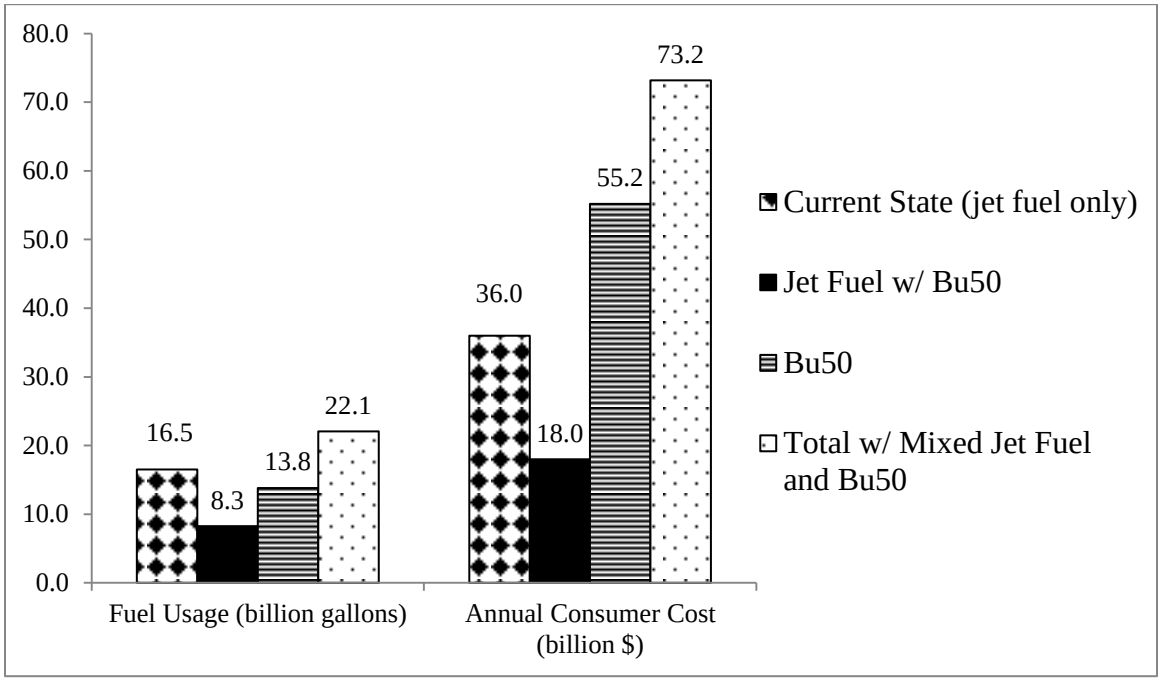

Fig. 4.46. Histogram comparing fuel utilization and consumer costs for a scenario where half of the aviation fuel consumed is replaced by Bu50

From the plot in Fig. 4.46 it is obvious that at the current state mixing Bu50 with conventional aviation fuel at 50/50 concentrations would boost annual consumer expenditures for aviation fuel. It also increases the overall fuel utilization because Bu50 is less energy dense than conventional jet fuel. It may not look attractive as an alternative fuel source from this data but more aspects must be considered. For example, the United States has a large trade deficit. If Bu50 was utilized as an alternative for just 13% of aviation fuel it would account for all the imported aviation fuel and still allow for the current export rate. Reducing petroleum imports can help to reduce the trade deficit and the United States' dependency on foreign oil fields. Importing less petroleum would slow down the flow of U.S. currency into the world markets. Consumer costs would likely decrease with increasing demand of Bu50 causing the annual expenditures to decrease. The short CO_2 lifecycle of the SBO and cleaner burning butanol would also be

more environmentally friendly than burning the petroleum based jet fuels currently in use.

4.4.5 SBO/butanol Blends as an Alternative Source of Distillate Fuel Oil

Fuel oil could potentially be replaced or see reduced usage with increased utilization of biofuels like SBO/butanol blends. Fuel oils have different classifications. Some are residual fuel oils and some are distillate fuel oils. Most residual fuel oils need to be pre-heated for their relevant applications and are less commonly used than distillate fuel oils. Distillate fuel oils are primarily used in boilers for heat generation but some classes can be used for power generation and transportation as well. Distillate fuels oils were the leading single component contributor for CO_2 emissions of petroleum fuels for the residential, commercial and industrial sectors in 2010 [46]. It is of more interest to compare utilization of distillate fuel oils to alternative sources for these reasons.

Distillate fuel oil (DFO) was the United States' number one petroleum product export in 2010. It also accounted for nearly 9% of petroleum product imports that year. In 2010 the value of imported petroleum products was about $73.23 billion exceeding the value of exported petroleum products by just over $10 billion [46]. If the amount of imported distillate fuel oil (81.4 million barrels in 2010) was replaced by an equivalent amount Bu50 by energy content the difference between petroleum import value and export value would be decreased by more than $6 billion assuming all petroleum products have equal value. The histogram in Fig. 4.47 models a scenario where the amount of imported distillate fuel oil is replaced by Bu50 accounting for energy consumption needs based on 2010 data. The Bu50 fuel could be used as a direct replacement or mixed with conventional DFOs at low concentrations. The total fuel usage will be expected to increase because of the lower energy density of the Bu50 and the cost will be expected to increase because of the higher costs. Petroleum product imports will decrease as a result which is beneficial to current economic state. The histogram is only a comparison for one particular situation and different amounts of Bu50 fuel could be used as an alternative fuel source. If more renewable fuels are used there could be more distillate

fuel oil exported or stored which seems to be the trend. Also utilizing more short CO_2 life cycle fuels instead of the DFOs would positively impact the environment.

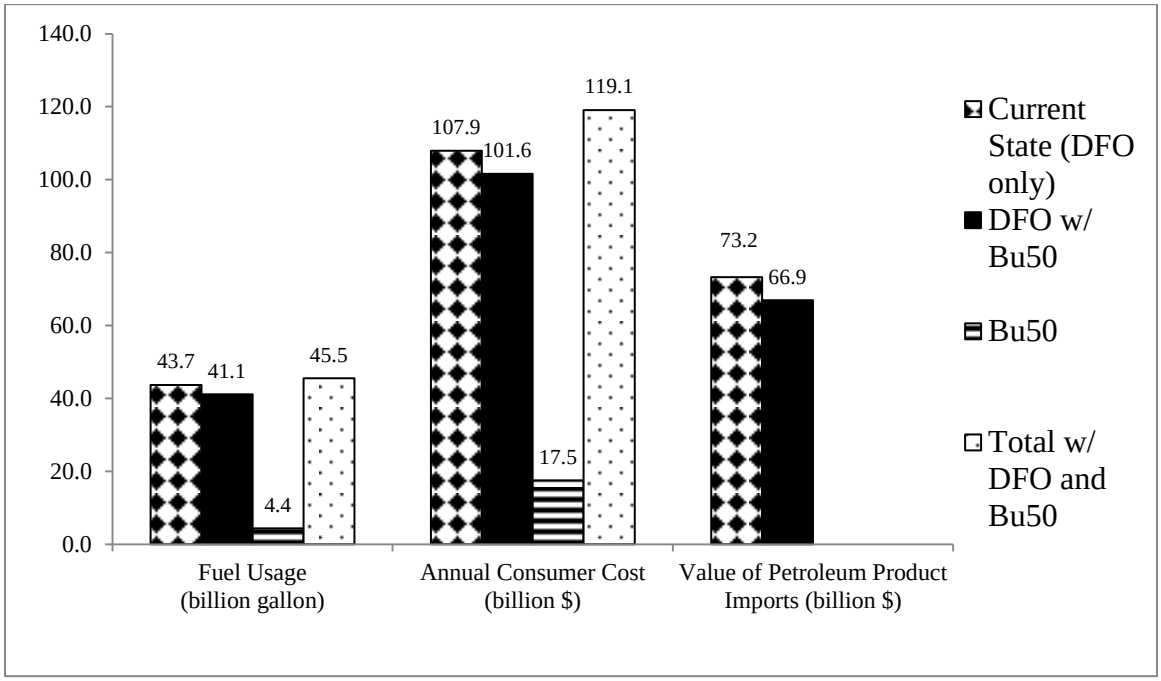

Fig. 4.47. Histogram comparing fuel utilization, consumer costs and import costs for a scenario where all imported distillate fuel oil is replaced by Bu50

Just a few different scenarios for the alternative use of renewable biofuels (Bu50) have been reported. These scenarios can be expanded and many other possibilities such as changing the comparable conventional fuels in each scenario can be analyzed. This report gives quick insight on the possibility of using the Bu50 fuel mixture as an alternative fuel source for various applications. The results show that with some sacrifices this could be a possibility in the future. Comparisons between the most common biofuels currently in use today (fuel ethanol and biodiesel) and the Bu50 mixtures are also reported showing why a simple mixed fuel consisting of SBO and butanol could essentially play similar roles as these fuels. Consumer costs and fuel consumption are the drawbacks for increasing the amount of biofuels used but future tax incentives may help offset the high production prices while increased demand could lower sales costs. Future engineering could help provide better and more efficient ways to produce such a fuel source as Bu50 as well as introduce mixing methods to increase

energy content which would lower consumption rates. Machines, engines, and boilers which depend on combustion will likely become increasingly efficient in the future resulting in reduced fuel usage as well. Better gas mileage in automobiles is a good example of this in the recent years.

5.0 Conclusions and Recommendations

5.1 Research Findings

A variety of testing techniques were applied to simply mixed soybean oil and butanol fuel blends in an effort to categorize simply mixed SBO/butanol blends as a viable alternative fuel source for combustion applications. Mixing rules and property estimation methods were studied and compared with experimental data for basic properties of RBD soybean oil-butanol mixtures. Linear regression showed that the relative density-temperature relationship is linear and that density for all blends decreases with increasing temperature. Kay's mixing rule proved to be an accurate method of predicting relative density based on blend composition. The kinematic viscosity-temperature relationship is exponential and the viscosity of the blends can accurately be predicted using the Andrade equation. The full form of the Grunberg-Nissan equation proved to be the most accurate for estimating kinematic viscosity based on blend composition. Kay's mixing rule was shown to be an accurate estimation of the higher heating values based on the composition. The surface tension-temperature relationship was linear and the surface tension of all the blends was nearly that of pure butanol. Linear regression showed that an approximate estimation could be made for each mixture using first order linear equations. The surface tension-composition relationship proved to be more difficult to estimate because the surface composition is not the same as the known bulk composition. Methods derived from thermodynamics proved to be more accurate than empirical equations for predicting surface tension based on blend composition. Likely more in depth research and regression on experimental data could provide interaction parameters that could be used to yield more desirable estimates. Cold flow tests showed that the addition of butanol had a limited effect on the CP and CFPP. The most significant

change was at butanol concentrations less than 25% by volume. Butanol showed a greater impact on PP, decreasing the mixture PP continuously with increasing butanol concentration.

Basic evaporation studies were performed using single droplets of SBO/butanol mixed fuel and their pure components. Evaporation constants (K) of Bu75, Bu50 and pure butanol were measured at a wide range of low temperatures using the Xcytex ProAnalyst^{TM} software. Experimental results showed that at temperatures of 29, 100, 118, 165 and 225°C SBO/butanol fuel blends had similar evaporation constants as that of pure butanol. Pure SBO did not show significant surface regression at temperatures below 285°C. Consequently, the evaporation constant for single droplets of pure SBO were measured at 285, 325 and 350°C. The evaporation rates of pure SBO were found to be much lower than that of the droplets containing butanol but increased with ambient temperature. For the mixed droplets, at temperatures at or below 225°C, surface regression of the liquid fuel ceased after a period of time depending on the ambient temperatures. As a result, a liquid fuel droplet, assumed to be that of pure SBO, was left on the fibers. Final diameters of the "left over" droplets were measured and compared to initial droplet diameters by calculating $(D/D_0)^2_{final}$. The $(D/D_0)^2_{final}$ values correlated with good accuracy to values which would suggest the final volume of the droplet was equal to a size corresponding to its initial SBO concentration. For example, the final volume of a Bu50 droplet was equal to 50% of its initial volume. Experimental results suggested that the gasification mechanism during pure evaporation at low temperatures was a diffusion type process where the butanol diffuses toward the surface of the droplet as it is vaporizing. A Peclet number, which Makino and Law suggest a diffusion-like gasification if its value is calculated to be >>1, was calculated using conservative values to be 60.12. Consequently, it is believed that the surface regression rate is slower than the mass diffusion rate of the butanol towards the surface resulting in a layer of butanol at the surface during vaporization. The droplets then vaporize until all butanol present has gasified, leaving behind an amount of pure SBO equal to its initial amount in the droplet. The results suggest that knowing the evaporation constant of pure butanol one can

estimate instantaneous concentration levels of single droplets at times between formation and ignition. The relative concentrations would depend on the temperature in the combustion chamber and time to ignition.

This work utilized single fuel droplets of mixed SBO/butanol fuel as well as their pure components to analyze combustion behavior. Ignition of all mixed droplets was possible at similar temperatures to that of pure butanol suggesting that any amount of butanol greater than 25% by volume added to the binary SBO/butanol mixture will lower the flashpoint to that of itself. The lower flashpoint can eliminate the need for preheating fuel and duel fuel tank systems. The single droplet combustion experiments introduced the concept of incomplete combustion. Experimental results showed that in some cases the mixed fuel droplets ignited but did not burn completely leaving liquid fuel on the testing fibers. This phenomenon is not previously discussed in literature due to the testing methods used by the select groups studying the combustion behavior of single fuel droplets. Microexplosions, a concept linked to burning fuel droplets with high volatility differentials, proved to be a common occurrence in this work. Microexplosions have been previously analyzed and reported upon by other research groups studying single mixed fuel droplets with volatility differentials similar to SBO/butanol. Incomplete combustion is an indicator of inefficient combustion and could be considered an undesirable combustion behavior. The occurrence of microexplosions is suggested by experts to be beneficial to the combustion process because it better mixes the fuel with surrounding oxidizing gasses. Analysis of the occurrence of incomplete combustion and microexplosions as well as microexplosion intensity allowed for an estimated range of fuel mixture concentrations which would be optimal for a spray combustion application. Because incomplete combustion occurred at a higher frequency for mixtures of Bu75 than Bu50 and Bu40, and microexplosions were much more common for the Bu50 and Bu40 mixtures, a range of 50-60% SBO by volume is predicted to be ideal for SBO/butanol fuel blends. The main factor which caused microexplosions proved to be the initial concentration of the droplets. Initial droplet size could not be proven to have a significant effect on whether or not microexplosions would occur or not. Time to

ignition also could not be proven to be a driving factor. It could be assumed that a much smaller droplet, like one produced from a nozzle in a spray combustion application, which is ignited much quicker than the single droplets used in this work would behave similarly because their relative concentrations at the time of ignition will be the same. Estimated concentrations at ignition and after the first burning stage were used in the analysis in an effort to gain insight as to why droplets of different initial concentrations burned so differently. Experimental results showed that less butanol was burned during the first combustion stage for droplets of nearly equal concentrations compared to the cases where more butanol was present (i.e. Bu75). The higher concentration of butanol trapped within the droplet at flame shrinkage is likely the reason that microexplosions occur more frequently and at a greater intensity. Results suggest that the droplets must have enough butanol gasified in the first stage to achieve a temperature great enough to superheat the droplet interior and there also must be enough butanol remaining in the droplet interior to explode the droplet and aid in the co-burning of the remaining fuel. Spray combustion testing including emission analysis will need to be performed to prove the accuracy of using single droplets to predict spray combustion behavior.

A literature review provided interesting data concerning how the utilization of biofuels like SBO/butanol mixtures could affect the environment and U.S. economy. After reviewing literature based on the use of alternative fuels as well as annual U.S. energy reviews some conclusions could be made about benefits and drawbacks of using SBO/butanol blends in place of both currently used biofuels as well as some petroleum fuels. All analysis and comparisons were done based on the utilization of Bu50 because of its property test results and performance in the combustion studies. First, it was shown that if Bu50 could be used in place of biodiesel (eliminating the costly transesterification process) there could be a possible economic advantage. More SBO would be utilized and the production of butanol would have to increase. However, the current stores of SBO would not be exceeded and the annual fuel cost would be decreased by about $70 million. Increased, commercialized production of butanol would likely lower the fuel cost even further. Secondly, butanol proved to have many advantages over ethanol, which is

currently the widest used biofuel. The main advantages discussed were that butanol is infinitely miscible with gasoline, has a higher energy content than ethanol, can be made from a wider variety of biomass and storage and transport of the fuel is more versatile due to its immiscibility with water. Current disadvantages of utilizing butanol as an alternative for ethanol directly, or as a mixed fuel, are its higher price due to butanol's low yield from the fermentation process and the fact that it is not currently recognized as a biofuel. Consequently, there are currently no tax incentives based on its use. Improved technology and more efficient fermentation techniques will likely increase butanol yields and lower costs in the future. As a result, its use is becoming more attractive and an increase in commercial production is expected in the near future. Other scenarios were analyzed which included a percentage of Bu50 utilization in place of conventional aviation fuels as well as distillate fuel oil used for heat and power generation. The Bu50 blend is shown to be nearly as energy dense as Jet A fuel which is the most common type of aviation fuel. As a result it is possible that it could be mixed with Jet A to provide an alternative renewable fuel source for the current petroleum based fuel. A scenario where Bu50 replaced 50% of the aviation fuel used in 2010 was analyzed. Because of its lower energy content there would have to be more Bu50 utilized to provide for the equivalent energy demand used that year. The annual fuel cost for consumers would double because Bu50 is nearly twice as expensive as petroleum based jet fuel. However environmental advantages would include the usage of a renewable source and usage of fuel with a shorter CO_2 lifecycle. The main economic advantage is that utilizing 50% alternative fuel source would eliminate the United States' need to import any aviation fuel and a lot less crude oil. This could help the trade deficit the U.S. is currently in and reduce cash flow to other world markets. The final scenario analyzed was one in which Bu50 replaced the amount of imported distillate fuel oil in the United States. The Bu50 blend has properties which would allow it to replace this type of petro-fuel for various applications such as heat production or power generation. It could be mixed with the fuel oil at various concentrations to provide sufficient energy for consumer demand. Results showed that if Bu50 replaced the imported distillate fuel oil a possible value of $6 billion in imported petroleum products could potentially be saved. Like the other scenarios,

more total fuel would need to be utilized because of the lower energy content Bu50 exhibits compared to distillate fuel oil but there would be similar positive economic and environmental tradeoffs. The use of a sustainable energy source would positively impact the environment both because of more environmentally friendly emissions as well as the renewable aspect of the fuel feedstocks. The impact on the economy would be that there is less need for imported petroleum products. The annual cost to the consumer would increase by about $11 billion. However, increased butanol production and possible tax incentives could help to offset the increased cost.

5.2 Limitations and future work

The limitations in this work were a result of testing procedures. The basic property testing revealed very little error and good repeatability as all tests excluding the surface tension tests were performed via ASTM standardized methods. The surface tension tests provided meaningful results but were measured with a calibrated Cole-Parmer EW-59780-90 surface tension apparatus employing the capillary rise method. This is an accurate method however it is not an ASTM standardized method. The results obtained, however, seemed to be correct and accurate. Other inaccuracies obtained during the evaporation and combustion studies could be minimized or eliminated by altering the testing procedure. The tests were done using a newly developed testing procedure based on literature review of experts attempting to obtain similar information. The testing methods were perceived to be the best for obtaining the desired results using fuels with properties similar to SBO/butanol blends. As experimental testing progressed, new, unexpected and unforeseen results were obtained and consequently strategic alterations to the testing apparatus and procedure were made to better analyze these findings and improve accuracy. The results discussed in this work were a collaboration of the most accurate experimental data obtained in the given time frame. After the experimental results had been analyzed more alterations to the procedure that would produce even better and more meaningful results became evident. These recommendations for future testing will be discussed.

The initial droplet diameter was hard to measure accurately for a few reasons. First, it was difficult to achieve a camera setting which would allow for similar lighting at time zero (just before the furnace passed the droplet) and when the furnace was in test position. This is because when the furnace is in test position the dark furnace surrounded the droplet and instantaneously before time zero the light from the ambient lab surrounded the droplet. This lighting problem could be eliminated by placing a second, non-heated shell around the furnace so that as the furnace is dropping the surrounding lighting mimics that of when the furnace is completely lowered. Secondly, as the furnace was lowered it caused a slight vibration on the main table. The high speed camera was attached to a tripod which was positioned directly on the main table so that the lens of the camera could be as close to the test droplet as possible. Consequently, for a short period of time after the furnace had been lowered a bouncing affect is observed in the video footage making it difficult for the tracking software to track the edges of the droplet. An easy solution to this problem would be to build a second bracket which would be attached to a different, solid base than the one the furnace sits on (main table) which would still allow the camera lens to be positioned near the sight port. A camera mounting arm would likely be needed as well to get the camera as close to the sight port as possible. More accurate initial droplet measurements will allow for better estimations of droplet concentrations at the time of ignition and possibly allow for better insight as to what the main cause of incomplete combustion is. The ignition procedure could also be improved by attaching the igniter to a push pull solenoid controlled by a timing trigger. This would allow the ignition of the droplets to be more consistent and at the exact same time from test to test. Flashpoint data would be more accurate as a result and the time to ignition could be better analyzed as a factor for influencing combustion behavior. A change from hot wire ignition to spark ignition may also be beneficial if it is possible to estimate the energy added to the droplet to the spark. A spark igniter would be much more useful to ignite pure SBO.

Since butanol evaporates at room temperature there is also the concern of the change in concentration between the time the droplet is placed on the fibers to time zero when the initial droplet diameter is measured. This concept was neglected in this study however could play a significant role in such tests which require great accuracy. This initial evaporation period could be completely eliminated if a droplet dispenser was built to drop a liquid fuel droplet on the fibers while the furnace is already in test position. This would also eliminate any inaccuracies involved in the initial droplet measurement because the droplet would be at its exact initial concentration and size when the experimental process begins. This alteration could likely have the largest effect on experimental accuracy for the testing procedure used in this study. Lighting improvements could also be made in an effort to observe the flame present when the butanol is burning. The way to do this is unknown and would require some trial and error tests as well as some research into camera lighting.

BIBLIOGRAPHY

[1] *usda.gov*. [Online]. Available: http://www.usda.gov. [Accessed: 20-Jul.-2011].

[2] R. Altin, S. Cetinkaya, and H. Yucesu, "The potential of using vegetable oil fuels as fuel for diesel engines," *Energy Conversion and Management*, vol. 42, pp. 529–538, Jan. 2001.

[3] T. W. Ryan, L. G. Dodge, and T. J. Callahan, "The Effects of Vegetable Oil Properties on Injection and Combustion in Two Different Diesel Engines," *JAOCS*, vol. 61, no. 10, pp. 1610–1619, Oct. 1984.

[4] P. Soltic, D. Edenhauser, T. Thurnheer, D. Schreiber, and A. Sankowski, "Experimental investigation of mineral diesel fuel, GTL fuel, RME and neat soybean and rapeseed oil combustion in a heavy duty on-road engine with exhaust gas aftertreatment," *Fuel*, vol. 88, no. 1, pp. 1–8, Jan. 2009.

[5] M. K. Tran, D. Dunn-Rankin, and T. K. Pham, "Characterizing sooting propensity in biofuel-diesel flames," *Combustion and Flame*, vol. 159, no. 6, pp. 2181–2191, Jun. 2012.

[6] R. O. Dunn and M. O. Bagby, "Low-Temperature Phase Behavior of Vegetable Oil/Co-solvent Blends as Alternative Diesel Fuel," *JAOCS*, vol. 77, no. 12, pp. 1315–1323, Jul. 2000.

[7] P. Benjumea, J. Agudelo, and A. Agudelo, "Basic properties of palm oil biodiesel–diesel blends," *Fuel*, vol. 87, no. 10, pp. 2069–2075, Aug. 2008.

[8] A. W. Schwab, M. O. Bagby, and B. Freedman, "Preparation and Properties of Diesel Fuels from Vegetable Oils," *Fuel*, vol. 66, pp. 1–7, Oct. 1987.

[9] C. E. Goering, A. W. Schwab, R. M. Campion, and E. H. Pryde, "Soyoil-Ethanol Microemulsions as Diesel Fuel," *Transactions of the ASAE*, pp. 1602–1604, Jan. 1983.

[10] A. Shihadeh and S. Hochgreb, "Diesel Engine Combustion of Biomass Pyrolysis Oils," *Energy Fuels*, vol. 14, no. 2, pp. 260–274, Mar. 2000.

[11] R. O. Dunn, "Low-Temperature Flow Properties of Vegetable Oil/Cosolvent Blend Diesel Fuels," *JAOCS*, vol. 79, no. 7, pp. 709–715, Jun. 2002.

[12] H. V. Panchasara, B. M. Simmons, A. K. Agrawal, S. K. Spear, and D. T. Daly, "Combustion Performance of Biodiesel and Diesel-Vegetable Oil Blends in a Simulated Gas Turbine Burner," *Journal of Engineering for Gas Turbines and Power*, vol. 131, pp. 1–11, May 2009.

[13] G. Pucher, W. Allan, M. LaViolette, and P. Poitras, "Emissions From a Gas Turbine Sector Rig Operated With Synthetic Aviation and Biodiesel Fuel," *Journal of Engineering for Gas Turbines and Power*, vol. 133, pp. 1–8, Nov. 2011.

[14] C. Allouis, F. Beretta, P. Minutolo, R. Pagliara, M. Sirignano, L. A. Sgro, and A. D'Anna, "Measurements of ultrafine particles from a gas-turbine burning biofuels," *Experimental Thermal and Fluid Science*, vol. 34, no. 3, pp. 258–261, Apr. 2010.

[15] A. Rehman, D. R. Phalke, and R. Pandey, “Alternative fuel for gas turbine: Esterified jatropha oil-diesel blend,” *Renewable Energy*, vol. 36, no. 10, pp. 2635–2640, Oct. 2011.
[16] D. Sequera, A. K. Agrawal, S. K. Spear, and D. T. Daly, “Combustion Performance of Liquid Biofuels in a Swirl-Stabilized Burner,” *Journal of Engineering for Gas Turbines and Power*, vol. 130, pp. 1–9, May 2008.
[17] M. E. Boucher, A. Chaala, and C. Roy, “Bio-oils obtained by vacuum pyrolysis of softwood bark as a liquid fuel for gas turbines. Part I: Properties of bio-oil and its blends with methanol and a pyrolytic aqueous phase,” *Biomass and Bioenergy*, vol. 19, pp. 337–350, Jun. 2000.
[18] R. G. Andrews, P. C. Patnaik, J. W. Michniewicz, L. J. Jankowski, V. I. Romanov, V. V. Lupandin, and A. V. Ravich, “Feasibility of utilizing a bio-mass derived fuel for industrial gas turbine applications,” Presented at *The International Gas Turbine and Aeroengine Congress and exposition*, Houston, Texas, Jun. 2002.
[19] D. Chiaramonti and M. Prussi, “Pure vegetable oil for energy and transport,” *Int. J. Oil, Gas and Coal Technology*, vol. 2, no. 2, pp. 186–198, 2009.
[20] C. K. Law, “Fuel options for next-generation chemical propulsion,” *AIAA Journal*, vol. 50, no. 1, pp. 19–36, Jan. 2012.
[21] B. E. Poling, J. M. Prausnitz, and J. P. O'Connell, *The Properties of Gases & Liquids*, 5th ed. New York, New York: McGraw Hill.
[22] M. E. Tat and J. H. Van Gerpen, “The Specific Gravity of Biodiesel and Its Blends with Diesel Fuel,” *JAOCS*, vol. 77, pp. 115–119, Jan. 2000.
[23] E. Alptekin and M. Canakci, “Determination of the density and the viscosities of biodiesel–diesel fuel blends,” *Renewable Energy*, vol. 33, no. 12, pp. 2623–2630, Dec. 2008.
[24] C. C. Enweremadu, H. L. Rutto, and J. T. Oladeji, “Investigation of the relationship between some basic flow properties of shea butter and their blends with diesel fuel,” *International Journal of the Physical Sciences*, vol. 6, pp. 758–767, Feb. 2011.
[25] M. E. Tat and J. H. Van Gerpen, “The Kinematic Viscosity of Biodiesel and Its Blends with Diesel Fuel,” *JAOCS*, vol. 76, no. 12, pp. 1511–1513, Jan. 1999.
[26] L. Grunberg and A. H. Nissan, “Mixture Law for Viscosity,” *Nature*, vol. 164, no. 4175, pp. 799–800, Jan. 1949.
[27] R. E. Tate, K. C. Watts, C. A. W. Allen, and K. I. Wilkie, “The viscosities of three biodiesel fuels at temperatures up to 300°C,” *Fuel*, vol. 85, no. 7, pp. 1010–1015, May 2006.
[28] R. C. Reid, J. M. Prausnitz, and B. E. Poling, *The Properties of Gases & Liquids*, 4th ed. Boston, Massachusetts: McGraw Hill.
[29] M. Matalon, “Combustion theory,” Presented at *CEFRC Summer School*, Princeton University, Jun. 2011.
[30] J. H. Bae and C. T. Avedisian, “Experimental study of the combustion dynamics of jet fuel droplets mixed with additives in the absence of convection,” *Combustion and Flame*, vol. 137, pp. 148–162, Feb. 2004.

[31] M. Ikegami, G. Xu, K. Ikeda, S. Honma, H. Nagaishi, D. L. Dietrich, and Y. Takeshita, "Distinctive combustion stages of single heavy oil droplet under microgravity," *Fuel*, vol. 82, pp. 293–304, Oct. 2002.

[32] C. H. Wang, X. Q. Liu, and C. K. Law, "Combustion and microexplosion of freely falling multicomponent droplets," *Combustion and Flame*, vol. 56, pp. 175–197, 1984.

[33] J. C. Lasheras, A. C. Fernandez-Pello, and F. L. Dryer, "Experimental observations on the disruptive combustion of free droplets of multicomponent fuels," *Combustion Science and Technology*, vol. 159, pp. 195–209, 1980.

[34] C. H. Wang, W. G. Hung, S. Y. Fu, W. C. Huang, and C. K. Law, "On the burning and microexplosion of collision-generated two-component droplets: miscible fuels," *Combustion and Flame*, vol. 134, pp. 289–300, Mar. 2003.

[35] M. L. Botero, Y. Huuang, D. L. Zhu, A. Molina, and C. K. Law, "Synergistic combustion of droplets of ethanol, diesel and biodiesel mixtures," *Fuel*, vol. 94, pp. 342–347, Nov. 2011.

[36] G. Xu, M. Ikegami, S. Honma, M. Sasaki, K. Ikeda, H, Nagaishi, and Y. Takeshita, "Combustion characteristics of droplets composed of light cycle oil and diesel light oil in a hot-air chamber," *Fuel*, vol. 82, pp. 319–330, Oct. 2002.

[37] J. C. Lasheras, A. C. Fernandez-Pello, and F. L. Dryer, "On the disruptive burning of free droplets of alcohol/n-paraffin solutions and emulsions," *The Combustion Institute*, Eighteenth Symposium on Combustion, pp. 293–305, 1981.

[38] K. L. Pan, J. W. Li, C. P. Chen, C. H. Wang, "On droplet combustion of biodiesel fuel mixed with diesel/alkanes in microgravity condition," *Combustion and Flame*, vol. 156, pp. 1926–1936, Aug. 2009.

[39] G. Gogos, S. Soh, and D. N. Pope, "Effects of gravity and ambient pressure on liquid fuel droplet evaporation," *Heat and Mass Transfer*, vol. 46, pp. 283–296, 2003

[40] T. Niioka and J. Sato, "Combustion and microexplosion behavior of miscible fuel droplets under high pressure," *The Combustion Institute*, Twenty-first Symposium on Combustion, pp. 625–631, 1986.

[41] M. Takei, T. Tsukamoto, and T. Niioka, "Ignition of blended-fuel droplet in high-temperature atmosphere," *Combustion and Flame*, vol. 93, no. 6, pp. 149–156, 1993

[42] H. Zhang and C. K. Law, "Effects of temporally varying liquid-phase mass diffusivity in multicomponent droplet gasification," *Combustion and Flame*, vol. 153, pp. 593–602, Mar. 2008.

[43] A. Makino and C. K. Law, "On the controlling parameter in the gasification behavior of multicomponent droplets," *Combustion and Flame*, vol. 73, pp. 331–336, 1988.

[44] A. L. Randolph, A. Makino, and C. K. Law, "Liquid-phase diffusional resistance in multicomponent droplet generation," *The Combustion Institute*, Twenty-first Symposium on Combustion, pp. 601–608, 1986.
[45] J.F. Sanz Requena, A.C. Guimaraes, S. Quiros Alpera, E. Relea Gangas, S. Hernandez-Navarro, L.M. Navas Gracia, J. Martin-Gil, and H. Fresneda Cuesta, "Life Cycle Assessment (LCA) of a biofuel production process from sunflower oil, rapeseed oil and soybean oil," *Fuel Processing Technology*, vol. 92, pp. 190–199, Mar. 2011.
[46] *eia.gov*. [Online]. Available: http://www.eia.gov. [Accessed: 24-Sep.-2012].
[47] N. Kou, and F. Zhao, "Techno-economical analysis of a thermo-chemical biofuel plant with feedstock and product flexibility under external disturbances," *Energy*, vol. 36, pp. 6745–6752, Nov. 2011.
[48] A.A. Apostolakou, I.K. Kookos, C. Marazioti, and K.C. Angelopoulos, "Techno-economical analysis of a biodiesel production process from vegetable oils," *Fuel Processing Technology*, vol. 90, pp. 1023–1031, Apr. 2009.
[49] *ers.usda.gov*. [Online]. Available: http://www.ers.usda.gov. [Accessed: 24-Sep.-2012]
[50] K. R. Szulczyk, "Which is a better transportation fuel – butanol or ethanol," *International Journal of Energy and Environment*, vol. 1, Issue 3, pp. 501–512, 2010.
[51] A. International, "ASTM D1298-99," ASTM International, West Conshohocken, PA, 1900.
[52] A. International, "ASTM D445-11a," ASTM International, West Conshohocken, PA, 1900.
[53] A. International, "ASTM D240-09," ASTM International, West Conshohocken, PA, 1900.
[54] A. International, "ASTM D6371-05," ASTM International, West Conshohocken, PA, 1900.
[55] A. International, "ASTM D6749-02," Sep. 2007.
[56] A. International, "ASTM D2500-09," ASTM International, West Conshohocken, PA, 1900.
[57] *nrel.gov*. [Online]. Available: http://www.nrel.gov/vehiclesandfuels/npbf/pdfs/24772.pdf. [Accessed: 4-Oct.-2012].
[58] M. J. Haas, A. J. McAloon, W. C. Yee, and T. A. Foglia, "A process model to estimate biodiesel production costs," *Bioresource Technology*, vol. 197, pp. 671–678, Jun. 2005.
[59] D. E. Ramey, "Butanol: The Other Alteranative Fuel," *Agricultural Biofuels: Technology, Sustainability and Profitability*, pp. 137–147, May. 2007.
[60] A. International, "ASTM D2880-03," ASTM International, West Conshohocken, PA, 2010.